

Generation of cluster beams

B M Smirnov

DOI: 10.1070/PU2003v046n06ABEH001381

Contents

1. Introduction	589
2. Character of cluster growth in gases and plasmas	590
2.1 Properties of clusters; 2.2 Mechanisms and rates of cluster growth in gases; 2.3 Peculiarities of a cluster plasma	
3. Processes in gases and plasmas involving clusters	596
3.1 Equilibrium of clusters in a hot vapor; 3.2 Chemical processes in a hot buffer gas; 3.3 Nucleation in a hot buffer gas with metal-containing molecules; 3.4 Charging of clusters in a plasma; 3.5 Charging of clusters by electron impact	
4. Methods of generation of cluster beams	604
4.1 Basic methods of generation of cluster beams; 4.2 Laser generation of metallic atoms and clusters; 4.3 Cluster generation at free jet expansion; 4.4 Cluster generation in a plasma; 4.5 Pulsed generation of intense cluster beams in a plasma; 4.6 Cluster beams for metal transport	
5. Processes in the generation of cluster beams	614
5.1 Peculiarities of nucleation at free jet expansion; 5.2 Character of formation of atoms in cluster generation; 5.3 Explosive emission as a method of atom generation	
6. Applications of cluster beams	621
6.1 Cluster beams for fabrication of films and materials; 6.2 Laser irradiation of cluster beams; 6.3 Collision of cluster beams	
7. Conclusions	625
References	625

Abstract. The processes are considered in a cluster plasma consisting of a dense plasma of a buffer gas and a metal admixture. These processes involving clusters in a gas or plasma include nucleation processes in a supersaturated vapor, formation of metallic clusters in a dense gas from metal-containing compounds, and chemical processes in the course of this conversion, processes of cluster charging in a plasma and under the action of an electron beam. The basic methods are analyzed for cluster generation including formation and growth of clusters in free jet expansion of a gas, under laser action on the metallic surface, and growth of clusters in a plasma resulted from injection of metal-containing molecules into a plasma. Some applications of cluster beams are discussed, which include fabrication of thin films, new materials, and creation of a hot nonuniform plasma.

1. Introduction

A cluster as a system of bound atoms constitutes a physical object that is of interest both from the fundamental and

applied standpoints [1–10]. Use of clusters in the form of cluster beams is convenient for both the generation and application of clusters. This provides high rates of cluster formation and allows one to transport clusters in a simple way to the place where they will be used. Cluster beams were first generated in Germany [11–13] as a result of the expansion of a vapor formed in a chamber through a small nozzle into a vacuum. The subsequent evolution of the experimental technique [14–18] led to the development of various schemes of cluster generation with identical elements. Indeed, in all cases of cluster generation a nucleating vapor passes through a nozzle. Then a buffer gas or non-nucleating gas is pumped out, the clusters are charged by a crossing electron beam, the beam of charged clusters formed is accelerated and is operated by standard electric optics.

The yield cluster beam is used for the formation of thin films and in other identical applications [19–28] and for the fabrication of new materials, especially where such clusters are embedded in a continuous matrix [29–33], the latter being a type of nanostructured material [34]. But the chain of processes in the course of the generation of cluster beams is complex and nonequilibrium. Therefore, the yield parameters of the generators of cluster beams depend remarkably on the processes which proceed there. Moreover, yield parameters of cluster beams may be improved in some cases by changing the basic processes and correspondingly by changing the regime of cluster generation. Along with applications, some processes are of basic importance since they dominate and can be studied in the course of investigating cluster generation. The goal of this paper is to review the processes and phenomena which are important for cluster beam generation and to

B M Smirnov Institute for High Temperatures,
Russian Academy of Sciences,
Izhorskaya ul. 13/19, 127412 Moscow, Russian Federation
Tel./Fax (7-095) 190 42 44
E-mail: smirnov@oivtran.iitp.ru

Received 15 December 2002, revised 17 April 2003
Uspekhi Fizicheskikh Nauk 173 (6) 609–648 (2003)
Translated by B M Smirnov; edited by A Radzig

analyze these processes both from their fundamental and applied standpoints.

2. Character of cluster growth in gases and plasmas

2.1 Properties of clusters

Large clusters as macroscopic systems of bound atoms can be found in both the solid and the liquid aggregate states, the solid cluster being more interesting as a specific physical object because some parameters of solid clusters show a nonmonotonic dependence on the cluster size (or the number of atoms in it). The optimal cluster sizes correspond to completed structures, and the numbers of atoms in such clusters are called magic numbers. If the number of cluster atoms is one higher or lower than the magic number, the atomic binding energy for these clusters, as well as other cluster parameters such as the ionization potential and the electron affinity, is lower than that at the magic number of cluster atoms [35–37]. This means that various parameters of solid clusters are nonmonotonic functions of the number of cluster atoms and take optimal values (minimal or maximal) at magic numbers of atoms. Since the family of a completed cluster structure includes an infinite number of cluster sizes, a solid cluster is characterized by an infinite number of magic numbers.

Large clusters consisting of a many atoms are the object of our consideration. Solid clusters consisting of magic numbers of atoms are similar to completed crystalline particles. In this case a nonmonotonic dependence of the cluster parameters on the number of cluster atoms is observed when charged clusters are extracted from the cluster source, and currents of charged clusters of different sizes are measured on the basis of mass-spectrometric separation of clusters. This is the method for determining the magic numbers of charged clusters, and sufficiently large clusters can be analyzed by this method. In particular, magic numbers of sodium clusters are observed in clusters consisting of up to 22,000 atoms [38].

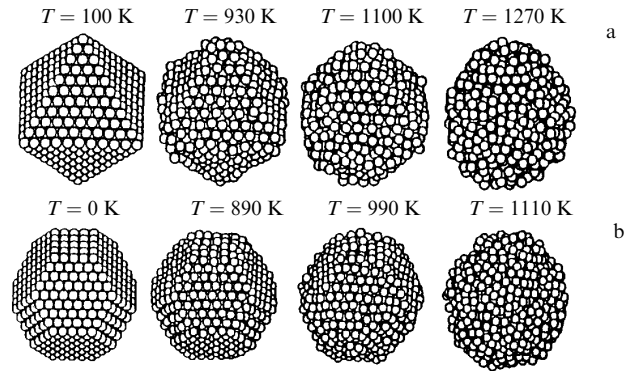


Figure 1. The character of amorphization of the cluster structure on heating copper clusters [39] (the cluster temperature is indicated): (a) $n = 891$, and (b) $n = 1291$. (These clusters have an octahedral structure and the structure of a regular truncated octahedron, respectively, at zero temperature.)

When a cluster melts, it loses its crystal structure as well as its magic numbers as a characteristic of the cluster structure. We give an example of cluster melting in Fig. 1 [39]. As a result of the melting, a shapeless particle is formed, and we will model it by a spherical liquid drop. Moreover, in considering a large liquid cluster, we will assume its density to be identical to that of a macroscopic liquid. Then the cluster radius r is given by [10]

$$r(n) = r_W n^{1/3}, \quad (2.1)$$

where n is the number of cluster atoms, and r_W is the Wigner–Seitz radius

$$r_W = \left(\frac{3m}{4\pi\rho} \right)^{1/3}. \quad (2.2)$$

Here, m is the mass of an individual atom, and ρ is the density of the cluster material. The model of a liquid drop for a cluster, where the cluster is changed by a macroscopic liquid drop with the bulk density, will be used below. Table 1

Table 1. Parameters of large liquid clusters based on the data derived from Ref. [40].

Element	T_m , K	T_b , K	r_W , Å	k_0 , 10^{-11} cm ³ s ⁻¹	ε_0 , eV	p_0 , 10^5 atm	A , eV	ΔH_f , eV	$N_{\text{sat}}(T_m)$, 10^{13} cm ⁻³
Ti	1941	3560	1.67	5.82	4.89	300	3.2	4.91	0.64
V	2183	3680	1.55	4.86	4.9	46	3.7	5.34	8.4
Fe	1812	3023	1.47	4.18	3.83	11	3.0	4.32	24
Co	1768	3200	1.45	3.96	4.10	3.5	3.1	4.41	3.7
Ni	1728	3100	1.44	3.70	4.13	47	2.9	4.46	2.0
Zr	2128	4650	1.85	5.18	6.12	52	3.8	6.31	0.005
Nb	2750	5100	1.68	4.23	7.35	360	4.5	7.47	0.2
Mo	2886	4912	1.60	3.78	6.3	59	4.5	6.82	7.4
Rh	2237	3968	1.55	3.42	5.42	7.7	3.8	5.78	1.5
Pd	1828	3236	1.58	3.50	3.67	4.4	2.9	3.92	16
Ta	3290	5731	1.68	3.30	8.1	250	4.7	8.12	1.2
W	3695	5830	1.60	2.73	8.59	230	4.7	8.82	10
Re	3459	5880	1.58	2.64	7.36	63	5.3	7.99	8.1
Os	3100	5300	1.55	2.52	7.94	230	4.7	8.16	1.0
Ir	2819	4700	1.58	2.60	6.44	130	4.9	6.93	6.4
Pt	2041	4098	1.60	2.65	5.6	170	3.6	5.87	0.04
Au	1337	3129	1.65	2.80	3.65	12	2.5	3.80	0.007
U	1408	4091	1.77	2.93	4.95	5.4	3.8	5.53	1.2×10^{-6}

Note. Here, T_m is the melting point of the metal, T_b is its boiling point, the Wigner–Seitz radius r_W is defined by formula (2.1), the reduced rate constant k_0 of atom attachment [see formula (2.8)] relates to the temperature 2000 K, the parameters ε_0 and A are defined according to formula (2.4), the parameter p_0 is included in formula (2.10), ΔH_f is the enthalpy per atom for transformation of a solid into a monatomic gas at a pressure of 1 atm and a temperature of 298 K, and $N_{\text{sat}}(T_m)$ is the number density of atoms at the melting point and saturated vapor pressure.

contains the parameters of some heat-resistant metallic clusters near and above the melting point [10, 41] if we employ the liquid drop model. Note that the number density of atoms $N_{\text{sat}}(T_m)$ at the melting point and saturated vapor pressure is the parameter that characterizes the maximum number density of free atoms above the metallic surface if it is not destructed. We express the pressure in atm and determine the saturated vapor pressure by the formula

$$p_{\text{sat}}(T) = \exp\left(\frac{\varepsilon_0}{T_b} - \frac{\varepsilon_0}{T_m}\right), \quad (2.3)$$

where we took into account that the saturated vapor pressure is 1 atm at the boiling point T_b .

In contrast to the solid state, parameters of liquid clusters depend monotonically on the cluster size. In particular, the total binding energy E of cluster atoms can be determined by the expression [42, 10]

$$E(n) = \varepsilon_0 n - An^{2/3}, \quad (2.4)$$

where ε_0 is the sublimation energy of bulk per atom, the second term in the right-hand side of this formula includes the surface energy that can be expressed through the surface tension of a macroscopic system, and the formula is an expansion of the cluster energy over a small parameter $\sim n^{-1/3}$. The parameters of this formula for large liquid clusters near the melting point are given in Table 1 and they were obtained on the basis of the parameters of bulk liquid metals. In so doing, we assume the atom binding energy ε_0 to be large in comparison with the typical thermal energy of atoms, which is $\sim T_m$ (T_m is the melting point, and throughout this paper we express the temperature in energy units).

Thus, we assume the atom binding energy at the melting point, ε_0 , and at zero temperature to be identical, and such an assumption leads to an error of several percent. One can become convinced of this accuracy by comparing ε_0 with the specific enthalpy ΔH_f of transformation of a metal into a monatomic gas under normal conditions (a pressure of 1 atm and temperature of 298 K), whose values are given in Table 1. Note that ΔH_f relates to the solid state and hence exceeds the value of ε_0 , and the accuracy of the data for ε_0 is better than the difference between ε_0 and ΔH_f . According to Table 1, the average ratio $\varepsilon_0/\Delta H_f$ is equal to 0.94 ± 0.03 . Therefore, the accuracy of the parameters in formula (2.4), presented in Table 1, is on average better than several percent. Below we will neglect the temperature dependence of parameters ε_0 and A in formula (2.4).

As follows from expression (2.4), the atomic binding energy for a liquid cluster is

$$\varepsilon_n = \frac{dE(n)}{dn} = \varepsilon_0 - \frac{\Delta\varepsilon}{n^{1/3}}, \quad \Delta\varepsilon = \frac{2}{3} A. \quad (2.5)$$

Of course, the atomic binding energy tends to that of a bulk system, ε_0 , for an infinite cluster, but the contribution of the surface energy to this quantity is remarkable even for large clusters. The reason for this is the developed cluster surface because many cluster atoms are located on or near the cluster surface. Therefore, surface effects are of importance for clusters. From this it follows that the parameters of large clusters, expressed in the form of a series expansion over a small parameter $n^{-1/3}$, depend on the cluster size. On the

other hand, this expansion simplifies the cluster analysis, and we will use that below.

The liquid drop model applied to a large liquid cluster allows us to analyze the kinetic parameters of a cluster located in a gas or plasma. In particular, within the framework of this model, the cross section of atom attachment to the cluster surface is equal to

$$\sigma(n) = \pi r^2, \quad (2.6)$$

where r is the cluster radius in accordance with formula (2.1). In the above formula we assumed that each contact of an incident atom with the cluster surface leads to its attachment, and the radius of action of atomic forces is small compared to the cluster radius, i.e., this formula is valid for large clusters. From this we obtain the following expression for the rate of atom attachment to a cluster surface:

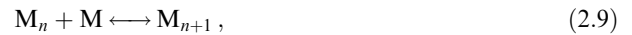
$$v(n) = Nv\sigma(n) = Nk_0n^{2/3}, \quad (2.7)$$

where N is the atom number density, v is the average atom velocity, and $\sigma(n)$ is the cross section of atom attachment to a cluster consisting of n atoms, in accordance with formula (2.6). The reduced rate constant k_0 is given by the formula [43, 44, 10]

$$k_0 = \sqrt{\frac{8T}{\pi m}} \pi r_w^2, \quad (2.8)$$

where T is the gaseous temperature expressed in energy units, and m is the atomic mass. Because of the simple temperature dependence, this is a universal parameter for a given type of clusters. Table 1 contains the values of k_0 for some metals at the temperature $T = 2000$ K.

The process of atom attachment to the cluster surface is the detailed inverse process with respect to evaporation of atoms from the cluster surface, so that both these processes are described by the scheme



where M is an atom. Hence, the evaporation rate $v_{\text{ev}}(n)$ can be expressed through the attachment rate (2.8) on the basis of the principle of detailed balance. In deriving this connection, we take into account that for an infinite cluster, when the atom binding energy ε_n coincides with that of a bulk system, ε_0 , the equilibrium between processes of atom attachment and evaporation takes place at the saturated vapor pressure $p_{\text{sat}}(T)$ that corresponds to the saturated number density $N_{\text{sat}}(T)$ of cluster atoms, and we have for an atomic vapor:

$$p_{\text{sat}}(T) = TN_{\text{sat}}(T).$$

The temperature dependence of the quantities takes the form [45, 46]

$$p_{\text{sat}}(T) = p_0 \exp\left(-\frac{\varepsilon_0}{T}\right), \quad (2.10)$$

and we have the same dependence for $N_{\text{sat}}(T)$ since the main temperature dependence for these quantities is exponential.

Switching to the equilibrium of an individual cluster in an atomic vapor and using the exponential temperature dependence for the equilibrium number density of atoms, we obtain

the following expression for the atom evaporation rate $v_{ev}(n)$ from the cluster consisting of n atoms [43, 44]:

$$v_{ev}(n) = v(n) \frac{N_{sat}(T)}{N} \exp\left(-\frac{\varepsilon_n - \varepsilon_0}{T}\right), \quad (2.11)$$

where the binding energy of the cluster atoms is given by formula (2.4), and the rate of atom attachment is given by formula (2.7). Thus, the rate of cluster evaporation is expressed through the atom number density at the saturated vapor pressure, and the parameters of formula (2.11) are represented in Table 1 for metallic clusters.

As follows from the above analysis, usage of the liquid drop model for a large liquid cluster allows us to consider some parameters of such a cluster and its kinetic parameters in a simple way. In particular, formulas (2.7) and (2.11) govern the rates of atom attachment and cluster evaporation for a large liquid cluster, so that if a cluster consisting of n atoms is located in an own vapor with a number density N of atoms, the character of evolution of the cluster size is given by the equation

$$\frac{dn}{dt} = k_0 n^{2/3} N - v_{ev}(n), \quad (2.12)$$

and we accounted for the fact that the processes of cluster growth proceed step by step. Thus, the liquid drop model is able to describe some properties of large liquid clusters and their behavior in an atomic vapor.

2.2 Mechanisms and rates of cluster growth in gases

The growth of clusters in gases and plasmas is one of the nucleation processes which are studied for other systems, such as the formation of coagulation processes in solutions, the formation and growth of islands on the surface, and condensation processes in gases and gaseous mixtures. Hence, cluster growth is analogous to other processes of nucleation and is governed by the same mechanisms, and then a cluster is an analog of condensation nuclei in other cases. We now enumerate these mechanisms, which are represented in Fig. 2 [47].

The first mechanism (Fig. 2a) of growth of condensation nuclei results from the attachment of individual or free atoms to a test nucleus and the evaporation of growing clusters or nuclei of condensation, i.e., these processes proceed according to scheme (2.9). Evidently, this mechanism of nucleation takes place if free atoms (or molecules) dominate. If the pressure of free atoms exceeds the saturated vapor pressure at a given temperature not so strongly, then the size distribution function for clusters that are not large in size is close to equilibrium, like that realized in the absence of cluster growth. One can introduce the critical cluster size for which the rate of atom attachment and the rate of cluster evaporation are identical. Then clusters whose size is less than the critical one evaporate, and clusters whose size exceeds the critical one grow. This situation corresponds to the classical case of the nucleation process [48–52], when the rate of atom attachment to clusters is almost equal to the total rate of evaporation of clusters, i.e., the difference in these rates is less in comparison to each of them. In considering cluster growth in a plasma, we will be guided by another limiting case, when the degree of vapor supersaturation is high and the processes of cluster evaporation are not important for cluster growth.

When all the atoms are bound in clusters, the subsequent cluster growth can be a result of joining individual clusters

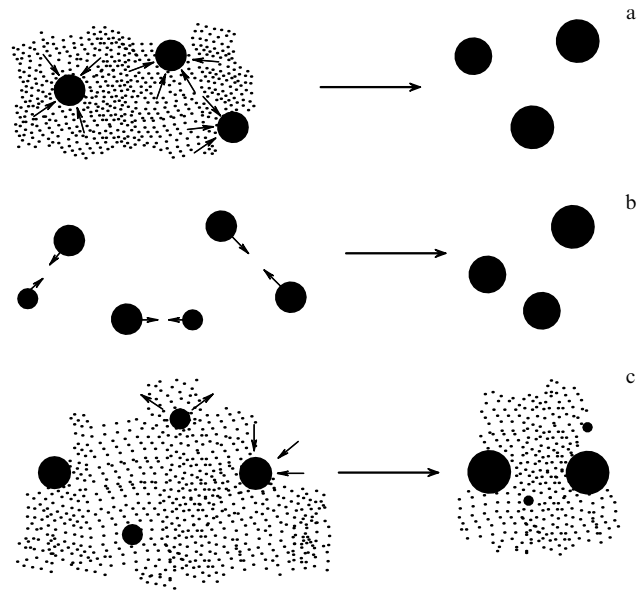


Figure 2. Mechanisms of cluster growth: (a) attachment of atoms to the cluster surface if an individual cluster is located in an atomic vapor; (b) coagulation or joining of clusters, and (c) coalescence or Ostwald ripening, where small clusters evaporate and large clusters grow due to an equilibrium between clusters and an atomic vapor.

according to the scheme



This is the coagulation process (Fig. 2b) [53], and its name shows that such a process was studied first for solutions and liquids. This process of the growth of condensation nuclei can proceed in various physical systems containing clusters or small particles. As an example of this nucleation process, we can point to the sticking of dusty particles in a gravitational field [54].

One more mechanism of cluster growth (Fig. 2c), namely Ostwald ripening [55] or coalescence, takes place when the two previous mechanisms of nucleation are forbidden or are quite weak. For example, in the case of the growth of islands on the surface [56–62], the nucleation process results from evaporation of atoms bonded to the surface in small islands, and these atoms then move along the surface and attach to large islands; the coagulation process does not occur there because of the small mobility of islands on the surface. In the case of charged clusters, when the coagulation process is forbidden because of a Coulomb repulsion of charged clusters, the coalescence nucleation mechanism follows from an equilibrium between clusters and free atoms, which are formed as a result of cluster evaporation and the attachment of atoms to the cluster surface. In the case of very large clusters, the pressure of free atoms corresponds to the saturated vapor pressure at a given temperature. The equilibrium between an individual cluster and an atomic vapor depends on the competition for the processes of cluster evaporation and attachment of free atoms to the cluster. For small clusters, the evaporation process dominates, whereas the attachment of free atoms is stronger for large clusters, compared with the evaporation process. Therefore, small clusters evaporate and large clusters grow, leading to an effective growth of clusters and a decrease in the number density of clusters. When the mean cluster size becomes large,

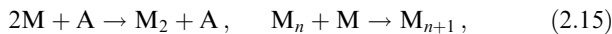
the automodel regime of cluster growth [63–65, 51] is established. In this limiting case, the form of the size distribution function of clusters does not vary in time, whereas the average cluster size increases in time.

The rate of cluster growth for this mechanism of the nucleation process is proportional to the number density of free atoms. For a large average cluster size, the equilibrium pressure of free atoms is close to the saturated vapor pressure that depends strongly on the temperature. Therefore, this mechanism of nucleation, namely coalescence or Ostwald ripening, is triggered at high temperatures. This nucleation mechanism dominates when the clusters are charged and the number density of free atoms is respectively small and is determined by its equilibrium with clusters or condensation nuclei.

We now demonstrate the character of these general mechanisms of nucleation and cluster growth in the widespread case of cluster generation as a result of the expansion of a gas or vapor if the gas flow passes through a nozzle. In the course of expansion, the gas temperature decreases sharply and the transformation of this gas into growing clusters is thermodynamically favorable. For definiteness, we consider the case where a metallic vapor is found in a buffer gas, and only metallic atoms are converted into clusters. Denoting the number density of free metallic atoms and atoms of a buffer gas by N and N_a , respectively, and introducing the number density N_{cl} of clusters and cluster size n (a number of cluster atoms), we obtain the following balance equations

$$\begin{aligned} \frac{dN}{dt} &= -N_{cl} k_0 n^{2/3} N - KN^2 N_a, & \frac{dN_{cl}}{dt} &= KN^2 N_a, \\ \frac{dn}{dt} &= k_0 n^{2/3} N. \end{aligned} \quad (2.14)$$

Here, K is the rate constant of formation of a diatomic molecule in three-body collisions, its typical value in this case being $K \sim 10^{-32} \text{ cm}^6 \text{ s}^{-1}$. The last equation in the set (2.14) is equation (2.12) where we ignored the process of cluster evaporation, i.e., the gas temperature is supposed to be relatively low. This set of balance equations shows the character of the cluster growth process and corresponds to the scheme



where M and A are the metallic atom and the atom of a buffer gas, respectively. Formation of a diatomic metallic molecule is a slow process because of its three-body nature. Therefore, the formed diatomic molecules next play the role of nuclei of condensation and are transformed quickly into large clusters by the attachment of metal atoms in pairwise collisions. From this it follows that at the end of the nucleation process, when initially free atoms become bonded to clusters, the formed clusters are large. Note that, in contrast to the classical theory of nucleation in a supersaturated vapor [48–52], when the degree of supersaturation is not high and the competition for the attachment and evaporation processes creates a barrier to cluster formation and growth, we now consider the case of a

high supersaturation, and evaporation processes are not essential then.

This character of the cluster growth process is realized at large values of the parameter

$$G = \frac{k_0}{N_a K} \gg 1. \quad (2.16)$$

Taking a typical value of k_0 at high temperatures to be $\sim 3 \times 10^{-11} \text{ cm}^3 \text{ s}^{-1}$ (see Table 1) and $K \sim 10^{-32} \text{ cm}^6 \text{ s}^{-1}$ [66, 44], we find that this inequality is satisfied at $N_a \ll 3 \times 10^{21} \text{ cm}^{-3}$, i.e., for gaseous densities of atoms one has $G \gg 1$.

The ratio of the first to second terms on the right-hand side of the first balance equation (2.14) is of the order of a current cluster size n , and since $n \gg 1$, one can neglect the last term in the first equation. We solve the set of equations (2.14) under the assumption $N(t) = \text{const}$. Then we arrive at the size distribution function f_n of clusters in the form

$$\begin{aligned} f_n &= \frac{N_{cl}}{n_{\max}}, & n &\leq n_{\max}, \\ f_n &= 0, & n &> n_{\max}. \end{aligned}$$

and the solutions of Eqns (2.14) in this approximation give

$$\begin{aligned} n_{\max} &= \left(\frac{k_0 N t}{3} \right)^3, & \bar{n} &= \frac{n_{\max}}{2}, \\ N_{cl} &= KN^2 N_a t = \frac{3N n_{\max}^{1/3}}{G}, & N_b &= N_{cl} \bar{n} = \frac{3N n_{\max}^{4/3}}{2G}, \end{aligned} \quad (2.17)$$

where \bar{n} is the average cluster size, N_b is the number density of bound atoms, and N is the number density of initially free metallic atoms which partake in the formation and growth of clusters. We assume the gas temperature at which the nucleation process proceeds to be relatively small, so that one can ignore evaporation of cluster atoms. From relations (2.17) we find the characteristic time τ_{cl} of the clusterization process, when all the free atoms are converted into bound atoms of clusters. From the relation $N_b = N$, where N is the number density of free atoms at the beginning of the cluster growth process, it follows by that time:

$$n_{\max} = \left(\frac{2G}{3} \right)^{3/4}, \quad \tau_{cl} = \frac{(54G)^{1/4}}{k_0 N}, \quad N_{cl} = \frac{54^{1/4} N}{G^{3/4}}. \quad (2.18)$$

As evidenced by the solutions (2.18), these processes lead to the formation of large clusters at the end of the conversion of free metallic atoms into clusters. We collected in Table 2 some parameters of this process when the concentration of metallic atoms at the beginning is 1% with respect to the total number of buffer and metallic atoms at a pressure of 1 atm. We introduce the critical temperature T_{cr} such that the saturated vapor pressure at this temperature is $p_{sat}(T_{cr}) = 0.01 \text{ atm}$, and we choose a current temperature T from the relation $p_{sat}(T) = 0.0001 \text{ atm}$, i.e., at this temperature free metallic

Table 2. Parameters characterizing formation of metallic clusters in a buffer gas if the total pressure of the buffer gas is 1 atm and the concentration of metallic atoms is 1%.

Metal	$T_{cr}, 10^3 \text{ K}$	$T, 10^3 \text{ K}$	$N, 10^{17} \text{ cm}^{-3}$	$G, 10^3$	$N_{cl}, 10^{15} \text{ cm}^{-3}$	$\tau_{cl}, 10^{-6} \text{ s}$	n_{\max}	$\tau_2, 10^{-6} \text{ s}$	ξ
Mo	3.8	3.0	2.4	2.7	1.7	1.2	280	2.4	38
W	4.6	3.8	1.9	2.7	1.4	1.9	280	3.7	38
Ir	3.6	3.0	2.2	1.8	2.4	1.6	200	2.7	30

atoms are 1% of the total number of metallic atoms under thermodynamically equilibrium conditions. Hence, in considering the kinetics of the nucleation process, one can ignore evaporation of clusters at this temperature. In addition, we take the rate constant k_0 from Table 1, and the rate constant of a three-body process is $K = 1 \times 10^{-32} \text{ cm}^6 \text{ s}^{-1}$ [44] with regard to the data [66] where this value was obtained by averaging several experimental results, and the statistical error in this value may be as great as 2. The data in Table 2 give a representation of this stage of the nucleation process.

Note that the kinetics of nucleation at this stage, when the basic portion of atoms is free, differs in principle from the classical case of gas nucleation [48–52] when the degree of supersaturation is not large. The rate of atom attachment is then comparable to the rate of cluster evaporation, and the latter brings down the total rate of conversion of free atoms into bound ones. In the case under consideration, when the supersaturation degree is large, evaporation of clusters is not significant, and this decreases the typical time of the nucleation process.

When this stage of the nucleation process is terminated, and all the atoms are converted into clusters, subsequent cluster growth results from the coagulation process (2.13) (see Fig. 2b) according to the scheme



where M is a metallic atom, and the clusters are neutral. According to the definition of the average cluster size we have $\bar{n} = N_b/N_{cl}$, where N_{cl} is the number density of the clusters, and N_b is the total number density of bound atoms in clusters. This gives

$$\bar{n} = 3.5(N_b k_0 t)^{1.2} \quad (2.20)$$

for the cluster growth through a time t after the beginning of the process for neutral clusters [67, 68]. We assume here that the reduced rate constant k_0 of atom attachment to a cluster and the number density N_b of bound atoms do not vary in time, and this formula is valid under the condition

$$\xi = k_0 N_b t \gg 1. \quad (2.21)$$

In order to estimate the rate of the coagulation process in reality, we give in Table 2 the values of a typical time τ_2 during which the average cluster size is doubled, as well as the values of the parameter ξ at this time.

2.3 Peculiarities of a cluster plasma

According to the definition, a cluster plasma is a weakly ionized gas containing clusters. Being guided below by the processes of cluster generation, we will consider a specific cluster plasma which includes a dense buffer gas and metallic clusters. These clusters can grow and evaporate, but a buffer gas does not change in the process. On the other side, a dense buffer gas prevents the metallic clusters from attaching to the walls which enclose this plasma. Next, plasma particles can destroy clusters at collisions, and such processes are not essential for clusters with large binding energies of their atoms. Therefore, we consider below a cluster plasma which consists of a dense buffer gas, usually an inert gas, and clusters of heat-resistant metals.

We mark the principal difference between a cluster plasma and a dusty plasma. In a cluster plasma, clusters grow and evaporate, and therefore even a uniform cluster plasma is

unstable with respect to the slow process of cluster growth. Clusters are less than particles of a dusty plasma (they are usually of micron size). Particles of a dusty plasma are stable and can form stable structures in external fields [69–73]. These structures are the main problem of study of dusty plasmas and their applications (see, for example, Ref. [74]). One more example of a dusty plasma is a cosmic plasma [75–77] whose investigation is connected with astrophysical problems. The structures arising in a dusty plasma are impossible for a cluster plasma because of its instability, and therefore the investigation of a cluster plasma is connected with other problems. One of these problems relates to the formation of clusters from a condensed phase, allowing one to convert a metal of a condensed phase into cluster beams and to realize in this manner the transport of large metal masses. Thus, cluster and dusty plasmas have different properties and are of interest for different applications.

It is convenient to use a cluster plasma for the generation of intense cluster beams. One can expect that the average number density of bound atoms in clusters does not exceed the number density of free atoms before formation of the clusters. If metallic clusters are formed as a result of joining free atoms, and free metallic atoms are emitted by a metallic surface, the number density of bound atoms is restricted by the number density of free atoms in a saturated vapor at the melting point, which is relatively small. In particular, Table 1 contains the number density $N_{sat}(T_m)$ of metallic atoms over a liquid surface at the saturated vapor pressure and the melting point. Evidently, if clusters are formed from free metallic atoms ejected by a metallic surface, the total number density of bound atoms does not exceed $N_{sat}(T_m)$.

This results from an equilibrium between the atoms formed and a metallic surface from which the atoms are generated. One can ignore this restriction if the atoms are produced under nonequilibrium conditions. Probably, the best method to achieve a high density of metallic atoms is the use of molecules containing metallic atoms instead of free metallic atoms. This method is implemented for generation of intense fluxes of metallic atoms and was employed first for generation of metallic clusters for a cluster light source in experiments by Scholl and his co-workers [78–81]. In particular, in experiment [78] a microwave discharge of frequencies 2.3–2.5 GHz and a power of about 100 W provided a temperature in the range of 4000–5000 K at the center of the vessel. WO_2Br_2 molecules which were injected into the discharge evaporated completely from the walls kept at a temperature of 1000 K, and these molecules were destroyed at the center of the discharge cell where tungsten clusters were formed from this time on. The clusters formed revert back to the tungsten chemical compounds near the walls of the vessel. This method is called chemical regeneration and was used for the formation of various clusters of heat-resistant metals for cluster lamps on the base of such molecules as Re_2O_7 , OsO_4 , MoO_2X_2 , TaX_5 , $TaOX_5$, NbX_5 , $NbOX_3$, HfX_4 , ZrX_4 , and TiX_4 , where X is a halogen atom [78–81]. This list testifies to the universal character of the chemical regeneration process. For definiteness, below we analyze this method for molecules MX_k , where M is the metal atom, X is the halogen atom, and k is an integer.

We first consider the chemical equilibrium of such molecules in a hot buffer gas, being guided by an arc plasma of high pressure. Under these conditions, a hot buffer gas or a dense weakly ionized gas is kept at a certain temperature that leads to a relevant distribution of components of this

molecule. We consider the total chemical equilibrium for this gaseous compound, which is described by the scheme



Along with the chemical equilibrium (2.22), equilibrium is established between the metal atoms and clusters in accordance with the scheme (2.9):



Let us introduce the binding energy per halogen atom, ε_X , so that the total binding energy of atoms in the compound MX_k is $k\varepsilon_X$, and the binding energy per atom for a bulky metal is ε_M . From these chemical equilibria, one can estimate a typical temperature T_1 at which this compound MX_k decomposes into atoms, as well as a typical temperature T_2 at which clusters are converted into atoms:

$$T_1 \approx \frac{\varepsilon_X}{\ln(N_0/[\text{X}])}, \quad T_2 \approx \frac{\varepsilon_M}{\ln(N_0/[\text{M}])},$$

or $[\text{M}] \approx N_{\text{sat}}(T_2),$ (2.24)

where $[\text{X}]$ is the total number density of free and bound atoms X , N_0 is a typical value of the atomic number density, $[\text{M}]$ is the total number density of free and bound metal atoms, and $N_{\text{sat}}(T_2)$ is the number density of atoms at the saturated vapor pressure and temperature T_2 .

From the above analysis we find that clusters exist stably in the temperature range [82–85]

$$T_1 < T < T_2, \quad (2.25)$$

where, on the one hand, molecules inserted into a hot gas decay into individual atoms, and, on the other hand, metallic atoms join in the clusters. This criterion is possible under a certain relation between the atomic binding energies. Since the formation of molecules MX_k at low temperatures is favorable energetically, the following criterion must hold true:

$$\varepsilon_M < k\varepsilon_X. \quad (2.26)$$

As a demonstration of the reality of criterion (2.26), Fig. 3 displays typical temperatures for evolution of the molecules WCl_6 in the course of formation of tungsten clusters. Note that the existence of a temperature range (2.25), where molecules MX_k are destructed and clusters M_n exist under thermodynamic equilibrium, corresponds to the criterion that follows from formulas (2.24) subject to the condition $[\text{X}] \sim [\text{M}]$:

$$\varepsilon_X < \varepsilon_M. \quad (2.27)$$

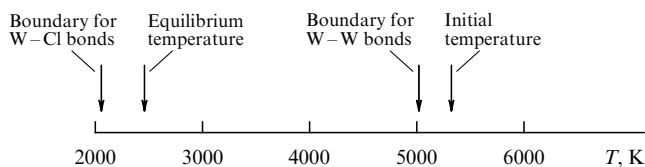


Figure 3. Typical temperatures for evolution of the metal-containing molecules WCl_6 of concentration 10% in a buffer gas (argon) at a pressure of 1 atm.

Table 3. Parameters of some compounds of heat-resistant metals at the initial number density 10^{16} cm^{-3} for the molecules MX_k . (Thermodynamic potentials per molecule are expressed in eV.)

Compound	ΔG_X	ΔG_M	ΔH_X	ΔH_M	$T_1, 10^3 \text{ K}$	$T_2, 10^3 \text{ K}$
HfCl ₄	—	6.0	4.2	6.4	(2.4)	3.15
SnCl ₄	2.1	2.8	2.6	3.1	1.2(1.5)	1.73
ThCl ₄	—	5.8	4.7	6.2	(2.6)	3.12
TiBr ₄	3.0	4.4	3.2	4.9	1.7(1.8)	2.28
TiCl ₄	3.5	4.4	3.8	4.9	2.0(2.1)	2.28
UCl ₄	3.8	5.1	4.1	5.5	2.1(2.3)	2.73
VCl ₄	3.0	4.7	3.3	5.3	1.7(1.8)	2.40
ZrCl ₄	4.3	5.9	4.8	6.3	2.4(2.7)	3.08
NbCl ₅	3.3	7.1	3.6	7.5	1.8(2.0)	3.41
NbF ₅	5.2	7.1	5.5	7.5	2.9(3.1)	3.41
VF ₅	4.1	4.7	4.4	5.3	2.3(2.5)	2.40
IrF ₆	2.2	6.4	2.5	6.9	1.2(1.4)	3.15
MoF ₆	3.9	6.3	4.2	6.8	2.2(2.4)	3.19
UCl ₆	3.0	5.1	3.3	5.5	1.7(1.8)	2.73
WCl ₆	—	8.4	3.0	8.8	(1.7)	4.04
WF ₆	4.5	8.4	4.9	8.8	2.5(2.7)	4.04

Thus, there is a temperature range where halogen-containing molecules of metals inserted in a hot buffer gas are converted into metallic clusters.

In order to reveal the reality of this possibility, we give in Table 3 the values of the above parameters. Note that the analog of the quantity ε_X is the Gibbs free energy ΔG_X of halogen molecules per atom or the enthalpy per atom ΔH_X for these molecules, and the analog of the quantity ε_M is the Gibbs free energy ΔG_M or the enthalpy per atom ΔH_M for a bulk metal. These quantities allow us to determine typical temperatures T_1 and T_2 for a given compound with an accuracy of 100–200 K for T_1 and better than 100 K for T_2 . Table 3 [41, 84–86] contains the values of T_1 obtained on the basis of ΔG_X (and on the basis of ΔH_X in parentheses), and the temperature T_2 is determined from the saturated vapor pressure of a metallic vapor. Note that only some compounds may be used for the formation of metallic clusters when they are inserted in a hot buffer gas. We do not include in Table 3 compounds for which formation of metallic clusters is not favorable thermodynamically at any temperature. Thus, though the chemical regeneration method allows us to obtain a high density of metallic atoms which are transformed later into bound atoms of clusters, this method is suitable for a restricted number of compounds.

We are coming to one more aspect of cluster behavior in a non-uniform dense buffer gas when an atomic vapor is also present in the space. Then clusters can move in the buffer gas as a result of diffusion, and we find the diffusion coefficient of the clusters within the framework of the liquid drop model. Using as we did earlier the assumption that the radius of action of atomic forces for buffer gas atoms is small in comparison with the cluster radius, we obtain that the diffusion cross section of collision between a buffer gas atom and a cluster is $\sigma = \pi r^2$, in accordance with formula (2.6). Then in the first-order Chapman–Enskog approximation, we have for the diffusion coefficient D_n of a cluster in a buffer gas [87, 88]:

$$D_n = \frac{3\sqrt{T}}{8\sqrt{2\pi m} N_a r_w^2 n^{2/3}}. \quad (2.28)$$

Here, r_w is the Wigner–Seitz radius [formula (2.2)], m is the mass of a buffer gas atom, N_a is the number density of atoms of the buffer gas, and T is the gaseous temperature. From this

Table 4. Parameters characterizing diffusion of large clusters in argon as a buffer gas. (The cluster diffusion coefficient is given by formula (2.28) for $T = 1000$ K, and Δ is defined by formula (2.33).)

Element	$D_0, \text{cm}^2 \text{s}^{-1}$	$\Delta\sqrt{N_0 N}, 10^{15} \text{cm}^{-2}$
Ti	0.91	1.59
V	1.05	3.51
Fe	1.17	2.13
Co	1.20	2.22
Ni	1.22	2.31
Zr	0.74	1.52
Nb	0.90	1.85
Mo	0.98	2.05
Rh	1.05	2.23
Pd	1.01	2.16
Ta	0.90	2.19
W	0.98	2.42
Re	1.01	2.49
Os	1.05	2.60
Ir	1.01	2.51
Pt	0.98	2.45
Au	0.93	2.32
U	0.81	2.11

we obtain the size dependence for the diffusion coefficient:

$$D_n = \frac{D_0}{n^{2/3}}, \quad (2.29)$$

and the temperature dependence is $D_n \sim \sqrt{T}$. In addition, the only dependence of the diffusion coefficient on the buffer gas parameters is that on the mass of a buffer gas atom: $D_n \sim 1/\sqrt{m}$. Table 4 gives the values of the parameter $D_n n^{2/3}$ for various metallic clusters in argon [41], if this parameter relates to the standard number density of atoms ($N_a = 2.69 \times 10^{19} \text{cm}^{-3}$), the unit mass of a buffer gas atom ($m = 1.66 \times 10^{-24} \text{g}$), and the temperature $T = 1000$ K.

Because of their large size, clusters move slowly in a space. This leads to specific phenomena in a cluster plasma. We consider the case when clusters are located in some region, while metallic atoms of number density N are distributed over a wider space. Under these conditions, atoms attach to clusters and clusters grow. On the other hand, clusters can propagate through a space as a result of diffusion. Neglecting the evaporation of clusters, we conclude that instability can occur when clusters grow faster than they can change their local positions. As a result, more mobile atoms come from all over the space and attach to the clusters, and in this way all the metal is collected in some region in the form of growing clusters.

For the analysis of this phenomenon, we use the balance equation for cluster size (2.14), which ignoring atom evaporation, takes the form

$$\frac{dn}{dt} = k_0 n^{2/3} N, \quad (2.30)$$

and the displacement of a test cluster is given by the equation

$$\frac{dx^2}{dt} = 2D_n, \quad (2.31)$$

where x is the coordinate for the cluster position along the gradients of the temperature or densities, an average is made over possible positions of the cluster, and D_n is the diffusion coefficient for a cluster consisting of n atoms in the buffer gas. Rewriting this equation in the form

$$\frac{dx^2}{dn} = \frac{2D_0}{k_0 n^{4/3} N}, \quad (2.32)$$

where we resorted to formula (2.30), we find a solution of this equation:

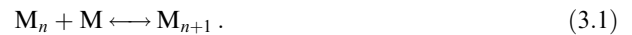
$$\overline{x^2} = \Delta^2 \left(\frac{1}{n_0^{1/3}} - \frac{1}{n^{1/3}} \right), \quad \Delta^2 = \frac{6D_0}{k_0 N}. \quad (2.33)$$

Here n_0 is the initial cluster size. As follows from this result, a cluster displacement in the course of the above processes cannot exceed a certain value. This means, on the one hand, that clusters remain in some region and, on the other hand, that growing clusters collect metallic atoms from other regions in this way. This instability [82, 41] with respect to the metal distribution in a space takes place in an inhomogeneous plasma with a temperature gradient, so that a metal is collected in the region which is favorable for the cluster's existence. Such an instability results from the cluster size dependence for both the rate of cluster growth and the cluster diffusion coefficient in a buffer gas.

3. Processes in gases and plasmas involving clusters

3.1 Equilibrium of clusters in a hot vapor

The cluster plasma under consideration consists of a dense buffer gas, clusters of a metal admixture, and an atomic metallic vapor that is found in equilibrium with clusters. Because of the high density of the buffer gas, there is a local thermodynamic equilibrium between clusters and their atomic vapor. This equilibrium is governed by processes of attachment of atoms to clusters and cluster evaporation:



In the adopted conditions, the number density N of free atoms is small compared to the number density N_b of bound atoms in clusters, which in turn is less significant than the number density N_a of buffer gas atoms, so that we have

$$N \ll N_b \ll N_a. \quad (3.2)$$

The local equilibrium established between the clusters and their atomic vapor is determined by the equality between the total rate of atom attachment to clusters and the total evaporation rate for cluster atoms. This means that the introduction of clusters into a given region of a space leads to the formation of free metal atoms in this region, and equilibrium corresponds to the equality between the rates of atom attachment to the clusters and cluster evaporation.

Let us introduce the size distribution function of clusters f_n (n is the number of cluster atoms) that is normalized by the condition

$$\int f_n n \, dn = N_b. \quad (3.3)$$

The equality between attachment and evaporation rates will lead to the relation

$$N \int k_n f_n \, dn = \int v_{ev}(n) f_n \, dn, \quad (3.4)$$

where k_n , $v_{ev}(n)$ is the rate constant of atom attachment to a cluster of $n \gg 1$ atoms and the rate of evaporation of this

cluster, respectively. In the limit of infinite cluster size, when the cluster surface is changed by a bulk surface, this equilibrium gives

$$N = N_{\text{sat}}(T), \quad (3.5)$$

where $N_{\text{sat}}(T)$ is the number density of metallic atoms at the saturated vapor pressure for a given temperature T .

We use the relation (2.11) that connects the rates of processes (3.1) due to the principle of detailed balance and for large clusters has the form [43, 44]

$$v_{\text{ev}}(n) = N_{\text{sat}}(T) k_n \exp\left(-\frac{\varepsilon_n - \varepsilon_0}{T}\right), \quad (3.6)$$

where ε_n is the atomic binding energy for a cluster consisting of n atoms, and ε_0 is the corresponding quantity for a bulk system ($n = \infty$). Modeling the cluster by a liquid drop, we have for large clusters on the basis of formula (2.4): $\varepsilon_n - \varepsilon_0 = \Delta\varepsilon/n^{1/3}$ ($\Delta\varepsilon = 2A/3$). Using formula (2.7) for the rate of atom attachment, we reduce formula (3.4) to the following expression

$$N \int n^{2/3} f_n dn = N_{\text{sat}}(T) \int \exp\left(\frac{\Delta\varepsilon}{Tn^{1/3}}\right) f_n n^{2/3} dn. \quad (3.7)$$

As follows from this formula, the equilibrium number density of free atoms near the clusters is larger than that for a bulk surface. In particular, in the case of a narrow size distribution function with an average cluster size n , this formula gives for the equilibrium number density of free atoms:

$$N = N_{\text{sat}}(T) \exp\left(\frac{\Delta\varepsilon}{Tn^{1/3}}\right). \quad (3.8)$$

If metallic clusters are injected into a buffer gas, the equilibrium between clusters and free atoms is established during a time when cluster evaporation will provide the equilibrium number density of free atoms. This system is not stable because small clusters evaporate and large clusters grow, i.e., the size distribution function f_n of clusters varies in time. Cluster growth in such a case is determined by the coalescence mechanism (see Fig. 2c). The typical time of this process leading to a change in the size distribution function is large in comparison with the typical time of establishment of this equilibrium and depends on the shape of the size distribution function f_n . Thus, the system under consideration, which includes clusters and their atomic vapor, is characterized by a certain hierarchy of times, which leads to the corresponding quasi-equilibrium in this system.

3.2 Chemical processes in a hot buffer gas

In order to reach a high metal concentration in a plasma, it is convenient to introduce a metal into a plasma in the form of metal-containing molecules. Indeed, if an atomic metal vapor is created by various methods of excitation of a metallic surface (see Fig. 4 [89]), the number density of metal atoms in the plasma does not exceed the number density of atoms at the saturated vapor pressure at the surface temperature. If we assume that the surface temperature does not exceed the metal melting point, the injection of a metal into a plasma in the form of its compound, which decays later in the plasma, increases the number density of

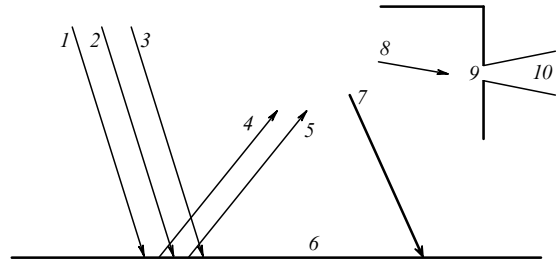


Figure 4. The mechanisms of generation of an atomic vapor as a result of excitation of the metallic surface: 1 — electron or ion beam, 2 — oven, 3 — laser, 4 — evaporation, 5 — erosion, 6 — metal surface, 7 — inverse flux, 8 — atomic vapor, 9 — nozzle or slit, 10 — metal flux.

metal atoms in the plasma by several orders of magnitude in comparison with excitation of the metallic surface. But injection of metal compounds into the plasma makes the character of the processes of formation and evolution of the metal components more complex, which requires an additional analysis. Below we consider this problem in the case where a metal is injected into a plasma in the form of molecules MX_6 , where M is a metal atom, and X is a halogen atom. This allows us to demonstrate the advantages of this method of injection of a metal component into a plasma.

Let us analyze the kinetics of decomposition of these molecules in a buffer gas. According to formulas (2.24), we have two typical temperatures T_1 and T_2 in this case, so that clusters exist below a temperature T_1 , and a chemical compound exists below a temperature T_2 . Taking the current plasma temperature in accordance with inequality (2.25) between T_2 and T_1 , we find that under equilibrium these molecules decompose, and metallic atoms are joined into clusters. But decay of these molecules is accompanied by a heat absorption that in turn decreases the rate of decay of metal-containing molecules. Below we consider the kinetics of decomposition of metal-containing molecules in a buffer gas when their concentration is enough to influence the rate of this process through a temperature decrease. It is then necessary to also account for the thermal conduction process that leads to the transport of heat from surrounding regions which do not contain these molecules.

In considering the decay of a metal-containing molecule MX_k that loses halogen atoms step by step, we use for describing this process a simple model which assumes the identical binding energies ε_X for each bond $\text{MX}_k - \text{X}$. Correspondingly, the rates of decay of molecules MX_6 and their radicals MX_k ($k = 1-5$) in collisions with buffer gas atoms are independent of k and are determined by the formula

$$v_d = N_a k_{\text{gas}} \exp\left(-\frac{\varepsilon_X}{T}\right). \quad (3.9)$$

Here, N_a is the number density of buffer gas atoms, T is the current temperature of buffer gas atoms, k_{gas} is the gas-kinetic rate constant for collisions of molecules and radicals with atoms of a buffer gas, and we assume the rate v_d to be independent of the number of halogen atoms k in the molecule or radicals. On the basis of this model, we analyze below the kinetics of destruction of metal-containing molecules in a hot buffer gas.

Under these conditions, the set of equations for the concentrations c_k of radicals with k atoms has the form

$$\begin{aligned} \frac{dc_0}{dt} &= v_d c_1, & \frac{dc_k}{dt} &= -v_d(c_k - c_{k+1}), & k &= 1-5; \\ \frac{dc_6}{dt} &= -v_d c_6. \end{aligned} \quad (3.10)$$

In the beginning, the system consists of molecules whose concentrations correspond to the following boundary conditions

$$c_6 = c_M, \quad c_k = 0, \quad k \neq 6, \quad (3.11)$$

where c_M is the total concentration of free and bound metallic atoms, and we ignore here the transport processes.

The set of equations (3.10) with the boundary conditions (3.11) can be solved analytically, and we obtain

$$c_k = c_M \frac{x^{6-k}}{(6-k)!} \exp(-x), \quad k = 1-6; \quad (3.12)$$

$$c_0 = c_M [1 - f(x)], \quad f(x) = \exp(-x) \sum_{k=0}^5 \frac{x^k}{k!}, \quad x = \int_0^t v_d dt,$$

where $f(x)$ is the part of molecules and radicals, i.e., $1 - f(x)$ is the part of free metallic atoms. Assuming a prompt cooling of the buffer gas after decomposition of molecules and radicals, we have the following balance equation for the temperature in the course of molecule destruction [89]:

$$\begin{aligned} \frac{dT}{dt} &= \delta T \sum_{k=0}^5 \left(\frac{dc_{k+1}}{dt} - \frac{dc_k}{dt} \right) = \delta T \left(\frac{dc_6}{dt} - \frac{dc_0}{dt} \right) \\ &= -v_d c_M \delta T f(x), \end{aligned} \quad (3.13)$$

where δT is the cooling temperature of the buffer gas per one percent of metal-containing molecules with respect to the number of buffer gas atoms and per one broken bond (we express the initial molecular concentration in percent).

Along with the rate of temperature variation, one can find the current temperature of a buffer gas for this character of molecular destruction. We have

$$T = T_0 - \delta T \sum_{k=0}^5 (6-k)c_k = T_0 - c_M \delta T F(x), \quad (3.14)$$

where

$$F(x) = 6 - \exp(-x) \left(\frac{x^5}{120} + \frac{x^4}{12} + \frac{x^3}{2} + 2x^2 + 5x + 6 \right). \quad (3.15)$$

Here, $F(x)$ is the number of broken bonds per molecule, $T_0 = T(0)$ is the initial temperature, and the total buffer-gas cooling temperature is defined as

$$T_0 - T(\infty) = 6c_M \delta T.$$

We ignore heat transport in this formula, so that it is valid at small c_M .

Since the binding energy ε_X of metal-containing molecules is large in comparison with a thermal energy $\sim T$, the process of molecule destruction acts strongly on the heat balance of a

buffer gas with a metal admixture in spite of the small concentration of metal-containing molecules in the buffer gas. In reality, metal-containing molecules are introduced into a narrow region, and therefore heat transport is of importance for the heat balance. Taking into account heat transport, we generalize the heat balance equation (3.13) to the form [89]

$$\frac{\partial T}{\partial t} = \chi \Delta T - v_d c_M \delta T f(x), \quad (3.16)$$

where χ is the thermal diffusivity of the buffer gas. We included in the heat balance equation heat transport due to the thermal conductivity of the buffer gas. We consider this equation when metal-containing molecules occupy a cylindrical region of radius ρ_0 in a plasma, ignoring diffusion of molecules and radicals outside this region.

For simplification of equation (3.16), we reduce it to a quasi-stationary regime when the buffer gas temperature remains to be T_0 in the region $\rho \geq \rho_0$, and T_* is the gas temperature at the center. Then equation (3.16) is replaced by

$$\frac{T_0 - T_*}{\tau_{\text{eq}}} = v_d c_M \delta T f(x), \quad \tau_{\text{eq}} = \frac{0.17 \rho_0^2}{\chi}. \quad (3.17)$$

The equation for the temperature T_* at the center of a cylinder takes the form [89]

$$T_0 - T_* = 100 N_m k_{\text{gas}} \delta T f(x) \frac{0.17 \rho_0^2}{\chi} \exp\left(-\frac{\varepsilon_X}{T_*}\right), \quad (3.18)$$

where N_m is the number density of metallic atoms at the center (by definition, $c_M = 100 N_m / N_a$), and metallic atoms join in clusters at the end of the process.

Table 5 contains parameters of compounds of metal-containing molecules [40] (ρ is the density of these compounds at room temperature, and T_m and T_b are their melting and boiling temperatures, respectively) which can be used for generating intense cluster beams. As is seen, these compounds are found in a condensed state at room temperature and are transformed into a gas of metal-containing molecules by heating. Table 5 also lists parameters

Table 5. Parameters describing evolution of metal-containing molecules in hot argon ($p = 1$ atm, $c_M = 10\%$, $\rho_0 = 1$ mm).

Compound	MoF ₆	IrF ₆	WF ₆	WCl ₆
ρ , g cm ⁻³	2.6	6.0	3.4	3.5
T_m , K	290	317	276	548
T_b , K	310	326	291	620
ε_X , eV	4.3	2.5	4.9	3.6
ε_M , eV	6.3	6.5	8.4	8.4
T_1 , K	2200	1200	2500	1700
T_2 , K	4100	4000	5200	5200
δT , K	120	37	130	48
T_0 , K	3700	6000	5000	5800
T_* , K	3600	2900	4600	4200
τ_{eq} , 10 ⁻⁵ s	12	17	8	9
τ_0 , 10 ⁻³ s	5	0.1	1	0.1
N_m , 10 ¹⁷ cm ⁻³	2.0	2.5	1.6	1.8

describing destruction of these metal-containing molecules in argon as a buffer gas under optimal conditions for the generation of intense cluster beams. In this table we take $x = 0$, i.e., $f(x) = 1$, and the buffer gas temperature is chosen in such a way that $N_m/N_{\text{sat}}(T_*) \approx 10$ for MoF_6 and WF_6 , and $N_m/N_{\text{sat}}(T_*) \approx 1000$ for IrF_6 and WCl_6 . This means that a small portion of the metal can be found in the buffer gas in the form of free atoms. We also assume that metal-containing molecules are injected at the beginning into a cylinder region of radius $\rho_0 = 1$ mm. In all the cases, the temperature is T_0 far from the center where metal-containing molecules are located, and is T_* at the center of this region. Next, we use the following formulas for the energy parameters of the compounds under consideration:

$$\delta T = -\frac{G(\text{MX}_k)}{250k}, \quad \varepsilon_X = \frac{1}{k} [-G(\text{MX}_k) + G(\text{M}) + kG(\text{X})],$$

$$\varepsilon_M = G(\text{M}), \quad k = 6, \quad (3.19)$$

where $G(Y)$ is the specific free Gibbs energy of formation of a given component Y , and $k = 6$ for these cases. We take into account that the energy for detachment of the halogen atoms is taken from the kinetic energy of the buffer gas atoms, for which the heat capacity is $c_p = 5/2$. In addition, we take the gas-kinetic cross section $\sigma_{\text{gas}} = 3 \times 10^{-15}$ cm² to be identical for various molecules and radicals and to be independent of the temperature.

Note that the temperatures T_1 in Table 5 are taken from Table 3, and they correspond to a current number density $N = 10^{16}$ cm⁻³ of halogen atoms, though this value depends on the rate of transport of halogen atoms; we recalculate here the temperature T_2 for this number density of bound metallic atoms. The criterion (2.25), namely

$$T_2 > T > T_1, \quad (3.20)$$

is satisfied for the parameters contained in Table 5, so that metal-containing molecules are decomposed in this region, while metallic atoms are joined in clusters. We have here two typical times for the process of evolution of this system. The first one, τ_{eq} , is a typical time for establishing the heat regime under consideration and it is given by formula (3.17). The second typical time, which is equal to

$$\tau_0 = \frac{6}{v_d(T_*)} = \frac{6}{N_a k_{\text{gas}} \exp(-\varepsilon_X/T_0)}, \quad (3.21)$$

is the total time for the destruction of the metal-containing molecules. Since the rate of attachment of metallic atoms to clusters is assumed to be high, this is a typical time of transformation of metal-containing molecules into metallic clusters. The values of these times are presented in Table 5. The character of the processes requires $\tau_{\text{eq}} \ll \tau_0$, and according to the data in Table 5, this inequality is fulfilled for the examples under consideration.

Thus, the heat balance of a system consisting of a dense hot buffer gas and metal-containing molecules includes heat absorption due to destruction of metal-containing molecules that is compensated for by heat transport from surrounding regions where metal atoms are absent.

3.3 Nucleation in a hot buffer gas with metal-containing molecules

We now consider the character of nucleation when metal-containing molecules are introduced into a hot buffer gas.

Then, the first stage of the evolution of this system consists in the destruction of molecules as described above. Atoms being formed are then joined in clusters. We assume the criteria (2.25) and (3.20) to be fulfilled, so that the thermodynamic equilibrium of the system corresponds to the destruction of molecules and the formation of a condensed metal. The rate of transformation of metal-containing molecules into metallic clusters in a plasma and a typical cluster size during cluster growth are determined by the kinetics of processes involving metallic atoms and clusters. In considering the evolution of the metal component, we restrict ourselves to the following scheme of the basic processes:



So, we shall deal with the stage of cluster growth when it is determined by metallic atoms originated from the destruction of molecules. We restrict ourselves only to pair processes, and, for example, the first stage of cluster growth resulting in the formation of diatomic molecules proceeds as follows



Neglecting three-body processes, we ignore the participation of buffer gas atoms in cluster growth, whereas metallic atoms, which constitute a basis of clusters, are formed in collisions of metal-containing molecules and radicals with buffer gas atoms. Next, we keep in mind that the process of cluster formation proceeds in a small region of a space occupied by a buffer gas, so that resultant free halogen atoms and molecules go out the cluster region and propagate through all the buffer gas region, whereas clusters remain in this region because of their low mobility. Thus, we neglect the role of halogen atoms in cluster growth, and though the nucleation process is considered to proceed in a uniform system, for other processes it is not uniform.

Under the above conditions, we obtain the following set of balance equations for the number density N of free metallic atoms, the number density N_{cl} of clusters, and a typical cluster size n in a uniform system [41]:

$$\frac{dN}{dt} = Q - N_{\text{cl}}k_n N, \quad \frac{dN_{\text{cl}}}{dt} = k_{\text{ch}}N^2, \quad \frac{dn}{dt} = k_n N. \quad (3.24)$$

Here, $Q = N_b v_d = N_a N_b k_d$ is the rate of formation of free metal atoms as a result of molecule destruction, so that N_a is the number density of buffer gas atoms, N_b is the number density of bound atoms at the end of molecule decomposition, v_d is the rate (3.9) of the process of destruction of metal-containing molecules and their radicals, k_n is the rate constant of atom attachment to a cluster that, according to formula (2.6), is $k_n = k_0 n^{2/3}$, and k_{ch} is the rate constant of the process of formation of a metal diatomic molecule M_2 . We consider a diatomic metallic molecule that is transformed later into a growing cluster as a nucleus of condensation, and attachment of atoms to a diatomic molecule proceeds at pair collisions (3.23), exactly like the attachment of atoms to larger molecules and clusters.

The analysis of the set of balance equations (3.24) shows that the cluster number density N_{cl} and cluster size n grow in time, while the number density N of free atoms increases in the first stage and drops in the second stage of cluster growth. Roughly, one can divide the time into three intervals, as is

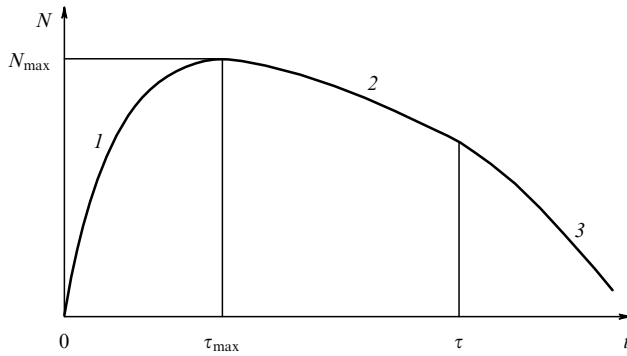


Figure 5. The time dependence of the number density of free metallic atoms in the course of formation of metallic clusters from metal-containing molecules in a buffer gas.

illustrated in Fig. 5, so that at $t \leq \tau_{\max}$ the number density of free atoms grows, and in a time $\tau \sim 1/\nu_d$ metal-containing molecules are destroyed. Note that we consider as free atoms that part of the radicals which can form metal compounds at pair collisions as in reaction (3.23).

In the second stage of the nucleation process ($\tau > t > \tau_{\max}$), we have

$$Q = N_a N_b k_d \sim N_{cl} \frac{dn}{dt} \sim k_{ch} N^2 n. \quad (3.25)$$

Assuming $k_d \sim k_{ch}$, in the second stage of the nucleation process we obtain

$$N \sim \sqrt{\frac{N_a N_b}{n}}. \quad (3.26)$$

Because of inequality (3.2), this relation holds true at large numbers of cluster atoms ($n \gg 1$). Next, from the first equation of set (3.24) at the maximum of N we have

$$\tau_{\max} \sim \frac{N}{Q} \sim \frac{N}{N_a N_b k_d}, \quad (3.27a)$$

and since by order of magnitude a typical decay time of metal-containing molecules is

$$\tau \sim \frac{1}{N_b k_d}, \quad (3.27b)$$

we arrive at the following result

$$\tau \gg \tau_{\max}. \quad (3.28)$$

This means that the time dependence of the number density N of free atoms has the form shown in Fig. 5, and the maximum of this quantity is achieved before the total destruction of metal-containing molecules. In addition, we have from the last equation of set (3.24) and relation (3.26) at the end of the nucleation process the following estimate

$$n \sim (k_0 N \tau)^3 \sim (k_0 \tau)^3 \left(\frac{N_a N_b}{n} \right)^{3/2}$$

that gives

$$n \sim (k_0 \tau)^{6/5} (N_a N_b)^{3/5} \sim \left(\frac{k_0}{k_d} \right)^{6/5} \left(\frac{N_a}{N_b} \right)^{3/5}, \quad (3.29)$$

and because each factor of the last product is large, we obtain large clusters at the end of the destruction of metal-containing molecules ($n \gg 1$).

In the same manner, using formula (3.27a) for τ_{\max} and formula (3.26), we have for a cluster size by that time:

$$n \sim \left(\frac{k_0}{n k_d} \right)^3,$$

with a consequent relationship

$$n \sim \left(\frac{k_0}{k_d} \right)^{3/4} \gg 1. \quad (3.30)$$

Since $k_0 \gg k_d$, we are dealing with large clusters at this stage of the nucleation process.

Thus, in considering the cluster growth process as a result of the decomposition of metal-containing molecules under the conditions (2.25) and (3.20), we find that this process of transformation of metal-containing molecules into metallic clusters proceeds mostly at large cluster sizes. In the course of this process, criterion (3.2) holds true, and also $N \gg N_{\text{sat}}(T)$, i.e., evaporation of clusters is a weak process, and one can ignore it. When all the metal-containing molecules have decayed, the other mechanisms of cluster growth are possible in accordance with Fig. 2. But these processes start at large cluster sizes, when the clusters contain the main part of metallic atoms.

3.4 Charging of clusters in a plasma

Let us consider the processes of the charging of clusters in a plasma. The simplest mechanism of cluster charging results from the attachment of plasma electrons and ions to the cluster surface. These processes lead to the establishment of a certain equilibrium in the plasma, such that a cluster charge creates a barrier for electrons, and resultant electron and ion currents to the cluster surface are equalized. Because of a small concentration of charged particles in the plasma under consideration, the motion of electrons and ions near a charged cluster is determined by their diffusion in a buffer gas and mobility under the action of a cluster electric field. Let a cluster be a spherical particle of a radius r_0 with a charge $-Z$ (in electron charges). Then the currents of electrons I_e and ions I_i to the cluster surface are equal to [10, 41, 90]

$$I_e = \pi r_0^2 \sqrt{\frac{8T}{\pi m_e}} N_e \exp(-x), \quad (3.31)$$

$$I_i = \pi r_0^2 \sqrt{\frac{8T}{\pi m_i}} N_i (1+x), \quad x = \frac{|Z|e^2}{r_0 T}.$$

We rely on the Maxwell energy distribution function for electrons and ions with a gaseous temperature T , and assume the cluster radius r_0 to be small in comparison with the mean free paths of electrons and ions in a buffer gas. Here, m_e and m_i are the electron and ion masses, e is the electron and ion charge, N_e and N_i are the electron and ion number densities, and we consider here a quasi-neutral plasma: $N_e = N_i$. Then the equilibrium cluster charge follows from the relation [10, 90]

$$|Z| = \frac{r_0 T}{e^2} \ln \left[\sqrt{\frac{m_i}{m_e}} \left(1 + \frac{|Z|e^2}{r_0 T} \right) \right]. \quad (3.32)$$

Table 6. Parameters of the electron current for thermoemission of metals (W is the metal work function, T_b is the boiling point, and i_b is the current density at the boiling point) [90, 92].

Metal	A_R , A (cm ² K ²) ⁻¹	W , eV	T_b , K	i_b , A cm ⁻²
Mo	51	4.3	5070	8.8×10^4
Nb	57	4.0	5170	2.1×10^5
Pd	60	4.8	3830	240
Re	720	5.0	5870	2.3×10^6
Ta	55	4.1	5670	3.3×10^5
Th	70	3.3	4470	2.2×10^5
Ti	60	3.9	3280	750
W	75	4.5	5740	2.8×10^5
Y	100	3.3	3478	3.5×10^3
Zr	330	3.9	4650	2.4×10^5

Note that this mechanism of cluster charging leads simultaneously to the effective recombination of electrons and ions in a plasma, i.e., clusters in a plasma serve as traps for electrons and ions.

The other process of the cluster charging is thermoemission of electrons from the cluster surface. For a plane surface of a metallic particle and the Fermi–Dirac energy distribution of electrons, the thermoemission current density of electrons is given by the formula

$$i_{th} = \frac{em_e T^2}{2\pi^2 \hbar^2} \exp\left(-\frac{W}{T}\right), \quad (3.33)$$

where W is the work function of a metallic surface, i.e., the electron binding energy. This formula can be reduced to the Richardson–Dushman formula [91–93]

$$i_{th} = A_R T^2 \exp\left(-\frac{W}{T}\right). \quad (3.34)$$

Here A_R is the Richardson parameter. According to formula (3.33), its value is $A_R = 120$ A (cm² K²)⁻¹, and Table 6 gives the values of this parameter for some heat-resistant metals.

If the thermoemission current is induced from the surface of a charged cluster which is assumed to be similar to a spherical bulk particle, formula (3.33) is transformed to [10]

$$i_{th} = \frac{em_e T^2}{2\pi^2 \hbar^2} \exp\left(-\frac{W}{T} - \frac{Ze^2}{r_0 T}\right). \quad (3.35)$$

We assume in this formula that an electron release from the cluster surface proceeds similarly to this process near the plane surface, but in the case of a charged cluster a removed electron must overcome the electric potential of cluster attraction.

Because the thermoemission current does not depend on the number density of plasma electrons, and the current of attaching electrons and ions is proportional to this quantity, the thermoemission character of cluster charging dominates at low electron number densities. Hence, there is an equilibrium number density N_{em} of electrons for a given temperature at which the thermoemission electron current is equal to the current of electron attachment to the cluster surface. The equilibrium cluster charge is zero at this electron number density, while it is negative for higher N_e and is positive for smaller N_e at a given temperature.

A thermoemission current charges a metallic cluster positively, and it can be taken into account if the thermoemission current from the cluster surface $4\pi r_0^2 i_{th}$ is comparable with the current I_i of ion attachment. Let us consider the limit of low number densities of plasma electrons and ions,

when a positive cluster charge is determined by the thermoemission current. In this limit

$$i_{th} \geq \sqrt{\frac{8T}{\pi m_i}} N_i, \quad (3.36)$$

so that the equilibrium cluster charge is established as a result of the thermoemission process and the attachment of plasma electrons to the cluster surface. The cluster charge is then negative at large electron number densities and is positive at low electron number densities. It becomes zero if

$$i_{th} = \sqrt{\frac{8T}{\pi m_e}} N_e. \quad (3.37)$$

Because for $T \ll W$ the thermoemission current density according to formulas (3.33) and (3.34) depends monotonically on the temperature, there is a neutralization temperature T_n for each electron number density, so that the cluster charge is zero at this temperature. The neutralization temperature is defined by formula (3.37), and its dependence on the electron number density for molybdenum and iridium is depicted in Fig. 6. Table 7 contains the values of the neutralization temperature for the electron number density $N_e = 10^{13}$ cm⁻³.

In the limit of low electron number densities we obtain

$$i_{th} \geq \sqrt{\frac{8T}{\pi m_e}} N_e, \quad (3.38)$$

and a cluster is charged positively. We assume that the thermoemission process near the cluster surface does not depend on the cluster charge, but if the energy of a releasing electron is small, it cannot be removed from the cluster and is captured by its electric field. In this limit, based on formula (3.37) for the balance of currents to the cluster surface and using formula (3.33) for the thermoemission current density, if the cluster charge is relatively small, instead of formula (3.32) for the cluster charge we arrive at [68, 10, 41]

$$\begin{aligned} Z &= \frac{r_0 T}{e^2} \ln \left[\sqrt{\frac{\pi m_e}{8T}} \frac{i_{th}}{N_e} \right] \\ &= \frac{r_0 T_e}{e^2} \left\{ \ln \left[\frac{2}{N_e} \left(\frac{m_e T}{2\pi \hbar^2} \right)^{3/2} \right] - \frac{W}{T} \right\}. \end{aligned} \quad (3.39)$$

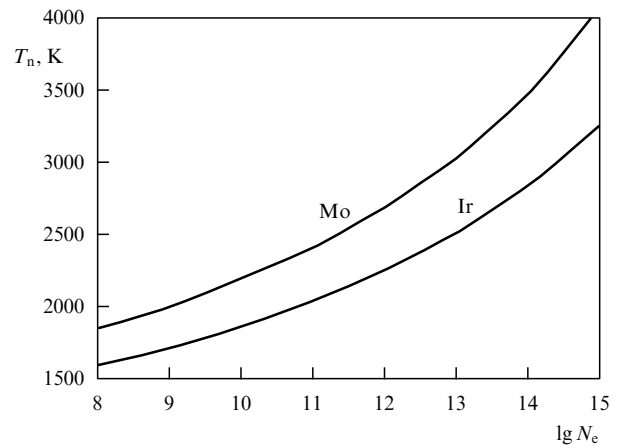


Figure 6. The neutralization temperature T_n for molybdenum and iridium clusters. For a given electron number density, the thermoemission current from the cluster surface is equal to the current of the attaching electrons.

Table 7. Parameters of charged metallic clusters.

Element	W , eV	T_n , 10^3 K	$Z_{Ar}/n^{1/3}$	k_* , 10^{-8} $\text{cm}^3 \text{s}^{-1}$	$Z_{cr}/n^{1/2}$	$\varphi_{cr}/n^{1/6}$, V
Ti	3.92	2.51	0.084	1.7	1.4	12
V	4.12	2.63	0.078	1.5	1.4	13
Fe	4.31	2.75	0.074	1.3	1.2	12
Co	4.41	2.82	0.073	1.3	1.2	12
Ni	4.50	2.87	0.072	1.3	1.2	12
Zr	3.9	2.51	0.093	2.1	1.6	12
Nb	3.99	2.57	0.085	1.7	1.6	14
Mo	4.3	2.74	0.081	1.6	1.6	14
Rh	4.75	3.00	0.078	1.5	1.4	13
Pd	4.8	3.04	0.080	1.5	1.3	11
Ta	4.12	2.65	0.085	1.7	1.7	14
W	4.54	2.90	0.081	1.6	1.6	14
Re	5.0	3.12	0.080	1.5	1.7	16
Os	4.7	3.01	0.078	1.5	1.6	15
Ir	4.7	3.03	0.080	1.5	1.6	15
Pt	5.32	3.38	0.081	1.6	1.4	13
Au	4.30	2.85	0.083	1.9	1.2	10

Averages 2.8 ± 0.2 0.080 ± 0.005 1.6 ± 0.2 1.4 ± 0.2 13 ± 2

Note. Here, W is the metal work function, T_n is the temperature at which the average cluster charge is zero in accordance with formula (3.37), Z_{Ar} is the average cluster charge according to formula (3.39) at a temperature of 1000 K for argon as a buffer gas, the rate constant k_* is defined by formula (3.47), and the parameters Z_{cr} and φ_{cr} are given by formulas (3.51) and (3.52), respectively.

We assume here that the number density N_e of plasma electrons does not depend on the presence of clusters in the plasma, i.e., we are dealing with the equilibrium conditions for an individual cluster in the plasma.

We now consider the equilibrium between plasma electrons and a cluster charge when the thermodynamic equilibrium is sustained by processes



and we find the distribution of clusters over charges. Introducing the probability $P_Z(n)$ for a cluster consisting of n atoms and having a charge Z , and assuming the temperatures of bound electrons in metallic clusters and free plasma electrons to be identical, we use the Saha formula for ionization equilibrium [51, 90]:

$$\frac{P_Z(n)N_e}{P_{Z+1}(n)} = 2 \left(\frac{m_e T}{2\pi\hbar^2} \right)^{3/2} \exp \left[-\frac{I_Z(n)}{T} \right], \quad (3.41)$$

where $I_Z(n)$ is the ionization potential of the cluster consisting of n atoms and having a charge Z . In this approximation, the cluster ionization potential is equal to

$$I_Z(n) = W + \frac{Ze^2}{r_0}. \quad (3.42)$$

Introducing the average cluster charge through the relation $P_Z(n) = P_{Z+1}(n)$, we have [10, 68]

$$\bar{Z} = \frac{Tr_0}{e^2} \left\{ \ln \left[\frac{2}{N_e} \left(\frac{m_e T}{2\pi\hbar^2} \right)^{3/2} \right] - \frac{W}{T} \right\}. \quad (3.43)$$

This formula coincides with formula (3.39), which is obtained by another method.

Under equilibrium conditions, the charge of clusters located in a weakly ionized gas depends on the electron

temperature of this plasma (or the mean energy of electrons), and also on the electron number density. If an ionization equilibrium (3.40) is established between the clusters and the plasma, the relation for the number densities of clusters of different charges is given by the Saha formula (3.41). From this formula it follows that at high electron temperatures clusters are charged positively, while at low electron temperatures they can have a negative charge. In particular, let us find plasma parameters where, in accordance with experiment [94], 80% of clusters formed Cu_{1000} have a unit negative charge, and 20% of these clusters are neutral. Using the Saha formula (3.41) and values of the electron affinities for clusters, we find that such a situation takes place at the electron temperature 2800 K, if the electron number density is $N_e = 10^{13} \text{ cm}^{-3}$; this also corresponds to the electron temperature of 2510 K, if $N_e = 10^{12} \text{ cm}^{-3}$, and the electron temperature is 2250 K for the electron number density $N_e = 10^{11} \text{ cm}^{-3}$. Note that the cluster temperature is usually less than the electron temperature.

Let us consider the other limiting case when plasma electrons are produced from clusters. For simplicity, we assume the clusters to have an identical number of atoms n . In this limit, an equilibrium (3.37) yields

$$N_e = ZN_{cl}, \quad (3.44)$$

where N_{cl} is the number density of the clusters. Let us introduce the rate v_{th} of electron emission as a result of thermoemission from the cluster surface:

$$v_{th} = 4\pi r_0^2 i_{th} = v_0 n^{2/3}, \quad v_0 = 4\pi r_W^2 i_{th}, \quad (3.45)$$

where r_0 is the cluster radius, r_W is the Wigner–Seitz radius, and v_0 is the reduced electron emission rate. The temperature dependences for the reduced emission rates v_0 are given in Fig. 7 for molybdenum and iridium clusters. The cluster charge in this limiting case is equal to

$$Z = \frac{v_0}{N_{cl}k_e}, \quad k_e = \pi r_W^2 \sqrt{\frac{8T}{\pi m_e}}. \quad (3.46)$$

As can be seen, in this limit the cluster charge Z does not depend on its size. The parameter k_e depends weakly on the cluster material. In particular, for clusters of Mo, Rh, W,

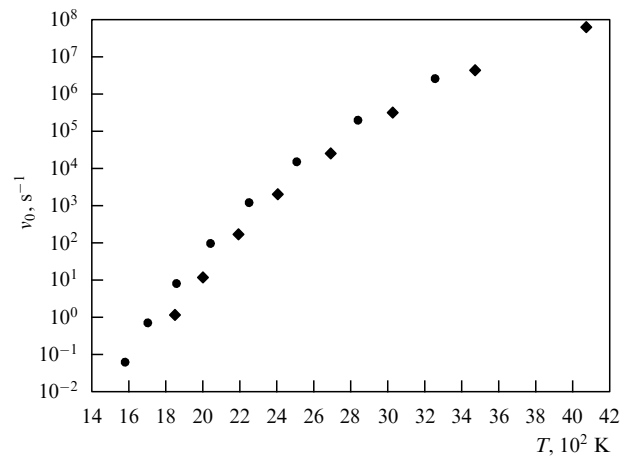


Figure 7. The temperature dependence of the reduced emission rate $v_{em}n^{-2/3}$ for thermoemission of molybdenum (●) and iridium (○) clusters.

Re, Os, or Ir the average value of the Wigner–Seitz radius (see Table 1) is $r_W = 1.58 \pm 0.02 \text{ \AA}$, so that at the temperature $T = 3000 \text{ K}$ we have for clusters of these metals: $k_e = (2.67 \pm 0.07) \times 10^{-8} \text{ cm}^3 \text{ s}^{-1}$. Let us represent the rate constant k_e in the form

$$k_e = k_* \left(\frac{T}{1000} \right)^{1/2}, \quad (3.47)$$

where k_* is the same rate constant at the temperature of 1000 K. Table 7 contains the values of k_* for some metallic clusters. Note that the parameters of Table 7 are found in a narrow range, and we give in Table 7 statistically averaged values of the parameters for the cases under consideration.

3.5 Charging of clusters by electron impact

Usually in generating cluster beams, when a cluster beam passes through a nozzle, the beam is crossed by an electron beam, and the clusters are charged as a result of ionization of the clusters by electron impact. A formed beam of charged clusters is governed by electric fields. Therefore, the character of cluster ionization by electron impact is of interest, and we will find below the cross section of cluster ionization by electron impact. For simplicity, we assume that each contact of an incident electron with the cluster surface leads to electron release, so that the cross section of ionization of a neutral cluster by electron impact is equal to πr_0^2 , where r_0 is the cluster radius. If a cluster is charged positively, an incident electron of energy ε has the energy $\varepsilon + Ze^2/r_0$ near the cluster surface, and a releasing electron is removed from the cluster if its energy exceeds Ze^2/r_0 (Z is the cluster charge). We find the cross section of cluster ionization by electron impact by assuming the statistical character of the distribution of scattered electrons over energies near the cluster surface. Because in this case the probability of an electron having an energy in the range from ε to $\varepsilon + d\varepsilon$ is proportional to $\varepsilon^{1/2} d\varepsilon$, the ionization cross section σ_{ion} within the framework of this model equals

$$\sigma_{\text{ion}} = \sigma_{\text{cap}} \frac{\int_{Ze^2/r_0}^{\varepsilon} (\varepsilon')^{1/2} d\varepsilon' \int_{Ze^2/r_0}^{\varepsilon - \varepsilon' + Ze^2/r_0} (\varepsilon'')^{1/2} d\varepsilon''}{\int_0^{\varepsilon + Ze^2/r_0} (\varepsilon')^{1/2} d\varepsilon' \int_0^{\varepsilon - \varepsilon' + Ze^2/r_0} (\varepsilon'')^{1/2} d\varepsilon''},$$

where the cross section σ_{cap} of electron contact with the cluster surface in electron–cluster collisions is given by

$$\sigma_{\text{cap}} = \pi r_0^2 \left(1 + \frac{Ze^2}{r_0 \varepsilon} \right).$$

We take into consideration that near the cluster surface the energy of an incident electron equals $\varepsilon + Ze^2/r_0$, if ε is the energy of an electron far away from the cluster.

Thus within the framework of this model, we have for the reduced cross section of ionization of a charged cluster by electron impact:

$$\frac{\sigma_{\text{ion}}}{\pi r_0^2} = \frac{16(1+x)}{\pi x^4} \int_1^x y^{1/2} [(x+1-y)^{3/2} - 1] dy, \quad (3.48)$$

$$x = \frac{\varepsilon r_0}{Ze^2} \geq 1.$$

For simplicity, we suppose the metal work function W to be small in comparison with Ze^2/r_0 . According to these formulas, the maximum cross section is equal to $1.29\pi r_0^2$ and

corresponds to the collision energy $4.7Ze^2/r_0$. The ionization cross section (3.48) is approximated by the dependence

$$\frac{\sigma_{\text{ion}}}{\pi r_0^2} = 1.2 \{ 1 - \exp[-1.5(x-1)] \}, \quad 1 < x < 12. \quad (3.49)$$

As follows from the above results, electrons of a given energy can ionize the cluster up to a charge $Z < \varepsilon r_0 / e^2$. Therefore, one can govern the cluster charge in a beam using a suitable electron energy of the electron beam.

Since the cluster charge creates a strong tension inside the cluster, the value of the charge is restricted, and the limiting cluster charge that leads to cluster destruction depends on the binding energies of the atoms in the cluster. Modeling a cluster by a liquid drop and assuming its charge to be spread over the surface, we can find the limiting charge as the threshold of the Rayleigh instability, when the surface tension energy $4\pi r_0^2 \gamma = An^{2/3}$ (γ is the surface tension) averts the cluster from destruction due to the Coulomb interaction $Z^2 e^2 / (2r_0)$ of elementary charges. This gives the limiting cluster charge as the threshold of the Rayleigh instability due to small deformations of the liquid cluster [95]:

$$Z_{\text{cr}} = \left(\frac{16\pi\gamma r_0^3}{e^2} \right)^{1/2} = \left(\frac{4Ar_W n}{e^2} \right)^{1/2}. \quad (3.50)$$

Since there are various versions of the Rayleigh instability [95–97], the numerical coefficient of this formula may differ slightly from the value given above. Using the limiting sizes of krypton and xenon clusters for the critical cluster charges $Z = 2–4$ according to measurements [98–102], we represent this formula in the form

$$Z_{\text{cr}} = \left(\frac{5Ar_W n}{e^2} \right)^{1/2} \times (1.00 \pm 0.06). \quad (3.51)$$

We consider in these formulas the limiting cluster charge Z_{cr} as a continuous variable. Table 7 contains values of the reduced critical charge for some large metallic clusters.

Note that the electric potential on the cluster surface, induced by its critical charge $\varphi_{\text{cr}} = Z_{\text{cr}} e / r_0$, depends weakly on the cluster size. According to formula (3.50), this electric potential is equal to

$$\varphi_{\text{cr}} = \frac{Z_{\text{cr}} e}{r_0} = \left(\frac{5A}{r_W} \right)^{1/2} n^{1/6}. \quad (3.52)$$

Table 7 lists the values of the parameter $\varphi_{\text{cr}} / n^{1/6}$ for some metallic clusters, and these values are found in a narrow range for various metals.

A crossing electron beam, which charges the clusters in a cluster beam as a result of collisional ionization, can lead simultaneously to the destruction of large clusters. Therefore, the electron beam can influence the cluster size. We have the following balance equation for the cluster charge Z if it is created by an electron beam:

$$\frac{dZ}{dt} = \sigma_{\text{ion}} J,$$

where σ_{ion} is the cross section of cluster ionization by electron impact, and J is the intensity of the electron beam (the number of incident electrons per unit area and per unit time). Taking the ionization cross section as $\sigma_{\text{ion}} = \pi r_0^2$, where r_0 is the cluster radius, we have for the cluster charge by the time t , if

cluster charging is determined by this ionization process:

$$Z = \frac{t}{t_0} n^{2/3}, \quad (3.53)$$

where t_0 stands for a value which is identical for clusters of any size. From this it follows that the critical charge (3.50) is achieved firstly for large clusters, and then large clusters are destructed. Hence, cluster charging by an electron beam as a result of cluster ionization leads to a change in the size distribution function of clusters because of destruction of large clusters. Note that the ionization process is permitted if the electron energy in the beam exceeds the value of $e\varphi_{cr}$ [see formula (3.52), and Table 7].

4. Methods of generation of cluster beams

4.1 Basic methods of generation of cluster beams

Clusters as physical objects occupy an intermediate place between atoms and molecules, on the one hand, and condensed systems, on the other hand. Clusters are thermodynamically nonequilibrium systems, and their evolution over a long time period leads to the formation of a gaseous phase as a result of cluster evaporation or to the formation of a condensed phase through the joining of clusters. Clusters have a high reactivity, so that contact between two clusters leads to their joining, and the properties of the incident clusters are lost in the resulting cluster. Therefore, clusters are used in the form of beams where they are separated and therefore conserved in beams. Among the applications of cluster beams is the manufacturing of thin films as a result of cluster deposition on a target and the fabrication of new materials as a result of simultaneous deposition of an amorphous target and a beam of solid clusters. It is convenient to transport a metal by means of cluster beams. Therefore, cluster beams constitute the most widespread form of cluster applications. Table 8 lists the basic methods for generating cluster beams and their peculiarities, and we will briefly analyze these methods.

One can divide the methods of cluster generation into two groups according to the character of material transformation into the clusters. In the first case, clusters are formed as a result of the destruction of an original material with the direct formation of clusters. An example of such a method is the formation of clusters through the bombardment of an object by fast ions, where destruction of the target is accompanied by the formation of fragment-clusters. Another example of this type is the sputtering of a liquid with the formation of small liquid drops or aerosols. In the case of methods of the second group of cluster generation, a target is transformed into atoms (or molecules) at the first stage of the process of cluster generation, and then clusters are formed from free atoms. At the second stage of such a cluster generation, expansion of a gas or vapor through a nozzle into a vacuum is used, and the condensed phase is a thermodynamically

stable state of a system of atoms at the end of the expansion process. Transformation of an atomic vapor or gas into a condensed phase through the formation of clusters does not lead to formation of a stationary state, since clusters are not stable thermodynamically and have a tendency to increase in size as a result of the coagulation or coalescence processes (see Fig. 2). Nevertheless, clusters can have a fairly large lifetime in a gas or in a cluster beam.

Generation of clusters as a result of the bombardment of a target with ions of keV energies [103–113] is based on the fact that collisions of fast ions with a surface lead to the formation of different fragments, which include clusters, as well as atoms and molecules. Clusters resulting from ion impact with a surface can acquire a charge, which allows one to separate the clusters and accelerate them. Cluster beams formed in this way are characterized by a small size and low beam intensity. This method is used for the generation of selective beams of small clusters for research applications.

Other methods of generating cluster beams from a vapor or a gas are based on the transformation of an excess of an atomic gas or vapor into a condensed phase when the vapor pressure exceeds the saturated vapor pressure at a given temperature. As this takes place clusters are formed in nucleation processes and grow in time. Through infinite time they would be transformed into a condensed phase, but the process of cluster growth finishes due to vapor expansion. A cluster beam is then formed as a result of the evolution of an expanding vapor. There are various methods for the formation of an expanding vapor depending on the cluster material and output parameters of the cluster beam. An oven is used for fusible metals, so that an atomic vapor forming in the oven expands through a nozzle into a vacuum together with a buffer gas. The cooling of this mixture during expansion causes nucleation of the vapor and formation of clusters. This method provides for the generation of fairly intense cluster beams which are deposited onto a substrate for the production of thin films (for example, see Refs [114–118]). In the case of heat-resistant metals, a laser beam is employed to evaporate them and form free atoms [119–124]. The atoms evaporated are mixed with a flow of the buffer gas, and the subsequent expansion of the mixture leads to the formation and growth of clusters.

Along with these methods, mixed methods of cluster generation are possible. As an example, we describe the cluster aggregate source [125, 126] for cluster generation. In the first stage of the aggregation process, clusters of rare gases (for example, argon clusters) are formed as a result of the adiabatic expansion of the gas through a small orifice (300 μm in diameter). These clusters are injected into a scattered chamber where the material of resultant clusters (for example, NaCl) is evaporated in a resistively heated oven. Molecules produced in these conditions are captured by rare gas clusters and finally evaporate them. As a result, molecular clusters are formed, which may or may not contain rare gas atoms, depending on the conditions of aggregation. In this

Table 8. Methods for generating cluster beams and their peculiarities.

Method	Material	Peculiarities
Bombardment of a target with keV-ions	—	Small-sized clusters, low intensity
Free jet expansion of a vapor from an oven	Low-evaporated	Moderate cluster size and intensity
Laser evaporation and free jet expansion	Heat-resistant	Low intensity
Free jet expansion of a vapor after erosion of electrodes	Electrode material	Moderate cluster size and intensity
Nucleation in a dense plasma	Heat-resistant	Large-sized clusters, high intensity

way one can transform clusters of rare gas atoms into molecular clusters.

Comparison of the two groups of methods of cluster generation shows that the first is simpler because it provides for direct cluster formation from a condensed system. But one can control the cluster sizes in the second case, and cluster beams can have a higher intensity. Hence, these methods of cluster generation, when a vapor or gas is formed at the first stage of cluster growth, are preferable in practice, especially in the case of material decomposition into atoms or molecules in the first stage of the process, and later these atoms or molecules are joined in growing clusters. Below we shall focus on such methods of cluster generation.

4.2 Laser generation of metallic atoms and clusters

Figure 4 illustrates various methods for the excitation of a metallic surface in the generation of atoms. The number density of atoms in a space near the surface then does not exceed the atomic number density at the saturated vapor pressure for the surface temperature, and the coincidence of these quantities corresponds to equilibrium between the formed vapor and surface. If we assume that the surface loses stability at melting, i.e., the surface temperature does not exceed the metal's melting point, the number density of metallic atoms in the space does not exceed the number density of atoms in the saturated vapor at the surface temperature. For most metals this limit gives relative vapor pressures, but this restriction can be escaped if evaporation of atoms proceeds under nonequilibrium conditions. This situation takes place for the laser method of cluster generation [119–124], and a typical scheme for such a method is depicted in Fig. 8. A focused laser beam directed to a metallic surface then causes generation of an atomic beam that is mixed with a buffer gas flow. After an expansion of this mixture its temperature decreases, and metallic atoms are joined in metallic clusters. We now consider the first stage of this process, when an atomic beam arises from a spot irradiated by a laser beam.

There are various regimes of interaction of a laser beam with a surface [127–129]. Because absorption by a surface depends on its temperature, which in turn depends on thermal processes on the surface, a self-consistent character of interaction of laser radiation with the surface can lead to a specific structure of thermal distributions over the surface

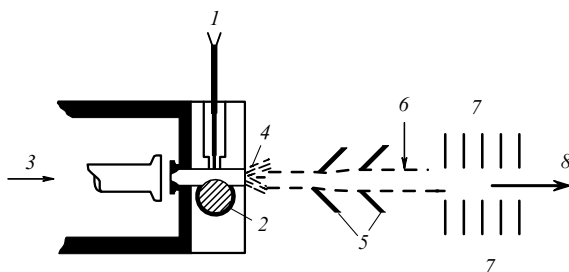


Figure 8. Schematic of a cluster generator on the basis of the laser method: 1 — laser beam; 2 — rod-target; 3 — flow of a buffer gas; 4 — stream of a buffer gas and clusters after the nozzle; 5 — skimmers; 6 — crossing electron beam; 7 — ion optics and accelerator; 8 — emergent cluster beam. Atoms of a metallic vapor are formed as a result of laser irradiation of a metallic rod, then the atoms are transformed into clusters as a result of expansion in a cold buffer gas and expansion of the mixture formed into a vacuum.

[130–132]. In the case under consideration, a laser beam is focused upon a small spot on the surface, and the character of absorption and heat balance is more or less uniform across this spot. As a result, a gasdynamic stream of metallic atoms is formed near an irradiated spot on the surface. Along with atoms, electrons are produced, and their density increases sharply with an increase in the power of the laser beam propagated to the surface. Interaction of the formed electrons with the laser beam through bremsstrahlung leads to an increase in the electron energy and therefore can cause a breakdown of the atomic beam formed [133, 134, 129]. As a result of this process, laser radiation is absorbed by electrons and does not reach the surface, and the threshold of this instability for the specific laser power lies above 10^7 W cm^{-2} [133, 134, 129], if the laser pulse duration amounts to $\sim 10^{-6} - 10^{-5} \text{ s}$, and the size of the irradiated spot is $\sim 10 - 100 \mu\text{m}$. Below we consider such a regime of this process [127, 135, 136] when an absorbed laser energy is consumed mostly by evaporation of atoms, and the evaporated atoms form a gasdynamic stream. Note that because of a high density of evaporated atoms, fractal aggregates, namely bound solid clusters of a sparse structure, can be formed in this regime [137–142], i.e., solid clusters can form sparse bound structures.

We consider this process under the simplest conditions, when the vapor pressure in the stream significantly exceeds the pressure of the buffer gas, and since the angle of divergence of a stream is usually $5 - 15^\circ$ [143], we assume the stream to be cylindrical near the surface. In this regime, we arrive at the heat balance equation

$$P_{\text{abs}} = j(\epsilon_0 + 2T_{\text{sur}}), \quad (4.1)$$

where P_{abs} is the specific absorbed laser power, j is the atomic flux from the surface, ϵ_0 is the metal binding energy per atom, and T_{sur} is the surface temperature. We make use of the semi-Maxwell velocity distribution function of evaporated atoms near the surface and the expression in the parentheses of this formula defines the average energy consumed per one released atom. Because the beam pressure exceeds the buffer gas pressure, a formed stream under the adiabatic character of beam generation moves with the velocity of sound, which is $u = (\gamma T_b/m)^{1/2}$, where γ is the ratio of the specific heat capacities at a constant pressure and volume, and this constant is $5/3$ for an atomic gas. Introducing the probability $\zeta(T_{\text{sur}})$ of atom attachment to the surface at a given temperature in the case of their contact, on the basis of the principle of detailed balance we obtain the atomic flux from the surface in the form

$$j(T_{\text{sur}}) = \zeta(T_{\text{sur}}) \times \frac{1}{4} \sqrt{\frac{8T_{\text{sur}}}{\pi m}} N_{\text{sat}}(T_{\text{sur}}), \quad (4.2)$$

where $N_{\text{sat}}(T)$ is the number density of atoms at the saturated vapor pressure for a given temperature.

The semi-Maxwell distribution function of atoms over velocities at the surface is transformed into the distribution function of beam atoms, and assuming that the atoms of a beam do not return to the surface, we have the following balance equations which connect the parameters of the atomic distribution at the surface and in the beam:

$$j = uN_b, \quad 2T_{\text{sur}} = \frac{mu^2}{2} + \frac{5}{2} T_b. \quad (4.3)$$

Table 9. Parameters characterizing atomic evaporation from a metallic surface under the action of a laser pulse with the specific power of 10^7 and 3×10^6 W cm $^{-2}$ (in parentheses). (The data were obtained on the basis of formulas (4.1)–(4.4) and from data in Table 1 under the assumption that 30% of the laser energy is absorbed by the surface and the sticking probability is $\zeta(T_{\text{sur}}) = 1$.)

Metal	Cu	Mo	Ag	W	Ir
$T_{\text{sur}}, 10^3$ K	3.6 (3.2)	5.9 (5.3)	3.8 (3.3)	7.3 (6.7)	5.8 (5.3)
$N_{\text{sur}}, 10^{19}$ cm $^{-3}$	5.3 (1.7)	2.8 (0.89)	46 (15)	2.6 (0.81)	3.9 (1.2)
$p_{\text{sur}},$ atm	26 (7.4)	22 (6.4)	240 (68)	26 (7.4)	31 (8.9)
$T_{\text{b}}, 10^3$ K	2.5 (2.2)	4.0 (3.7)	2.6 (2.3)	5.0 (4.6)	4.0 (3.7)
$N_{\text{b}}, 10^{19}$ cm $^{-3}$	1.3 (0.42)	0.70 (0.22)	11 (3.8)	0.64 (0.20)	0.96 (0.31)
$p_{\text{b}},$ atm	4.5 (1.3)	3.8 (1.1)	41 (12)	4.4 (1.3)	5.3 (1.5)
$p_{\text{sat}}(T_{\text{b}}),$ atm	0.19 (0.03)	0.08 (0.01)	0.32 (0.05)	0.054 (0.009)	0.09 (0.015)
$J,$ g (cm 2 s) $^{-1}$	490 (150)	410 (120)	5700 (1800)	580 (180)	800 (240)
$\sigma T_{\text{sur}}^4/P_{\text{abs}}, 10^{-3}$	0.32 (0.69)	2.2 (5.1)	0.18 (0.39)	5.3 (12)	2.2 (5.0)
G	560 (1700)	1300 (3900)	310 (920)	1100 (3500)	650 (2000)
\bar{n}	43 (96)	80 (180)	27 (62)	73 (170)	48 (110)
$u\tau_{\text{cl}}, \mu\text{m}$	12 (49)	24 (97)	4.9 (20)	25 (100)	15 (61)

We make use of the Maxwell distribution function of atoms in a beam, and then T_{b} is the temperature of these atoms, N_{b} is their number density in the beam. The balance between the fluxes of atoms and energy near the surface (4.3) leads to the following relationships between the parameters of the atomic vapor before and after formation of an atomic beam [129, 135, 136]:

$$T_{\text{b}} = 0.69T_{\text{sur}}, \quad N_{\text{b}} = 0.25N_{\text{sur}}. \quad (4.4)$$

This velocity distribution function in a beam is established as a result of collisions between atoms, so that the transfer from the surface to a beam proceeds at distances of the order of the mean free path λ for atoms. Evidently, this one-dimensional scheme is valid if the radius r of an irradiated spot on the surface exceeds significantly the mean free path λ of atoms, i.e., this regime does not relate to low laser powers. Table 9 demonstrates the character of this regime of atomic generation for some metals, which relates to high local intensities J of atomic fluxes. Note that in these cases the typical mean free path of atoms is $\lambda \sim 0.1 - 1 \mu\text{m}$. Table 9 also gives the ratio of the specific radiation power σT^4 (σ is the Stephan–Boltzmann constant) at the surface temperature (if this surface emits as a blackbody) to the absorbed specific power P_{abs} . As can be seen, thermal emission of the surface makes a small contribution to the heat balance.

We note the peculiarity of the nucleation process in this regime of laser irradiation of a metallic surface. As a result of transformation of a surface vapor into an atomic beam, the vapor temperature decreases, and the vapor pressure in the beam can become lower than the saturated vapor pressure $p_{\text{sat}}(T_{\text{b}})$ at the beam temperature, whose values are given in Table 9. The excess of atoms is then converted into clusters whose parameters are given by formula (2.18), and τ_{cl} is the time of this transformation, $\tau_{\text{cl}}u$ is the distance from the surface where the clusterization process finishes, the parameter G is given by formula (2.16), and \bar{n} is the average cluster size at the end of the transformation of atoms into clusters. We do not account for the influence of heat release as a result of the nucleation process on gasdynamical parameters of the atomic beam.

The laser method of cluster generation is of a pulse nature, and a laser beam cannot act on a cluster beam because in the opposite case laser radiation acts on clusters and leads to their decomposition and the heating of the beam, so that the atomic temperature increases and the beam decays. Of course, one can suggest a continuous version of laser generation of clusters, where a laser beam takes a small angle with the surface, but then other troubles occur. Next, the size of the irradiated spot on the surface and, correspondingly, the beam diameter are restricted, allowing us to escape convection in the beam. Under these conditions, the atomic beam and, subsequently, the cluster beam are formed in the nonequilibrium conditions, providing a relatively large metal flux J in this case. But because of the pulse character of the laser beam and the small beam size, the laser method does not give high rates of metal transport. Note the role of the buffer gas which carries clusters from the region of the laser action and takes the excess heat as a result of nucleation processes. In addition, the buffer gas promotes subsequent cluster growth.

4.3 Cluster generation at free jet expansion

If an atomic gas or vapor passes through a nozzle, it expands after the nozzle, so that the temperature and density of this gas decrease significantly, thus the gas pressure after the nozzle can exceed the saturated vapor pressure at the current gas temperature. An excess of gas can then transform into clusters. Since the number density of atoms decreases with subsequent gas expansion, there is a finite time of favorable conditions for the nucleation process. Therefore, though the free jet expansion method of cluster generation is the simplest and most convenient method of conversion of an atomic gas into clusters, the nucleation process is realized under certain conditions with respect to the gas pressure and expansion parameters. We consider below the character of the processes for this method of cluster generation and formulate optimal conditions for these processes.

If a gas expands when being passed through a nozzle, it is practically motionless before the nozzle, whereas a gas flow is formed after the nozzle, and the parameters of this gas flow depend both on the distance from the nozzle and on the distance from the flow axis. The spatial parameters of this

flow depend also on the nozzle profile; in particular, they differ slightly for hyperbolic and straight conical nozzles [144]. We will below ignore these peculiarities of the gas flow and define a typical time of gas expansion, i.e., a typical time of passage of atoms through a nozzle region, as follows

$$\tau_{\text{ex}} = \frac{d}{u \tan \alpha}. \quad (4.5)$$

Here, d is the nozzle diameter, α is the angle of beam divergence, the current speed u of gas flow is given by the formula

$$u = \sqrt{\frac{5T_0}{m}} \quad (4.6)$$

for the adiabatic expansion of interest, and T_0 is the gas temperature before the nozzle. This expression follows from the law of conservation of the entropy of an expanding atomic vapor and differs from formula (4.3) when a gas stream is formed by a jump.

The asymptotic expressions for the number density N of atoms and the temperature T far from the nozzle at a distance x from it are [15, 16]

$$N = 0.15N_0 \left(\frac{d}{x}\right)^2, \quad T = 0.282T_0 \left(\frac{d}{x}\right)^{4/3}. \quad (4.7)$$

Here, N_0 is the initial number density of atoms in the chamber, d is the nozzle diameter, and the above expressions are valid if $x > 4d$. These asymptotic expressions for the gas parameters far off a nozzle and the boundary conditions near the nozzle allow us to approximate the gas parameters in the intermediate region by the following expressions

$$T = T_0 \left[1 + 3.55 \left(\frac{x}{d}\right)^{4/3} \right], \quad N = N_0 \left[1 + 6.7 \left(\frac{x}{d}\right)^2 \right]. \quad (4.8)$$

Note that the asymptotic expressions (4.7) satisfy the relation

$$\frac{N}{N_0} = \left(\frac{T}{T_0}\right)^{3/2} \quad (4.9)$$

and this corresponds to the adiabatic character of expansion [45, 145] in neglecting the nucleation process.

Our task now is to describe the nucleation process in the course of free jet expansion of a gas or vapor after passage through a nozzle, when its temperature drops significantly and the gas pressure becomes more than the saturated vapor pressure at a given gas temperature. This leads to formation and growth of clusters. Let us apply to this process the scheme of processes (2.15) with evolution of gas parameters according to formula (2.17). In this problem, a typical parameter of the time dimensionality is the expansion time τ_{ex} , and T is the current gas temperature. Based on the scheme (2.15) of nucleation processes and using the corresponding set of balance equations (2.14), we find out that an expanding gas is transformed into clusters if the following inequality is valid:

$$\tau_{\text{ex}} \gg \tau_{\text{cl}},$$

where τ_{cl} is given by formula (2.18). Correspondingly, the character of the nucleation process is governed by the parameter (2.21):

$$\zeta = N_0 k_0 \tau_{\text{ex}} = \frac{3.2N_0 r_W^2 d}{\tan \alpha} \gg 1, \quad (4.10)$$

where we made use of the expression (4.5) for the expansion time.

A convenient semiempirical method for analyzing the nucleation process in an expanding beam was developed by Hagena [16, 146–151] who applied a scaling law for a beam on the basis of the experimental data. The reduced Hagena parameter Γ^* is introduced as

$$\Gamma^* = \frac{\Gamma}{\Gamma_{\text{ch}}}, \quad \Gamma = N_0 d^q T_0^{0.25q-1.5}, \quad (4.11)$$

$$\Gamma_{\text{ch}} = r_{\text{ch}}^{3-q} T_{\text{ch}}^{0.25q-1.5}, \quad r_{\text{ch}} = \left(\frac{m}{\rho}\right)^{1/3}.$$

Here, N_0 is the initial number density of atoms before the nozzle, T_0 is the initial temperature, m is the mass of the atom, d is the nozzle diameter, ρ is the density of the condensed material, and T_{ch} is the specific sublimation energy of the material per atom. The values of q can be varied within the range 0.5–1 depending on the experimental data, and the optimal value of this parameter is $q = 0.85$. Table 10 lists the values of Γ_{ch} for some materials [147] for this value of q . As follows from the analysis of various gases and vapors, total nucleation occurs when $\Gamma > 200$.

Table 10. Values of the reduced Hagena parameter for some vapors and gases [146].

Gas, vapor	$\Gamma_{\text{ch}}, 10^{14} \text{ m}^{-2.15} \text{ K}^{-1.29}$	Gas, vapor	$\Gamma_{\text{ch}}, 10^{14} \text{ m}^{-2.15} \text{ K}^{-1.29}$
Ar	347	Zn	17.8
Kr	210	Cd	16.9
Na	11.5	Hg	32.4
K	9.1	Al	5.5
Rb	6.4	Ga	5.8
Cs	7.8	In	5.6
Cu	6.3	Ge	3.4
Ag	6.0	Fe	5.0
Au	4.3	Ni	6.6

As can be seen, the parameters used in the Hagena theory, excluding q , are the parameters of the nucleation process and nucleating vapor. In particular, r_{ch} differs by a numerical factor from the Wigner–Seitz radius r_W in accordance with formula (2.1), T_{ch} corresponds to the parameter ε_0 in Table 1, and other parameters N , T , and d are identical in both cases. In the stage of nucleation of an atomic vapor, the nucleation rate within the framework of a simple scheme of nucleation processes (2.15) also depends on the three-body rate constant K , which, being averaged over several processes, is equal to $1 \times 10^{-32} \text{ cm}^6 \text{ s}^{-1}$ within a factor of 2 as follows from the experimental data [66] and the appropriate analysis [44]. If we consider this parameter to be constant for various gases and vapors, one can assume the rate of nucleation within the scheme (2.15) to be dependent only upon the parameter ζ that is determined by formula (4.10). Thus, comparing the Hagena model with the scheme of nucleation (2.15), i.e., the parameters Γ and ζ for these two models, we obtain the identical dependence of these basic parameters on the number density of atoms N_0 before the nozzle, almost identical dependence on the nozzle diameter, and different dependences on the initial gas temperature. We compare also the parameters of nucleation Γ and ζ for these two models under the conditions of the Hagena experiment [148, 149] for nucleation of a silver vapor at free jet expansion ($T_0 = 2200\text{--}2400 \text{ K}$, $p_0 = 18\text{--}140 \text{ kPa}$, $d = 0.35\text{--}1 \text{ mm}$, $\alpha = 5\text{--}8.5^\circ$), where the

highest intensities of formed cluster beams have been achieved. Under these conditions we obtain

$$\frac{\Gamma}{\zeta} = 0.4 \pm 0.1 \quad (4.12)$$

in this range of parameters, where the Hagedorn parameter Γ^* varies in the range 50–1000. As is seen, the parameters of both models with the accuracy indicated (about 30%) can be taken as the nucleation parameter in this range of parameters, where the nucleation parameter varies by more than an order of magnitude. This can be used both for evaluation of the nucleation rate and the accuracy of the results.

The above model, which uses the scheme of nucleation processes (2.15) and takes the parameter τ_{ex} as a characteristic of the expansion process, is valid if the nucleation process proceeds in a small region. According to research for free jet expansion in monatomic gases, it is not fulfilled in reality. Hence, for a numerical analysis of the nucleation process at a free jet expansion, it is necessary to account for the gas dynamics of a flux after a nozzle. Then, the nucleation process influences the flow temperature and therefore is of importance for the gas dynamics of an expanding beam. Thus, the correct computer analysis of this problem requires accounting for the process of cluster growth during expansion of a gas and its influence on the heat balance of the gaseous flow together with the gasdynamics of the flow of a nucleating gas. The above simple model, using processes (2.15) for the formation and growth of clusters and parameter (4.10) for the description of expansion of the gaseous flow, gives the correct character of current processes and allows one to obtain semiquantitative results for the rate of the nucleation process under real conditions.

4.4 Cluster generation in a plasma

The first stage for the second group of the above methods of cluster generation is the preparation of a supersaturated gas or vapor, and subsequently this vapor is transformed into clusters as a result of nucleation processes. Supersaturation of the vapor may be attained by its cooling, and the rate of the nucleation processes is determined by both the number density N of atoms in this supersaturated vapor and its lifetime τ with respect to the expansion. In any case, formation of clusters is possible, if the following criterion holds true:

$$Nk_0\tau \gg 1, \quad (4.13)$$

where the rate constant k_0 is defined by formula (2.8), and its values are given in Table 1. Criterion (4.13) is similar to the criterion (2.21) or (4.10), and according to this criterion, for cluster formation it is necessary that, along with supersaturation, the gas or vapor be found in this state long enough for the nucleation process. In particular, according to the data in Table 1, the number density of atoms of heat-resistant metals at the melting point and the saturated vapor pressure is $\sim 10^{13} \text{ cm}^{-3}$, so that criterion (4.13) takes the form $\tau \gg 10^{-3} \text{ s}$, whereas the expansion time for passage of a vapor through a nozzle of diameter $\sim 100 \mu\text{m}$ is $\sim 10^{-6} \text{ s}$. From this it follows that the method of cluster generation by free jet expansion is not suitable for the generation of clusters of heat-resistant metals, if an atomic vapor is accumulated in a space near a metallic surface.

This problem for heat-resistant metals can be overcome if clusters are formed in a plasma flow involving metallic atoms or metal compounds injected into a plasma flow. Then the

typical time of cluster growth in formula (4.13) is determined by the typical time of plasma flow, which greatly exceeds the typical time of vapor passage through a nozzle, so that criterion (4.13) can be fulfilled. We note that this plasma method is suitable only for clusters with a large binding energy of atoms, since a relatively high cluster temperature and the presence of energetic and active atomic particles in a plasma lead to destruction of clusters with a small binding energy. Hence, the plasma method of cluster generation is utilized in addition to other methods and is convenient mostly for clusters with a high sublimation energy, in contrast to the method of free jet expansion that is applied to clusters of low sublimation energy. In considering this method, we will relate it to a vapor of a heat-resistant metal that is a small additive to a dense buffer gas. Below we discuss the method of cluster generation in a plasma flow in detail.

Note one more peculiarity of cluster generation for heat-resistant metals if metallic atoms are formed by destruction of metal-containing molecules. This process requires a high specific energy for conversion of metal-containing molecules into metallic clusters, which leads to cooling of the buffer gas. Therefore, the concentration of metal-containing molecules in the buffer gas is limited. But this concentration can be increased if these molecules are injected into a restricted region near the center of the buffer gas flow [152, 153], so that an energy needed for the destruction of metal-containing molecules is taken from neighboring regions of the flow. This allows one to attain a high efficiency of the plasma method for cluster generation.

Thus, we use the following scheme for this process. A plasma flow of a buffer gas emerges from a plasma generator of small power, and a metal in the form of metal-containing molecules is injected into the central region of this plasma. For definiteness, we take molecules MX_6 as metal-containing molecules (M is a metal atom, X is a halogen atom), and assume that the plasma temperature satisfies criterion (2.25). Then these molecules decay in the plasma, and metallic atoms are joined in clusters. Next, metal-containing molecules are injected into the center of the plasma flow, so that the metallic clusters formed remain in the region of molecule injection because of a low mobility of clusters, while formed halogen atoms and molecules propagate through all the flow space.

A general scheme of the cluster generator is presented in Fig. 9 and includes the following basic elements. A plasma

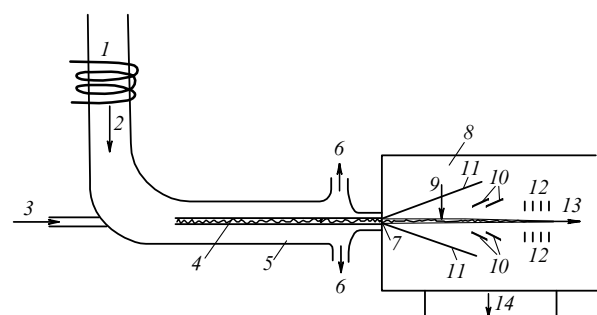


Figure 9. Schematic of a generator of clusters from an arc afterglow: 1 — plasma generator; 2 — plasma flow; 3 — injection of a gaseous compound of heat-resistant metal; 4 — cluster beam in plasma flow; 5 — afterglow tube; 6 — output plasma flow; 7 — nozzle for plasma expansion into a vacuum; 8 — vacuum chamber; 9 — electron beam; 10 — skimmers; 11 — expanding buffer gas; 12 — electric field optics; 13 — cluster beam; 14 — pumps.

generator of low power (~ 1 kW) creates a flow of an arc plasma of a buffer gas (for simplicity and definiteness, we will consider below argon as the buffer gas at a pressure of 1 atm and temperature of several thousand kelvins, so that this plasma is characterized by a small ionization degree). A narrow beam of metal-containing molecules is injected in the form of a liquid jet into this flowing buffer gas near the flow center. As a result of the evolution of this flowing afterglow plasma, metal-containing molecules are decomposed, and the metallic atoms formed attach to growing clusters in this region, so that the metal is collected near the flow center in the form of growing clusters, while halogen atoms and molecules, another component of metal-containing molecules, spread out over all the buffer gas. At the end, the central part of the plasma flow contains a weakly ionized buffer gas and growing metallic clusters, whereas the halogen concentration is small at the flow center. The central part of the flow passes through a separate nozzle or slit, and standard methods are used for pumping the buffer gas after the nozzle, for charging the clusters by a crossing electron beam, and for acceleration of the charged clusters in an external electric field. The noncentral part of the plasma flow, which contains the main part of the buffer gas and does not contain metallic atoms, is extracted separately and is purified from admixtures, so that the purified buffer gas may be utilized once more.

The average number density of bound metallic atoms in clusters for the plasma method of cluster generation (see Table 5) is lower than that obtained by the method of free jet expansion for clusters containing gaseous atoms or molecules. It is comparable to the average number density of atoms in metallic clusters obtained by laser irradiation of a metallic surface (see Table 9). But because the width of cluster beams as a result of the laser method is relatively small, and the laser method is usually used in a pulse regime, the total intensity of the cluster beam (the total metal mass in clusters transferred per unit time) generated by the plasma method is several orders of magnitude higher than that for the laser method.

Figure 10 shows the character of variation of the electron number density in the course of evolution of the plasma flow

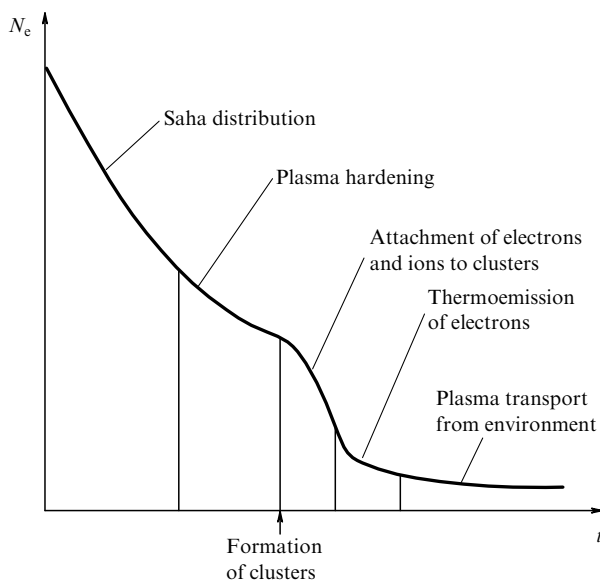


Figure 10. Character of plasma relaxation in the course of plasma evolution in the plasma generator of continuous cluster beams.

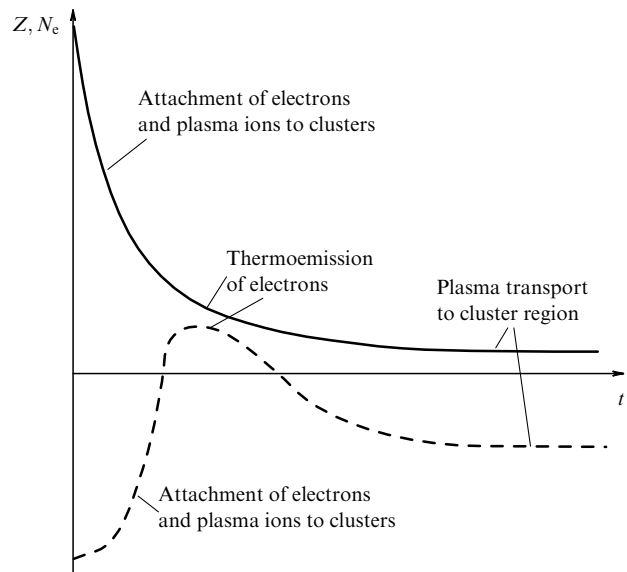


Figure 11. Variation of electron number density (solid curve) and cluster charge (broken curve) during evolution of a cluster plasma in the plasma generator of cluster beams.

at the flow center. Plasma obtained from a plasma generator is an equilibrium one, i.e., the electron number density is connected with the electron temperature by the Saha formula. As the electron temperature decreases in the flow during the plasma cooling, the number density of electrons decreases sharply. Ultimately, this leads to violation of the ionization equilibrium, if the rate of three-body recombination of electrons and ions that is responsible for the equilibrium maintenance in the course of plasma cooling cannot reestablish a decreasing equilibrium number density of electrons, and the current number density of electrons exceeds the equilibrium one. The subsequent sharp decrease in the electron number density takes place after formation of clusters as a result of attachment of plasma electrons and ions to clusters. Then, until the plasma temperature is no longer small, the electron number density results from electron thermoemission from the cluster surface. At low plasma temperatures, the electron number density in a cluster region becomes small and is determined by plasma transport from a surrounding region which does not contain clusters, and recombination of electrons and ions in a cluster region results in attachment of electrons and ions to clusters. As can be seen, evolution of the plasma under consideration includes several stages with a different character of the balance between plasma electrons and ions.

Figure 11 illustrates a variation of the cluster charge in the course of plasma evolution. At the stage when the clusters are formed and the balance of charged particles in the plasma is determined by the attachment of electrons and ions to the clusters, the cluster charge is negative because the electron mobility in a buffer gas exceeds the ion mobility, and a cluster negative charge equalizes the electron and ion currents to the cluster surface. When the number density of plasma electrons is low but the temperature is not low, the number density of plasma electrons is determined by thermoemission of electrons from the cluster surface, and the cluster charge is positive, though it is relatively small. Next, when the plasma temperature becomes low and the thermoemission process is weak, the electron number density in the cluster region and

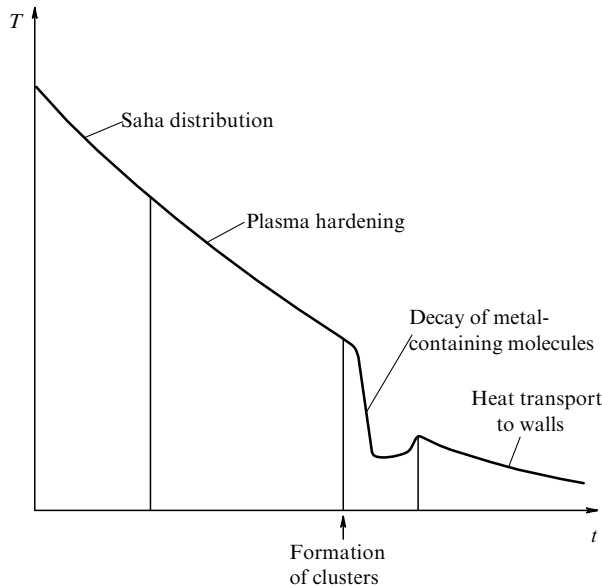


Figure 12. Heat regime of evolution of a cluster plasma.

the charge of an individual cluster result from the transport of the plasma from regions surrounding the cluster region. Then the cluster charge becomes negative again.

Figure 12 shows the evolution of the plasma temperature in a center of the cluster region, where the first stage of processes relates to a pure buffer-gas plasma without clusters. When metal-containing molecules are injected into the plasma, its temperature drops strongly because the thermal energy of the buffer gas is consumed on destruction of the metal-containing molecules and formation of metallic clusters. Later on this heat absorption is compensated for by heat transport from neighboring regions without clusters, and when cluster growth is over, i.e., all metal atoms are bound in clusters, the heat balance of a cluster region is maintained by heat transport to the walls. Such a development of plasma and cluster parameters in a plasma generator of cluster beams exhibits the character of processes which determine properties of this cluster plasma.

4.5 Pulsed generation of intense cluster beams in a plasma

The general character of the generation of metallic clusters by the pulsed plasma method of cluster generation is similar to that of continuous generation of metallic clusters in a plasma [152, 153], but because of a higher number density of bound atoms in the pulsed method of cluster generation, we rely on another scheme of cluster generation. Briefly, a drop with metal-containing molecules is injected into a dense buffer gas and is heated fast, leading to its transformation into a gas, the destruction of free molecules, and the formation of free metallic atoms, which then are joined in metallic clusters in a weakly ionized buffer gas. When a buffer gas with these clusters flows through a nozzle or orifice, atoms of the buffer gas are pumped out, and the resultant beam contains metallic clusters only. The pumping out does not affect the clusters because of their large mass compared to the atomic mass, and therefore clusters possess large momenta in comparison with atomic momentum. One can expect that the pumping out also allows one to obtain a beam of van der Waals-bonded clusters, liberating them from free atoms. But because of the small binding energy of atoms, these clusters evaporate atoms up to an equilibrium

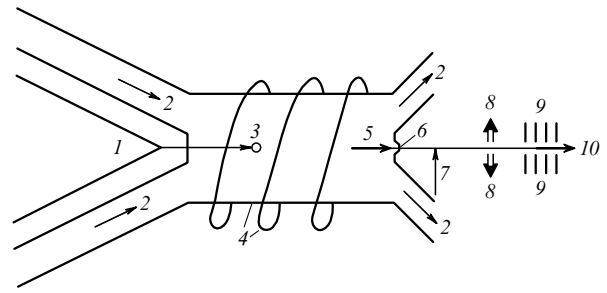


Figure 13. Schematic of the method of generation of a cluster beam as a target for laser pulse irradiation: 1 — source of liquid drops; 2 — flow of buffer gas; 3 — liquid drop in the flow of the buffer gas; 4 — waveguide and gas discharge; 5 — flow of the buffer gas with metallic clusters; 6 — nozzle or orifice; 7 — electron beam; 8 — pumping out; 9 — electric field optics; 10 — beam of charged clusters.

between the evaporation and attachment processes. For metallic clusters, the equilibrium number density of free atoms is very small, i.e., one can ignore the presence of free metallic atoms in the space between clusters.

The general scheme of a generator of a pulsed cluster beam (Fig. 13) is outlined as follows. A liquid drop consisting of metal-containing molecules is injected into a dense buffer gas, and is then heated by gas discharge. The drop also contains lightly ionized admixtures, and an electromagnetic wave of microwave discharge is absorbed mostly in the vicinity of the drop because of the higher degree of plasma ionization there. This leads to strong heating of the drop and surrounding gas up to temperatures of several thousand kelvins during a short time by virtue of consumption of a small amount of electromagnetic energy. Under this action, compounds of the drop are decomposed into atoms, the metallic atoms join in clusters, and other components spread over the buffer gas as a result of diffusion in the form of atoms and molecules, while the diffusion coefficient of clusters formed is small and they remain in the initial region. Cluster growth proceeds until the buffer gas with clusters expands through a nozzle into a vacuum. After the nozzle or orifice, as a result of standard methods [146, 154], atoms of a buffer gas are pumped out, and clusters are charged by a crossing electron beam and governed by electric fields. The resultant pulsed beam contains large charged metallic clusters, whereas free atoms are absent in this beam, and this cluster beam can be a target for laser irradiation that leads to X-ray emission. This is the general scheme for the preparation of a cluster target, and this regime of evolution is realized only under certain conditions. Below we focus on processes of evolution of a liquid drop consisting of metal-containing molecules in a buffer gas and find the conditions when this character of processes is realized.

We suppose for simplicity that the liquid drop inserted in the buffer gas has a spherical shape and conserves this shape after transformation into a gas. The buffer gas is located in a waveguide, and a pulsed gas discharge causes a fast heating of the gas up to a certain temperature T_0 . As a result, the drop is transformed into a gas of molecules, which are destructed into atoms, and an atomic metallic vapor is transformed into a gas of clusters. This system is characterized by two typical temperatures T_1 and T_2 , [82, 41], so that above temperature T_1 the thermodynamic equilibrium corresponds to the breaking of all bonds between halogen and metal atoms, and below temperature T_2 the formation of metallic clusters is favorable

thermodynamically. We assume the criterion (2.25) to be valid and the operation time of gas discharge to be relatively small, so that the processes of destruction of radicals and metal-containing molecules proceed mostly when the breakdown pulse is over. We will be guided by compounds whose parameters are given in Table 5.

We demonstrate the reality of this system through the example of a drop of 10 μm radius, consisting of metal-containing molecules in a condensed state (the densities of these compounds at room temperature [40] are given in Table 5), is injected into argon at a pressure of 50 atm. The drop also contains lightly ionized additives and it is heated by a short pulse ($\sim 10^{-6}$ s) of an electromagnetic wave. As a result, the drop evaporates and expands, and argon penetrates to the drop's interior. For definiteness, we assume the concentration of argon atoms inside the drop in the course of the process to be $c = 50\%$. In Table 11, we give the total mass M of metal atoms in the drop and the total number n_M of metallic atoms in it. Note that in this case the input energy for heating and destruction of the drop is not large; in particular, the energy that is consumed for transformation of this drop into metal and halogen atoms is about 10^{-4} J, i.e., various types of gas discharges are available for this. Next, we introduce the temperature T_2 as $N_{\text{sat}}(T_2) = N_m$, where N_m is the total number density of bound metallic atoms in the drop evaporated, and the number density $N_{\text{sat}}(T)$ corresponds to the saturated vapor pressure at a given temperature. We take the temperature T_0 of argon outside the drop such that $N_{\text{sat}}(T_0) = 0.1N_m$, and its values are listed in Table 11. Note that since the temperature T_* at the drop's center is lower than T_0 , the number density $N_{\text{sat}}(T_*)$ of metallic atoms at this temperature is less significant (see Table 11).

Table 11. The parameters characterizing cluster formation as a result of destroying a drop of 10 μm radius. The drop consists of metal-containing molecules and is located in argon at a pressure of 50 atm.

Molecule	MoF ₆	IrF ₆	WF ₆	WCl ₆
$r, \mu\text{m}$	45	48	46	40
$M, 10^{-9}$ g	4.9	16	8.9	6.8
$n_M, 10^{13}$	3.1	5.0	2.9	2.2
$T_2, 10^3$ K	5.9	5.7	7.3	7.3
$T_0, 10^3$ K	5.0	4.9	6.2	6.2
$T_*, 10^3$ K	4.3	2.8	5.2	4.4
$N_m, 10^{19}$ cm ⁻³	4.2	6.6	3.5	4.2
$N_{\text{sat}}(T_*), 10^{17}$ cm ⁻³	0.05	5×10^{-4}	1	0.05
$\tau_{\text{eq}}, 10^{-6}$ s	0.3	0.8	0.3	0.3
$\tau_0, 10^{-6}$ s	15	4	10	2
$\bar{n}, 10^5$	10	2	4	0.6
$n_M/\bar{n}, 10^7$	3	26	8	35
$\Delta x, \mu\text{m}$	1	1	1	1

The heat regime of this drop is similar to that considered in Section 3.2. Indeed, the energy needed for destruction of metal-containing molecules is taken from the surrounding buffer gas that does not contain metallic atoms. Halogen atoms formed as a result of the destruction of metal-containing molecules and their radicals leave the drop's region, while metallic atoms join in clusters and remain in this region. Such

a regime is established during a typical time

$$\tau_{\text{eq}} = \frac{r^2}{3\chi(T_*)},$$

where χ is the thermal diffusivity of argon, whose values are taken from Refs [155, 156], as are the values of the diffusion coefficient for halogen atoms (they are modeled on inert gas atoms) in argon. The halogen atoms formed leave the drop region rapidly, and the inverse process of their attachment to metal-containing radicals is not significant. The total time of transformation of metal-containing molecules into metal clusters, given by formula (3.21), is determined mostly by destruction of these molecules and their radicals:

$$\tau_0 = \frac{1}{v_d(T_*)},$$

where $v_d(T_*)$ is the rate of destruction of molecules and radicals in collisions with argon atoms. Under these conditions, cluster growth is determined by the coagulation process, and the average number \bar{n} of cluster atoms by the time t is given by formula (2.20):

$$\bar{n} = 3.5(k_0 N_m t)^{1.2}, \quad (4.14)$$

where N_m is the total number density of bound metallic atoms, and k_0 is the reduced rate constant of cluster collisions [see formula (2.8) and Table I]. The longer the drop is located in the buffer gas, the larger the clusters that are formed in this process. We give in Table 11 the minimal value of the average cluster size $\bar{n}(\tau_0)$ if the time the cluster is located inside argon corresponds to the total time of destruction of metal-containing molecules. In reality, this process leads to larger cluster sizes. The ratio n_M/\bar{n} is the maximum number of clusters formed during this process.

The decay of metal-containing molecules with a release of halogen atoms leads to an increase in the gas pressure, while the joining of radicals and clusters causes a decrease in the pressure. We assume a soft regime for these processes, so that atoms of a buffer gas penetrate into this region, having compensated variations of the gas pressure. In addition, we suppose that the volume of the region, where bound metallic atoms are located, is conserved in the course of formation and growth of clusters; the concentration of bound metallic atoms in the volume where they are located with respect to atoms of a buffer gas was taken to be $c_M = 50\%$.

As a result of these processes, released halogen atoms spread over the space due to their diffusion in argon. Let us estimate the average displacement Δx of metallic clusters as a result of their diffusive motion that is given by the formula

$$\Delta x^2 = 2 \int D dt, \quad (4.15)$$

where the diffusion coefficient D of large clusters in a buffer gas is given by formula (2.28), and its values are listed in Table 4. Using the dependence (2.29) for the diffusion coefficient ($D = D_0/n^{2/3}$) and taking formula (4.14) for the current number n of cluster atoms, we find the average displacement Δx of metallic clusters as a result of their diffusion:

$$\Delta x^2 = \frac{3.7D_0 n^{1/6}}{k_0 N_0}, \quad (4.16)$$

where N_0 is the number density of buffer gas atoms. Note that the main contribution to Δx is made by clusters with large numbers of atoms, so that formula (4.14) for evolution of the average cluster size is valid, and we relied on this fact at integration of formula (4.15). Table 11 contains the values of Δx for the regimes under consideration and confirms our assumption that cluster diffusion is not essential.

Thus, the above-discussed pulsed method for generation of metallic clusters from a plasma allows one to obtain intense pulsed beams of clusters. The number density of bound atoms in cluster beams obtained by the pulsed plasma method is two orders of magnitude higher than that for the stationary plasma method of cluster generation (compare the data of Tables 5 and 12) and is comparable with that in intense beams of van der Waals-bonded clusters. But in intense beams of clusters consisting of gaseous atoms or molecules, free atoms or molecules are also present. They are found in equilibrium with clusters and can influence subsequent processes of application of cluster beams. In pumped out beams of metallic clusters, free metallic atoms are practically absent.

4.6 Cluster beams for metal transport

The above analysis shows that the generation of cluster beams of metals is problematic within the free jet expansion method when a metal vapor from a metallic surface is accumulated in a chamber and then this vapor is converted into a cluster beam by free jet expansion into a vacuum or a gas of low pressure. The reason for this is the low saturated vapor pressure of many metals at the melting point, and the equilibrium number density of atoms in a chamber does not exceed that at the saturated vapor pressure and surface temperature because an excess of the equilibrium vapor will attach to the hot surface. Evidently, the surface loses stability at the melting point, so that the vapor pressure in a space near the heated metallic surface is restricted by the saturated vapor pressure at the melting point. This value of pressure is usually not enough for conversion of a metallic vapor into a cluster beam because of the small time of expansion, and the standard scheme of generation of cluster beams is not suitable for most metals.

This trouble can be overcome if we use nonequilibrium conditions near the metal surface. A simple method for reaching this purpose is the formation of cluster beams in a chamber near a hot metallic surface by using a flow of cold buffer gas. Then an equilibrium between the metallic surface and the clusters is absent, and a part of the evaporable atoms attaches to the clusters in a cold region, leading to the transformation of a metallic vapor into clusters which are captured by the flow of the buffer gas.

Note that the problem of the generation of intense beams of metallic atoms is of importance for metal transport. Indeed, the basic applications of cluster beams consist of depositing cluster beams on a target with fabrication of thin films or creation of a new materials with embedded clusters, and such applications result from metal transport in the form of cluster beams between two objects. Because equilibrium between the clusters and the source of metallic atoms is absent, the number density of metallic atoms in cluster beams is not restricted by equilibrium conditions which must be fulfilled for atomic beams. Therefore, cluster beams constitute a more convenient form for metal transport than atomic beams.

Let us consider this problem for the simple geometry when a hot metallic surface and a cold surface are parallel planes,

and a dense buffer gas flows between them. We assume that the heat balance between these planes is due to thermal conductivity of the buffer gas, i.e., we have

$$q = -\kappa \frac{dT}{dx} = \text{const}, \quad (4.17)$$

where q is the heat flux between the planes, κ is the thermal conductivity coefficient for the buffer gas, T is its temperature, and x is the distance from the hot metallic surface. We assume for simplicity that the process of atom attachment to clusters does not make a contribution to the heat balance of the buffer gas. Then if clusters of a typical size n are found in equilibrium with metal atoms in the region of the buffer gas whose temperature is T , an equilibrium number density of free atoms in the cluster region according to formula (3.8) is given by

$$N_m^{\text{eq}} = N_{\text{sat}}(T) \exp\left(-\frac{2A}{3n^{1/3}T}\right), \quad (4.18)$$

where $N_{\text{sat}}(T)$ is the atomic number density at the saturated vapor pressure at a temperature T of the cluster region, and A is the specific surface energy of the cluster. Thus, the rate of cluster formation and growth is determined by the number density of atoms $N_{\text{sat}}(T_m)$ related to the saturated vapor pressure at surface temperature. These values are given in Table 1 for some metals, and in addition Fig. 14 contains the parameters of formula (2.10) for the saturated vapor pressure of liquid metals, together with the melting and boiling points of these metals, as well as the specific surface energy A of these metals, defined by formula (2.4).

In considering the dynamics of the cluster growth process, we base it on the scheme (2.15) of formation and growth of clusters. Atoms which are evaporated from the hot metallic surface propagate through the space in the form of a wave, and in the absence of the nucleation process, the number density of atoms is $N_{\text{sat}}(T_m)$ in the region that is attained by the wave (we take the surface temperature to be equal to the melting point T_m), and the number density $N_{\text{sat}}(T)$ corresponds to the saturated vapor pressure at the surface temperature T . According to formula (2.18), the time τ of conversion of a metallic vapor to clusters is given by

$$\tau = \frac{(54G)^{1/4}}{k_0 N_m}.$$

During this time atoms displace at a distance

$$l \approx \sqrt{2D\tau},$$

where D is the diffusion coefficient of metallic atoms in a buffer gas. Based on the scheme (2.15) of the nucleation process, we neglect the evaporation process, so that nucleation takes place in a cold region that is not located close to the hot surface. We take for definiteness the characteristic distance l_0 from the surface, where the equilibrium number density is low compared to the saturation number density $N_m = N_{\text{sat}}(T_m)$, as

$$l_0 \approx \frac{2T_m^2}{\varepsilon}, \quad \varepsilon = \varepsilon_0 - \frac{2A}{3n^{1/3}T_m}, \quad (4.19)$$

and the criterion

$$l \gg l_0$$

Table 12. Parameters describing a metal flux from a hot surface in a buffer gas.

Metal	l_0 , mm	p_0 , atm	$G(T_m)$	D , cm ² s ⁻¹	j_{dif} , cm ⁻² s ⁻¹	j_{dif} , μg cm ⁻² s ⁻¹	j_{ev} , cm ⁻² s ⁻¹	ξ , %	c_m
Ti	0.7	10	210	0.45	1.5×10^{14}	0.012	9.3×10^{17}	0.03	6.1×10^{-7}
V	0.8	3.7	570	1.5	1.6×10^{15}	0.14	2.0×10^{18}	0.08	6.8×10^{-6}
Cr	1.1	0.037	49000	150	2.3×10^{19}	2000	1.3×10^{22}	0.18	0.14
Fe	0.9	2.1	670	1.9	2.0×10^{15}	0.18	2.0×10^{18}	0.10	1.2×10^{-5}
Co	1.3	6.0	420	1.3	2.9×10^{14}	0.028	7.0×10^{17}	0.04	1.8×10^{-6}
Ni	0.81	50	24	0.072	2.4×10^{12}	2.3×10^{-4}	5.3×10^{16}	0.004	1.3×10^{-8}
Cu	0.77	50	17	0.046	1.3×10^{12}	1.4×10^{-4}	3.2×10^{16}	0.004	7.0×10^{-9}
Nb	0.69	86	30	0.085	3.9×10^{12}	6.0×10^{-4}	6.3×10^{16}	0.007	1.4×10^{-8}
Mo	0.87	20	120	0.39	6.7×10^{14}	0.11	3.0×10^{18}	0.022	3.0×10^{-6}
Rh	1.2	0.12	22000	79	4.3×10^{18}	730	1.3×10^{20}	3.3	0.023
Pd	1.0	1.3	920	2.8	5.1×10^{15}	0.90	2.7×10^{18}	1.4	3.4×10^{-5}
Ag	0.85	6.0	120	0.3	6.0×10^{13}	0.011	2.1×10^{17}	9.5	2.9×10^{-6}

holds true, if the nucleation takes place in a cold region. Evidently, the optimal pressure of a buffer gas corresponds to the approximate relation

$$l \approx l_0, \quad (4.20)$$

which provides for the maximum efficiency of conversion of evaporable atoms into clusters.

Table 12 contains the parameters of the process under consideration for some metals, when the temperature of a hot surface is the metal's melting point. Argon is taken as a buffer gas at a pressure p , which satisfies relation (4.20) [the diffusion coefficient of metallic atoms in a buffer gas is inversely proportional to the buffer gas pressure, as well as the parameter G according to formula (2.16)]. Then the temperature gradient near the surface is taken as T_m/L , where T_m is the melting point, and the distance between the hot and cold surfaces is $L = 1$ cm. The diffusion flux of atoms emerging from the metallic surface in the buffer gas is equal to

$$j_{\text{dif}} \approx D \frac{N_m}{l_0}, \quad (4.21)$$

whereas the flux of evaporable atoms near the surface is obtained from the expression

$$j_{\text{ev}} = \sqrt{\frac{T_m}{2\pi m}} N_{\text{sat}}(T_m),$$

where m is the atomic mass. Just the diffusion flux of free atoms determines the rate of cluster growth. The part of initially evaporable atoms which later attach to clusters is given by

$$\xi = \frac{j_{\text{dif}}}{j_{\text{ev}}}, \quad (4.22)$$

and Table 12 contains the above fluxes and the efficiency of conversion of evaporable atoms into clusters.

The heat regime under consideration is such that the nucleation process makes a small contribution to the heat balance of the buffer gas, and the corresponding criterion has the form

$$\kappa \frac{dT}{dx} \gg D \frac{N_m}{l_0} \varepsilon_0.$$

Introducing the concentration $c_m = N_m/N_a$ of metallic atoms, we rewrite this criterion as follows

$$c_m \ll c_0 = \frac{l_0}{\varepsilon_0} \frac{dT}{dx} \frac{\kappa}{DN_a}. \quad (4.23)$$

Taking as we did earlier $dT/dx = T_m/L$, where $L = 1$ cm, we obtain $c_0 \sim 1$ in this formula, while the concentration c_m of free metallic atoms in the buffer gas is lower by several orders of magnitude (see Table 12). Hence, the criterion (4.23) holds true, and the heat balance of the buffer gas is determined by the thermal conductivity of the buffer gas; a typical specific heat flux then amounts to ~ 100 W cm⁻² for the cases covered in Table 12.

Thus, the character of formation of clusters near a hot metallic surface may be described as follows. Evaporable atoms reach a cold region where formation of clusters is possible. Clusters are formed first at a distance l_0 from the hot surface, where an equilibrium number density of free metallic atoms is given by formula (4.18). The temperature gradient aimed away from the hot surface creates the gradient of the equilibrium number density of free metallic atoms, which in turn causes the diffusion flux of atoms in the case of equilibrium between free metallic atoms and clusters. Therefore, clusters are formed and grow in a narrow region, and expansion of this region as a result of atom attachment to clusters proceeds slowly in the course of atomic evaporation because of the strong temperature dependence (4.18) of the equilibrium number density of free atoms. Next, the rate of cluster formation is strongly distinguished for different metals (see Table 12). This quantity can be increased essentially if a liquid metal surface will be used for evaporation.

5. Processes in the generation of cluster beams

5.1 Peculiarities of nucleation at free jet expansion

Analyzing the character of nucleation in an expanding gas, we above assumed the gas temperature to be constant in the course of gas evolution, i.e., we ignored thermal processes during nucleation. We now consider the influence of the heat balance on the nucleation process that may be of importance for pure gases and vapors. Indeed, the binding energy per atom in the clusters formed exceeds significantly a typical thermal energy of free atoms, and heat release during the nucleation process can make a remarkable contribution to the heat balance of a nucleating gas. For the analysis of the heat process in the course of expansion of a nucleating vapor, we consider a mixture of a buffer gas with an admixture of a nucleating vapor, characterizing its amount by the concentration c of admixture atoms with respect to the total number of atoms in a given volume. We assume for simplicity the released energy per atom as a result of cluster formation to be ε_0 and this quantity is independent of cluster size, i.e.,

according to formula (2.4) we neglect the cluster surface energy. Taking a test volume of an expanding gas with a certain number g of atoms and considering free jet expansion of the gas into a vacuum as an adiabatic process, we apply the second law of thermodynamics to the given gas in the form

$$dE = dQ + p dV = 0, \quad (5.1)$$

where E is the total atomic energy in the volume, Q is the thermal energy of atoms in the volume, and p is the gaseous pressure. Correspondingly, the variation of the thermal energy of the gas is described by the equation

$$dQ = \frac{3}{2} g dT - \sum_k E_k dn_k = \frac{3}{2} g dT - g \varepsilon_0 dc, \quad (5.2)$$

where dT is the temperature variation, g is the total number of atoms in a given volume, n_k is the number of clusters consisting of k atoms and located in a given volume, and E_k is the total binding energy of atoms in a cluster containing k atoms [$E_k = \varepsilon_0 k$ according to formula (2.4) in which we ignore the cluster surface energy].

Considering the expanding gas to be ideal, we have the equation of state of the gas in the form $p = NT$, where N is the number density of gas atoms, and since the total number of atoms in a given volume equals $g = NV$, we have $p dV = -gT dN/N$. Then, the equation (5.1) for the adiabatic process in a gas ($dE = 0$) takes the form

$$-\frac{dN}{N} + \frac{3}{2} \frac{dT}{T} - \frac{\varepsilon_0}{T} dc = 0 \quad (5.3)$$

and is independent of the size of the volume under consideration. On the basis of this equation, one can consider two limiting heat regimes for an expanding gas. At high temperatures one can neglect the nucleation process, so that a current temperature T and number density of atoms N for an expanding atomic gas are connected with the initial values T_0 and N_0 of these parameters by the adiabatic law of expansion of an atomic gas [45, 145]:

$$\frac{N}{N_0} = \left(\frac{T}{T_0} \right)^{3/2}. \quad (5.4)$$

The other limiting case for the heat regime of an expanding nucleating gas is realized at low temperatures when the nucleation rate is high. Taking the gas parameters at the beginning of nucleation to be T_* , N_* , and setting $T = T_* = \text{const}$ in the course of nucleation, we have from equation (5.3) the following relation

$$c = \frac{T_*}{\varepsilon_0} \ln \frac{N_*}{N_f}, \quad (5.5)$$

where c is the concentration of bound atoms, and N_f is the number density of free atoms at the end of the nucleation process. This formula takes the form [68, 41]

$$c = \frac{T_*}{\varepsilon_0} \ln n. \quad (5.6)$$

Here, n is a typical number of atoms per cluster at the end of the nucleation process with the participation of free atoms, which takes the value ~ 10 under typical conditions of free jet expansion. In particular, in the case of generation of xenon clusters, assuming a typical temperature of nucleation $T_* = 150$ K, we have for xenon ($\varepsilon_0 = 158$ meV) according to

formula (5.6): $c \approx 20\%$. Thus, only part of an expanding pure gas or vapor can be transformed into clusters if the expansion process proceeds under adiabatic conditions. This is determined by the heat balance of an expanding gas, and the number of bound atoms in an expanded pure gas is practically $\sim 10-20\%$ [41, 68]. The reason for this finding is that a thermal atomic energy is small compared to the binding energy of a bound cluster atom, and since the energy released in the nucleation process remains in the gas, from this it follows that the number of bound atoms at the end of the expansion process is less significant than the number of free atoms.

Of course, this formula is based on the adiabatic character of gas expansion, when the nucleation energy is transformed into a thermal energy of free atoms. One can utilize a specific long nozzle where, due to gas-wall interaction, the heat liberated in the nucleation process is transferred to the walls, and the concentration of bound atoms in the end can be increased in this manner. But at low wall temperatures, free atoms can attach to the walls and form a condensed phase on the walls that complicates current processes and requires special analysis.

We give here an example when heat release retards the nucleation process on the basis of experiment [157], where the evolution of a copper vapor was studied. The initial vapor temperature was $T_0 = 2500$ K, the initial vapor pressure was $p_0 = 100$ Torr, and the nozzle diameter amounted to $d = 0.625$ mm. At the end of the expansion process, only a small part of the atoms was converted into diatomic molecules, and the vibrational T_{vib} and rotational T_{rot} temperatures of the dimers formed were measured as $T_{\text{vib}} = 950 \pm 100$ K and $T_{\text{rot}} = 800 \pm 50$ K. Polyatomic molecules or clusters were not observed in this experiment. One can estimate the character of nucleation under these experimental conditions. We have that the pressure of the copper vapor is close to the saturated vapor pressure at its temperature, i.e., formation of clusters can start from the initial temperature. We obtain with these parameters that $d/u = 0.4 \mu\text{s}$ (u is the speed of sound, i.e., the velocity of a beam being formed), and the typical expansion time that accounts for a small expansion angle is practically greater by one order of magnitude. A typical time of conversion of atoms into diatomic molecules is in this case: $(KN^2)^{-1} = 600 \mu\text{s}$. One can see that in spite of the high copper vapor density created in this experiment [157], which used laser ablation, the vapor density is small for the generation of clusters during expansion times. This example shows that high enough pressure is necessary for cluster generation in free jet expansion, as it takes place in the nucleation of a dense buffer gas.

One more peculiarity of the nucleation process relates mostly to the generation of gaseous clusters or van der Waals-bonded clusters where bonds between atoms are sustained by a weak van der Waals interaction. Let these clusters be generated by the free jet expansion method, and then free atoms are pumped out from the cluster beam. Then because of small binding energies of atoms, new atoms are formed in the course of the propagation of the cluster beam, and atoms evaporate from the cluster surface until an equilibrium is established between clusters and free atoms, and the portion of free atoms may be significant under real conditions. On the contrary, for clusters with a high binding energy of atoms, like metallic clusters, the portion of free atoms in cluster beams is small.

As a demonstration of this peculiarity, Table 13 contains a portion of free atoms in an equilibrium cluster beam depending on the pressure and temperature after the nozzle, and these portions refer to two typical cluster sizes, where the number n of cluster atoms is $n = 10^4$ and $n = 10^6$. These data were obtained from the equality of fluxes of atoms attaching to the cluster and evaporating from the cluster surface in accordance with Ref. [158]. As follows from data in Table 13, the portion of free atoms increases with an increase in temperature or a decrease in pressure. Note that the triple point for xenon is equal to 161.4 K, so that under the conditions examined in this table clusters can be found both in the solid and in the liquid states.

Table 13. The portion of free xenon atoms (in %) at a given temperature and pressure which is established at the total cluster vaporization. An equilibrium is maintained between free and bound atoms in the cluster beam, and the average size of clusters formed is $n = 10^4$ and $n = 10^6$ (data are given in parentheses).

p , atm	T , K			
	120	150	180	210
1	1.5 (1.2)	30 (25)	100 (100)	100 (100)
3	0.5 (0.4)	10 (8.3)	90 (77)	100 (100)
10	0.15 (0.12)	3.0 (2.5)	27 (23)	90 (79)
30	0.05 (0.04)	1.0 (0.83)	9.0 (7.7)	30 (26)

5.2 Character of formation of atoms in cluster generation

The first stage of the nucleation process, when clusters are formed from a condensed phase, is the formation of an atomic vapor; the efficiency and intensity of this process are the parameters which characterize this method of cluster generation. In particular, Fig. 4 depicts various methods of formation of metallic atoms as a result of excitation of a metallic surface. Below we shall analyze some of these methods of atom formation from the standpoint of their efficiency. We characterize the efficiency of atom formation by the energy consumed per atom — that is, the energy cost of one atom.

In the case of fusible metals, the optimal and effective method of generation of an atomic vapor uses a specific oven. The optimal method of atom formation for heat-resistant metals depends on certain conditions and requirements. In particular, we have considered above the laser method of generation of an atomic stream from a metallic surface (see Section 4.2), and the main problem of providing high efficiency in this process of atom formation is to prevent the interaction between the laser beam and the atomic flux. When it is attained by a pulse regime of the laser beam or by the removal of an atomic stream by a flux of a buffer gas, the efficiency of this method of atom generation may be high enough, though the rate of atom formation is limited. Along with this, other problems of atom formation may occur, and we consider below one more peculiarity of the atom generation process. If a surface is heated strongly, it emits radiation, and the contribution of the radiative process to the heat balance of the surface can be remarkable. In particular, in the case of tungsten, the radiative channel of energy losses is the basic one in a temperature range which is employed for atom generation, and the atomic energy cost in these conditions is equal to

$$\varepsilon = \frac{p}{j}, \quad (5.7)$$

where p is the radiation power per unit area, and j is the flux of evaporable atoms. Taking the parameters of the processes from Ref. [40], we determine the tungsten atomic energy cost $\varepsilon = 270$ keV at $T = 3000$ K, $\varepsilon = 28$ keV at $T = 3300$ K, and $\varepsilon = 4.2$ keV at $T = 3600$ K, when the tungsten melting point is $T = 3660$ K. The binding energy per tungsten atom for these temperatures according to Table 1 is about 8.6 eV. As can be seen, the method of formation of tungsten atoms by heating the tungsten surface (wire) is characterized by a low efficiency (or a high energy cost). The sharp temperature dependence of the atomic energy cost is due to the exponential temperature dependence for the evaporating atomic flux, as well as the fact that the radiation from the surface determines the energy balance at these temperatures. For materials with a low temperature of vaporization and a high saturated vapor pressure at temperatures where their surface is stable, the heating method may provide effective atom generation from the surface.

In the case of laser evaporation of surface atoms, the efficiency of atom generation is higher compared to the heating method because a higher surface temperature leads to another regime of the heat balance for the surface [formula (4.3)]. In this respect, gas-discharge methods based on cathode sputtering by an ion current may be more effective for the production of an atomic vapor because of the direct character of the atom formation process. In particular, magnetron discharge is used for the generation of metallic atoms in a buffer gas because this discharge is characterized by a high efficiency of cathode sputtering. Therefore, clusters of Ag, Al, Co, Cu, Fe, Mg, Mo, Si, Ti, and TiN were produced by this method with average cluster sizes falling within the range 500–10,000 atoms [159–161, 94]. The charged clusters formed are accelerated by an external electric field that allows one to obtain a cluster beam energy in the range 0.1–10 eV atom⁻¹. Thus, the experience acquired in generating cluster atoms from a condensed phase shows that an atomic vapor in this case may be obtained by various methods depending on the evaporated material and the parameters of the cluster beam.

The first stage of the gas discharge method for cluster generation is the formation of free metallic atoms as a result of electrode sputtering, and then the atoms later on join in clusters. Often gas discharge is triggered at low gas pressures, whereas transformation of atoms into clusters proceeds effectively at high pressures, and this contradiction can be overcome by separating the regions of atom generation and cluster generation. In particular, the above magnetron discharge technique for cluster generation [161, 94] uses an argon pressure of 10–100 Pa, while the gas pressure is of the order of 1 Pa for common discharges of this type.

The standard method is employed for the conversion of an atomic vapor into a cluster beam if this vapor passes through a nozzle or orifice and expands into a vacuum or into a gas of low pressure. For example, in the laser method of cluster generation [119–124], when clusters are formed after irradiation of a metallic rod by a laser beam, the metallic atoms formed and clusters resulting from their joining are captured by a flow of cool buffer gas, and then this buffer gas with metallic clusters passes through a nozzle. After the nozzle, metallic clusters are charged by a crossing electron beam, and a buffer gas is pumped out, as shown in Fig. 8. Then only charged clusters remain in the flux, and this beam of charged clusters is governed by electric optics in accordance with the scheme of the experiment in Fig. 8.

Along with the efficiency of formation of an atomic metallic vapor from a condensed phase, the intensity is an important parameter of a cluster beam. The upper limit of the metal flux from a metal surface can be found as follows. Evidently, the temperature of a stable surface cannot exceed the melting point T_m of the metal, and correspondingly the number density of metallic atoms in the space near the surface cannot exceed the number density $N_{\text{sat}}(T_m)$ of atoms at the saturated vapor pressure for this temperature. Indeed, if the number density of atoms is higher than this value, an excess of atoms attaches to the metal surface. If this vapor passes through a nozzle, the velocity of expansion of the vapor into a vacuum is equal to

$$v = \sqrt{\frac{c_p T_b}{m}} = \sqrt{\frac{5T_b}{2m}}, \quad (5.8)$$

where m is the atomic mass, and $c_p = 5/2$ is the heat capacity per atom at constant pressure. This leads to the flux of free atoms at the adiabatic passage of a gas through the nozzle or orifice:

$$j = N_{\text{sat}}(T_m) \sqrt{\frac{5T_m}{2m}}. \quad (5.9)$$

Under optimal conditions, all the atoms join in clusters in the course of cluster growth, and therefore formula (5.9) also defines the maximum flux of bound atoms in clusters. The number density of atoms N_f and temperature T_f after the nozzle are $N_f = 0.56N$ and $T_f = 0.68T$, where N and T specify appropriate quantities for a motionless vapor before the nozzle. Correspondingly, the maximum mass flux after the nozzle equals

$$J_{\text{max}} = m j_{\text{max}} = N_f \sqrt{2,5mT_f} = N_{\text{sat}}(T_m) \sqrt{mT_m}. \quad (5.10)$$

Table 14 contains the values of this flux together with the number densities of metallic atoms at the saturated vapor pressure at the melting point [90].

Table 14 also gives the values of $N_{\text{sat}}(T_m)$ and J_{max} for some metals, and the data for the saturated vapor pressure were taken from Table 1. As a matter of fact, J_{max} is the maximum metal flux that is transported by clusters under the condition that a saturated metal vapor is located before the nozzle, being in equilibrium with the surface. For example, the maximum flux of silver clusters is $0.8 \text{ g m}^{-2} \text{ s}^{-1}$ [150], whereas formula (5.10) gives the value of $0.6 \text{ g m}^{-2} \text{ s}^{-1}$. But if the equilibrium between the metallic vapor and surface is violated, one can heighten this limiting flux. In particular, in the plasma method of cluster generation, the above equilibrium between the metallic vapor and the walls is violated, and the metal flux exceeds significantly the limit imposed by formula (5.10). Therefore, for metals with a low density of saturated vapor, the nonequilibrium method of metal transport is preferable and allows one to increase the metal mass transported per unit time. It is convenient to use cluster beams for metal transport, because when atoms become bound in clusters, their equilibrium with the walls is broken.

5.3 Explosive emission as a method of atom generation

Since the generation of atoms in gas discharges may be effective due to erosion of electrodes, and this process is of importance for the ignition and sustaining of some discharges, we consider below the cathode phenomena from the standpoint of the generation of atoms which can be

Table 14. Parameters of large liquid clusters.

Element	T_m , K	ρ , g cm^{-3}	ε_0 , eV	$N_{\text{sat}}(T_m)$, 10^{13} cm^{-3}	J_{max} , $\text{mg cm}^{-2} \text{ s}^{-1}$	dl/dt , $\mu\text{m s}^{-1}$
Ti	1941	4.5	4.89	0.64	0.03	0.06
V	2183	6.0	4.9	8.4	0.4	0.7
Fe	1812	7.87	3.83	22	1.0	1.3
Co	1768	8.86	4.10	3.7	0.18	0.2
Ni	1728	8.90	4.13	2.0	0.1	0.1
Zr	2128	6.52	6.12	0.005	3×10^{-4}	5×10^{-4}
Nb	2750	8.57	7.35	0.17	0.013	0.015
Mo	2886	10.2	6.3	7.4	0.58	0.57
Rh	2237	20.8	5.42	1.5	0.11	0.05
Pd	1828	12.0	3.67	16	1.1	0.9
Ta	3290	16.4	8.1	1.2	0.14	0.08
W	3695	19.3	8.59	10	1.3	0.66
Re	3459	20.8	7.36	8.1	1.0	0.5
Os	3100	22.5	7.94	1.0	0.12	0.05
Ir	2819	22.5	6.44	6.4	0.71	0.32
Pt	2041	21.5	5.6	0.04	0.004	0.0018
Au	1337	19.3	3.65	0.007	5.6×10^{-4}	2.9×10^{-4}
U	1408	19.1	4.95	1.2×10^{-6}	1.1×10^{-7}	5.7×10^{-8}

Note. T_m is the melting point of a metal, ρ is its density at room temperature, the parameters ε_0 and $N_{\text{sat}}(T_m)$ were taken from Table 1, J_{max} is the maximum metal flux in clusters according to formula (5.10) under the assumption of equilibrium between the atomic metal vapor and solid, and dl/dt is the rate of film growth.

transformed later into clusters. We will be guided by the explosive emission mechanism of cathode erosion that takes place in vacuum discharges, sparks, and cathode spots of arcs. As a result of this phenomenon, a medium is created due to the erosion of small elements of the cathode under the action of the ion current that provides the passage of the electric current through a gaseous discharge. Therefore, the erosion process is a basis for this phenomenon of explosive emission of charged particles in gas discharges.

The regime of explosive emission [162–164] was discovered by Mesyats in sixties and sometimes is called the Mesyats mechanism of electron emission (see, for example, the book [90]). An electric current near the cathode is concentrated in a narrow region which determines the discharge current towards the cathode. A high electric current density leads to heating of this cathode region, causing erosion of the cathode and sputtering of the cathode material in the surrounding space. The evaporating substance is then transformed into electrons and ions which maintain the electric discharge current. This phenomenon occurs at a given cathode point during a restricted time τ , through which a current is suppressed at a given point and then arises at another point. Thus, this emission process consists of individual events when a current flows through a given cathode point, and an individual event or an individual emission center is called an ecton [163–166]. An ecton includes a certain number of evaporable atoms (in the form of individual atoms and sputtered drops), and its parameters follow from experimental data [162–166]. Theoretical models of the explosive emission phenomenon are not self-consistent and are able to explain some aspects of this phenomenon on the basis of experimental data. In addition, according to experimental data [167, 168], splashing the liquid metal out from the cathode surface under the action of electric current plays a principal role in this phenomenon. Below we consider some aspects of this phenomenon and discuss them from the standpoint of atom generation, which can be used for obtaining clusters.

The peculiarity of the explosive emission is the large current density observed during the existence of an ecton that is $i \sim 10^7 - 10^8 \text{ A cm}^{-2}$ according to experimental data [169–172]. From this one can estimate a size Δz near the cathode where the plasma becomes unipolar due to the ion current. In this unipolar layer, the cathode voltage $U \sim 10 \text{ V}$ is induced, and from the Poisson equation we have the next connection between the cathode voltage and the thickness of the cathode layer Δz :

$$U = 2\pi e N_i \Delta z^2, \quad (5.11)$$

where the number density of ions near the cathode is $N_i = i/(ev_i)$, and the ion velocity $v_i \sim 10^6 \text{ cm s}^{-1}$ is determined by the cathode voltage. Taking the current density $i \sim 10^8 \text{ A cm}^{-2}$, we obtain $N_i \sim 10^{19} \text{ cm}^{-3}$, and the thickness of the cathode layer is estimated as

$$\Delta z \sim 10^{-4} \text{ cm}. \quad (5.12)$$

This value is less or comparable to the mean free path of ions colliding with evaporable atoms, because if this condition is not valid, fast ions do not reach the cathode, and the ion current is quenched. The mean free path λ of ions is determined by the resonant charge exchange process involving the ion and its atom: $\lambda = (N_a \sigma_{\text{res}})^{-1} \sim 10^{-7} \text{ cm}$, where N_a is the number density of atoms, and the cross section of this process is $\sigma_{\text{res}} \sim 10^{-14} \text{ cm}^2$ [173]. From this it follows that the number density of atoms in the region of the ion current does not exceed the value of $N_a \sim 10^{18} \text{ cm}^{-3}$ during the existence of a given ecton.

A current toward the cathode creates a high pressure on the cathode where ions transfer their momenta. This pressure is equal to

$$p = \frac{i}{e} v_i. \quad (5.13a)$$

Assuming ions to be singly charged, and supposing the ion velocity to be determined by the cathode voltage, we obtain for the ion velocity v_i :

$$v_i = \sqrt{\frac{2V}{m_i}}, \quad (5.13b)$$

where m_i is the ion or atomic mass, V is the electric voltage in which the ion is accelerated up to the subsequent charge exchange event, and this voltage is less than the cathode voltage U . Table 15 contains the pressure of the ion current on the cathode surface, calculated according to formulas (5.13) and using the above parameters, if we take $V = 1 \text{ eV}$.

There are two mechanisms for the transformation of a cathode material into ions and electrons which are responsible for the electric current. The first relates to splashing out

the liquid cathode [167, 168] in the form of liquid drops to a plasma that is located about the cathode. The drops are converted into atoms which in turn give electrons and ions to sustain the discharge current. In the framework of the second mechanism, a flux of atoms is evaporated from the cathode surface, similar to that in the case of laser evaporation of a metallic surface (see Section 4.2). We first consider the second mechanism of metal transport, when it moves to a plasma in the form of an atomic beam [90]. When the atomic beam reaches the plasma, atoms are ionized, and ions and electrons are produced. Assuming ions to be singly charged, we arrive at the following connection between the atom flux j from the cathode surface and the ion current density i toward the cathode:

$$\kappa i = e j, \quad (5.14)$$

where the parameter κ is a part of the cathode material injected into the plasma in the form of an atomic flux, and the latter is determined by the cathode temperature according to formula (4.8). Table 15 contains the values of the cathode temperature T if $\kappa = 0.3$ and $\kappa = 0.1$ (in parentheses). Note that the number density of atoms drops 4 times [formula (4.4)] near the surface, when the Maxwell distribution of atoms near the surface is transformed into the distribution for an atomic beam formed. For completeness sake we give in Table 15 the number density of atoms in the beam.

Table 15 also contains the values of the mean free path λ for incident ions with respect to the atomic flux, where the mean free path λ of ions is given by the formula $\lambda = (N_b \sigma_{\text{res}})^{-1}$, with N_b being the number density of atoms in the beam (Table 15), and the cross sections of the resonant charge exchange process are taken from Ref. [173]. One can see that the criterion of a small cathode layer thickness as compared to the mean free path of ions is violated at a hot cathode because of a strong evaporation of atoms from the cathode surface.

Thus, the temperature of the cathode region is limited, since a high temperature causes a high atomic flux that locks the ion current. In addition, a restricted cathode temperature leads to a not high current density i_{th} of electron thermoemission that, according to the explosive emission mechanism, is small compared to the ion current density. Table 15 lists the values of the thermoemission current density which is determined by the Richardson formula (see, for example, Ref. [90]) and we use the parameters of this formula at room temperature. From the data in Table 15 it follows that the cathode temperature is not high, and evaporation of atoms from a hot cathode surface makes a small contribution to metal transport toward the plasma region.

From above reasoning one can see that heating of the cathode causes a high flux of evaporating atoms that blocks the ion current to a heated cathode region. This leads to an instability resulting in the quenching of the ion current which

Table 15. Parameters of the cathode region.

Metal	$i, \text{ A cm}^{-2}$	$p, 10^3 \text{ atm}$	$T, 10^3 \text{ K}$	$N_b, 10^{19} \text{ cm}^{-3}$	$\lambda, 10^{-6} \text{ cm}$	$i_{\text{th}}, \text{ A cm}^{-2}$
Cu	10^7	1.1	4.8 (4.2)	2.0 (0.7)	3.9 (11)	$3 \times 10^4 (5 \times 10^3)$
Cu	10^8	11	6.8 (5.6)	17 (5.8)	0.46 (1.3)	$2 \times 10^6 (2 \times 10^5)$
Mo	10^7	1.4	7.9 (7.0)	1.8 (0.65)	3.6 (10)	$7 \times 10^6 (2 \times 10^6)$
Mo	10^8	14	11 (9.2)	16 (5.7)	0.42 (1.2)	$6 \times 10^7 (2 \times 10^7)$
Ag	10^7	1.5	4.1 (3.6)	2.8 (1.0)	2.6 (7.2)	$5 \times 10^3 (7 \times 10^2)$
Ag	10^8	15	5.9 (4.9)	23 (8.5)	0.31 (0.84)	$5 \times 10^5 (5 \times 10^4)$
W	10^7	1.9	10 (9.2)	3.6 (1.3)	2.0 (5.6)	$5 \times 10^7 (2 \times 10^7)$
W	10^8	19	14 (12)	30 (11)	0.23 (0.64)	$3 \times 10^8 (1 \times 10^8)$

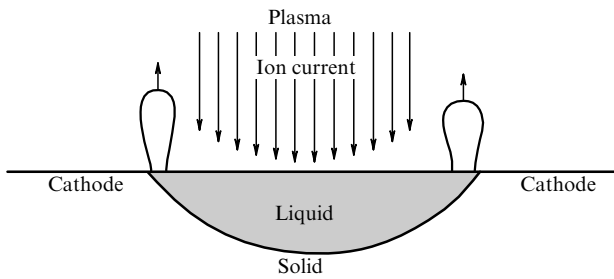


Figure 15. Character of sputtering of liquid drops from a cathode under the action of a discharge ion current from a plasma to the cathode.

does not reach the cathode surface and leaves off an emission at a given point. The time of development of this instability determines the ection lifetime, i.e., a time of emission from a given cathode point. Since the atomic flux is restricted, the basic mechanism of metal transport from the cathode to the plasma is the splashing out of the liquid metal of the cathode under the action of pressure produced by the ion current. Because of the pressure gradient, the peripheral part of the liquid metal is pushed outside the cathode toward the plasma (see Fig. 15). A typical velocity u of the splashing out of the liquid metal can be estimated from the Euler equation, which gives

$$u \sim \sqrt{\frac{p}{\rho}}, \quad (5.15)$$

where p is a typical pressure from the ion current to the cathode, and ρ is the typical density of the liquid metal. In particular, using the parameters of Table 15, we have $u \sim 10^4 \text{ cm s}^{-1}$, i.e., a typical time of transport of a liquid metal to a plasma equals

$$\tau \sim \frac{\Delta z}{u} \sim 10^{-8} \text{ s}, \quad (5.16)$$

where Δz is the thickness of the cathode layer. This estimate, $\tau \sim 10^{-8} \text{ s}$, is in accord with the available experimental data [162, 165, 174–176].

Along with the above hydrodynamic mechanisms for splashing out a liquid metal from a cathode surface in a plasma, other processes are possible because of the non-regular character of cathode heating under the action of the ion current. Indeed, fast cathode heating leads to its boiling, which is accompanied by formation of bubbles inside the metal. This leads to the ejecting of vapor from the cathode together with liquid drops. To such a cavitation character of cathode erosion that is typical for the boiling of fast heated liquids [177], or microexplosions inside solid surfaces [178–180] as a result of input of a high power density, is added the hydrodynamic model of splashing out the liquid metal from the cathode surface to a plasma in accordance with estimate (5.16). The explosive character of electron emission is observed upon investigation of the initial stage of amplification of the electric field in the course of explosive emission near a needle [181], which can result from the cavitation character of emission at the initial stage of this process. Note that the estimate (5.16) is conserved if we take into account the cavitation mechanism of metal transport from the cathode to a plasma, because this estimate assumes a cathode spray in the form of small liquid drops. This mechanism additionally restricts the cathode temperature in the emission region (see Table 15).

Because the process under consideration is not regular, its analysis on the basis of hydrodynamic theory is suitable for estimations only. We give one more confirmation that the atomic flux makes a small contribution to metal emission in the plasma. This flux has a large mean free path in the plasma, and its return to the cathode is problematic. In contrast, liquid drops are transformed into atoms and then into electrons and ions in the vicinity of the cathode, and these ions return to the cathode. Note that clusters and drops can be formed and grow in a cold region, and therefore the measurements of the size distribution of drops [182] cannot give information about the process of splashing out of the melted metal in a plasma.

Thus, metal emission from the cathode in a plasma proceeds mostly in the form of liquid drops as a result of the splashing out of the liquid cathode, but evaporation of atoms from the cathode heated under the action of the ion current also makes a contribution to the transport of the metal in the plasma. We now consider the rate of cathode erosion as a result of explosive emission and introduce the erosion rate as follows

$$\frac{dM}{dQ} = \frac{M}{\int I dt} = \frac{\gamma m}{2e}, \quad (5.17)$$

where M is the mass of the erosive material, $Q = \int I dt$ is the total charge, I is the discharge current, m is the atomic mass, and the coefficient γ is the probability that an evaporating atom which is converted into an electron and a singly charged ion, does not return to the cathode. Table 16 contains the experimental values of this parameter at not high currents [183, 166]. From this we find the average number of atoms which are removed from the cathode per one elementary charge $1/\gamma = 9 \pm 2$.

Table 16. The parameters characterizing the cathode processes.

Metal	$dM/dQ, \mu\text{g C}^{-1}$	γ	$1/\gamma$	T_m, K
Cu	39	0.12	8.5	1358
Mo	55	0.11	9.0	2886
Ag	90	0.16	6.2	1235
W	90	0.095	10.6	3695

Thus, the process of metal transport to a plasma results from a liquid metal splashing out of the cathode under the action of the ion current. One can recognize that the emission process starts near a surface nonuniformity, to which the ion current is directed and which is enforced due to heating. Then a typical size of such a nonuniformity, i.e., the size r of the emission center, is estimated as

$$r \sim (\chi\tau)^{1/2}, \quad (5.18)$$

if the ion current toward the cathode occupies a narrow region at the beginning. Here, τ is a typical time of development of this process, and χ is the thermal diffusivity of a surface material at a given temperature ($\chi \sim 1 \text{ cm}^2 \text{ s}^{-1}$). Evidently, we take a transversal size r of the emission region of the order of thickness Δz of the cathode layer, and this condition $r \sim \Delta z_{\text{max}}$ gives the following estimate for the typical time of the process under consideration:

$$\tau \sim \frac{\Delta z_{\text{max}}^2}{\chi} \sim 10^{-8} \text{ s}. \quad (5.19)$$

This value coincides with estimate (5.16) of transport of a liquid metal from the cathode to a plasma. From this we find a size $r \sim 1 \mu\text{m}$ of an individual emission center that coincides with the thickness of the cathode layer.

We now determine heat release in an intermediate region between the plasma and cathode layer, where the ion current is created. The plasma over the cathode layer is characterized by the electron temperature of 1–3 eV, which leads to significant or full plasma ionization. Therefore, the plasma conductivity can be estimated by the Spitzer formula [184] that relates to a fully ionized plasma, when the resistance is determined by electron–ion scattering. Assuming the plasma to be ideal, we have for the conductivity of this plasma [90]:

$$\Sigma = \frac{N_e e^2}{m_e v_{ei}}, \quad (5.20)$$

where N_e is the electron number density, and the rate of electron–ion collisions has the form [185]

$$v_{ei} = \frac{2\sqrt{2\pi}}{3} \frac{N_i e^4}{T_e^{3/2} m_e^{1/2}} \left(\ln \frac{T_e^3}{2\pi N_i e^6} - 2C \right), \quad (5.21)$$

where e is the electron charge, m_e is the electron mass, N_i is the ion number density, T_e is the electron temperature, and $C = 0.577$ is the Euler constant. This expression relates to the Maxwell distribution function of electrons over energies with the electron temperature T_e , and because the ionized gas is ideal ($N_e e^6 \ll T_e^3$) and quasi-neutral ($N_e = N_i$), the quantity in parentheses is large in comparison to unity. Formulas (5.20) and (5.21) give a typical conductivity of a hot plasma: $\Sigma \sim 100 \Omega^{-1} \text{cm}^{-1}$ at typical electron temperatures $T_e \sim 1-3 \text{ eV}$ (such temperatures lead to a fully ionized plasma under equilibrium conditions). Note that the plasma conductivity does not depend on the density of charged particles in this region, but the size of the intermediate region is large in comparison with the mean free path of electrons in the plasma. In addition, the energy density that is released in the intermediate region between the plasma and cathode layer is estimated as

$$\frac{i^2}{\Sigma} \tau \sim 10^4 - 10^6 \text{ J cm}^{-3}. \quad (5.22)$$

One can expect the same order of magnitude of the heat release on the cathode surface if we model a hot liquid metal of the cathode by a plasma.

From this one can formulate the character of the phenomena under consideration. The process proceeds between the cathode region and a rarefied plasma, which are separated by the cathode layer. When the depth of a metal that is melted and splashed out is compared to the thickness of the cathode layer, emission at this point is finished, because it significantly increases the thickness of the cathode layer, i.e., the distance between the cathode and plasma. From this we find the number n of atoms per one emission center — ecton:

$$n \sim r^3 \frac{\rho}{m} \sim 10^{11}, \quad (5.23)$$

where $r \sim 1 \mu\text{m}$ is an ecton size, ρ is the density of the cathode metal, and m is the atomic mass.

We now consider the ion current from a plasma to the cathode surface from another standpoint. Taking a plasma to be separated from the cathode surface by a gap of length l and

introducing the potential U_0 between them (the cathode voltage), one can find the charge distribution throughout the gap depending on the ion current density i toward the cathode. Taking the cathode surface and plasma surface to be flat and assuming the ion current density i to be constant in the gap, we have for the ion parameters in the gap:

$$i = e N_i(x) v_i(x) = \text{const}, \quad (5.24)$$

where x is the distance from the cathode, N_i is the electron number density, $v_i = \sqrt{2eU(x)/m_i}$ is the ion velocity, m_i is the ion mass, and the electric potential $U(x)$ is zero at the cathode surface — that is, $U(0) = 0$. An ion charge creates an electric field which decelerates the ions. The Poisson equation for the electric field strength $F = -dU/dx$ has the form

$$\frac{dF}{dx} = 4\pi e N_i(x) = 4\pi i \sqrt{\frac{m_i}{2eU}}.$$

Multiplication of this equation by $F = -dU/dx$ allows us to integrate it, which gives

$$F^2 = F_0^2 + 16\pi i \sqrt{\frac{m_i U}{2e}}, \quad (5.25)$$

where $F_0 = F(0)$.

Evidently, the maximum ion current corresponds to the boundary condition $F_0 = 0$ and leads to the following expression for the ion current density toward the cathode:

$$i = \frac{2}{9\pi} \sqrt{\frac{e}{2m_i}} \frac{U_0^{3/2}}{l^2}, \quad (5.26)$$

where U_0 is the cathode voltage, i.e., the difference in the voltages between the cathode and plasma. This coincides with the three-halves power law [90] for thermoemission of electrons from a heated cathode towards a plane electrode, if this current density is less than the thermoemission current density. One can see the analogy between these problems, and formula (5.26) gives the maximum current density. If the initial ion current density exceeds this value, a part of the ions reflects from the potential of this unipolar plasma and returns. This is the Bursian instability [186] which can be overcome by injecting electrons into the gap, where the electrons compensate for the ion charge. But if a current flows through a neutral plasma, a new instability occurs at a higher threshold current density in comparison with the threshold of the Bursian instability. This is so-called Pierce instability [187] which is created by the electric potential of the ion current in the gap, and the Debye shielding is of importance for this instability. The limiting current density in this case, i.e., the threshold of the Pierce instability, according to Refs [188, 186] (with an accuracy up to a factor of the order of one), equals

$$i_p = \frac{eU_0}{T_e} \sqrt{\frac{2e}{m_i}} \frac{U_0^{3/2}}{l^2}, \quad (5.27)$$

where T_e is the electron temperature. As is seen, the threshold of the Pierce instability differs from the threshold of the Bursian instability by the factor eU_0/T_e . Evidently, this mechanism of blocking the ion current in the cathode layer in the course of the passage of the ion current through it [189] also determines the generation of ion currents which move from the cathode [189–191]. For example, taking $U_0 = 20 \text{ V}$,

$i_p = 10^8 \text{ A cm}^{-2}$, and $T_e = 1 \text{ eV}$, we obtain from this formula the cathode layer thickness $l \approx 1.5 \times 10^{-6} \text{ cm}$ for the metals considered in Table 15. Of course, this is a rough estimate. Note that measurements of the voltage distribution in such a layer are problematic. In addition, we are guided by singly charged ions, whereas in reality they have a higher charge [166]. Nevertheless, the above estimates show the character of the processes in the cathode layer. We add to this that, along with the explosive emission, the thermoemission of electrons from the cathode, which makes a small contribution to the discharge current at the basic stage of evolution of the emission center, may be of importance at the stage of the origin of a new emission center.

This analysis reveals that the explosive emission or the Mesyats mechanism of emission leads to the effective erosion of the cathode material because of the nature of this phenomenon, where erosion of the cathode creates a medium which maintains the electric discharge current. From the standpoint of use of explosive emission for the generation of metallic atoms with the subsequent transformation of atoms into clusters, we arrive at the following conclusions. The explosive emission phenomenon is characterized by a high efficiency of transformation of the electric energy of gas discharge into the energy of atom formation at the cathode because of the nature of this process. Then atoms resulting from the cathode erosion are ionized, and the products of ionization (electrons and ions) sustain the gas discharge current, so that the ions go towards the cathode and the electrons move in the reverse direction. There are two types of ion currents in these processes. The first is directed from the gas discharge plasma and cathode layer to the cathode, so that the ions attach to the cathode and provide in this way the charge transport to the cathode. It is impossible to take these ions from the gas discharge without violating the current passage in it. The other type of ion current is directed from the cathode and results from reflection of part of the ion current from the electric potential of the cathode layer. This ion current amounts approximately to 10% of the total ion current (see Table 16) and is taken from the plasma in the simple way. These ions have an energy of several dozens or hundred eV and can be applied to ion technology such as ion implantation [192]. But these ions are not suitable for generation of clusters because of their high energy. Thus, though the explosive emission phenomenon is effective for generation of atomic ions, it is not of interest for generation of the beams of metallic clusters.

6. Applications of cluster beams

6.1 Cluster beams for fabrication of films and materials

Clusters have a high reactivity, and if the contact between two clusters leads to their joining, then the properties of incident clusters are lost in the cluster formed. Therefore in various applications clusters are used in the form of cluster beams. The main application of cluster beams is the production of so-called cluster-assembled materials [193–197] which have specific properties and constitute nanostructures [34]. There are two methods for using cluster beams for this purpose. The first one, the ‘Ion Cluster Beam Method’ [28], employs a beam of charged liquid clusters for the fabrication of thin films. In fact, by nature this method is similar to the method of film deposition by atomic beams. The advantage of the ion cluster beam method consists of the possibility of governing the energy

of charged clusters and also rests in a softer heat regime of film growth. A drawback of the ion cluster beam method is the relatively low intensity of beams and low rate of deposition, therefore its application is of interest for microelectronics. For example, the rate of cesium deposition by the ion cluster beam method with cesium clusters of 10^3 – 10^4 atoms in size is 4 nm s^{-1} [198], the maximum rate of silver deposition by silver clusters formed by free jet expansion of a silver vapor is 74 nm s^{-1} [149, 144], and the rate of zinc deposition with the use of zinc clusters measures about 100 nm s^{-1} [199]. Thin films result from the deposition of cluster beams, when the clusters are found in the liquid state [154]. Note that the specific heat release in the course of this deposition by cluster beams is as low as 0.1 – 1 W cm^{-2} . Because of the low intensity, the ion cluster beam method is only applied for fabrication of small elements of microelectronics.

The other method for using cluster beams employs the low-energy cluster beam deposition technique and involves a beam of neutral solid clusters of low energy [29]. In this case, deposition of a cluster beam is accompanied by a grow of the target itself. As a result, a new film consists of a deposited uniform matrix with embedded clusters. In contrast to the above method of deposition of uniform thin films, in this case clusters are found in the solid aggregate state. Because magic numbers of cluster atoms are preferable for the formation of solid clusters, a cluster beam consists here of solid clusters of almost identical sizes. Thus, this method allows one to create nanometer films deposited from a vapor with embedded clusters of identical sizes, deposited from cluster beams. It is impossible to produce such structures by other methods, and clusters of various materials and sizes can be useful for this purpose (see, for example, Refs [29, 31–33]).

Along with fabrication of materials by deposition of cluster beams on a target, cluster beams are used for cleaning and erosion of surfaces. In particular, the erosion rate 70 nm s^{-1} of a copper surface was achieved [200, 201] by a cluster beam. An example of such a treatment of materials is the RACE (reactive accelerated cluster erosion) method [202–204] that leads to microstructuring of a hard surface by cluster impact. For instance, the bombardment of a surface with accelerated clusters consisting of thousands of CO_2 molecules with an energy of 100 eV per molecule leads to formation of smoothly eroded surfaces of hard materials with hillocks less than 1 nm in height [202–204]. Though at the first stage of impacting with fast clusters craters are formed on the surface [205, 206], their subsequent evolution leads to the formation of such small hillocks. The surface with hillocks of a low height can be used later for deposition of various layers.

The advantage of a cluster beam lies in the possibility of charging clusters and governing cluster beams by electric fields, also changing the cluster energy. Fast cluster ions can even be utilized for thermonuclear fusion reactions [207–212]. Bombardment of foils by fast clusters allows one to make holes in the foils and to fabricate sieves in this manner [159]. Each fast cluster is like a bullet and the hole size depends on the cluster size and energy. Therefore, the density and size of the holes of the sieve formed can be adjusted.

From the standpoint of the interaction of impacting clusters with a surface, one can separate two limiting cases [213]. In the first, the cluster velocity is small compared to the speed of sound. A liquid cluster is then spread over the target surface, and there is an optimal cluster energy for the formation of a stable film on the target surface. For example,

in the case of molybdenum clusters, the optimal energy is about 10 eV per atom [214]. The local temperature reaches 8000 K, and a strongly adhering thin film forms on the surface of some metals. The other limiting case is realized if the cluster velocity exceeds the speed of sound. Then a shock wave accompanies the interaction of the impacting cluster with the surface, and craters are formed on the surface, whose depth weakly depends on the cluster energy [206]. A subsequent evolution of such craters leads to cleaning of the surface.

In spite of a small cluster size, cluster impacts with a surface do not lead to the creation of small nonuniformities on the surface, whose size is comparable to the cluster size. On the contrary, it is possible by using a focused beam of atomic ions. For example, the focused beam of gallium atomic ions allows one to form a spot 8 nm in size [215], while the size of holes in micron foils under the action of a beam of fast metallic clusters is of order 1 μm [159, 214], though the size of an individual cluster is less than 10 nm. Nevertheless, cluster beams permit one to fabricate uniform thin films of various materials, i.e., metallic, dielectric, semiconductor, and organic films (see, for example, Refs [19–28, 114–118]). In addition, new materials can be prepared by depositing some materials from the vapor by bombarding the films formed with a beam of solid clusters [29]. These materials are uniform films with embedded clusters of close sizes. Films with embedded clusters can be utilized as filters because clusters constitute absorbers in a certain spectral region. The spectral characteristics of these filters can be controlled by the sort, size, and density of embedded clusters. Alongside with filters, films consisting of a transparent matrix with embedded clusters can be used as elements of optoelectronics. Some transitions of clusters as atomic systems can be saturated, so that these films can be employed as optical locks due to their nonlinear transparency.

Films with embedded clusters of magnetic materials (Fe, Co, Ni) constitute magnetic nanostructures and are like multi-domain magnetic systems. In this context, the advantage of these films is as follows. First, the size of individual grains of these films, which coincides with the cluster size, is several times less than for normal magnetic films. This fact reduces the saturation magnetic field for such a magnetic material. Second, the nearby sizes of embedded clusters — magnetic grains — provide improved precision and selectivity for the devices developed on the basis of such magnetic materials. Third, the possibility to vary the type and size of embedded clusters enables one to operate the parameters of magnetic films. Therefore, films with embedded clusters as cluster-assembled materials are a new prospective material for precise devices.

6.2 Laser irradiation of cluster beams

A contemporary application of cluster beams is their excitation by a superpower and ultrashort laser pulse. Typical intensities of laser beams in these experiments are $10^{17}–10^{19}$ W cm $^{-2}$ [216], and the electric field strengths of appropriate electromagnetic waves exceed those of typical atomic fields. Hence, the electric field of a laser beam is able to ionize cluster atoms by the over-barrier ionization process. Moreover, this relates also to the ions formed, so that, as a result of interaction with a laser pulse, clusters are transformed into a system of multicharged ions and free electrons. Part of the electrons leaves the cluster and it is charged positively, whereas the other part of the electrons is kept by

a cluster self-consistent field. Of course, this system consisting of multicharged ions and electrons is unstable, and such a plasma decays as a result of ion motion. Nevertheless, since decay of an excited cluster is determined by ion velocities and a typical time of expansion of this system is less than the duration of the laser pulse, this stage of cluster evolution affects properties of a hot plasma produced. This character of interaction of a cluster beam with a powerful ultrashort laser pulse allows one to input into an electron subsystem a high specific energy that attains ~ 1 keV per released electron. Hence, the process of absorption of laser radiation by a cluster beam leads to the formation of a specific hot plasma.

The processes of evolution of this system are reviewed in Refs [216, 217] and briefly are as follows [218, 219]. In the first stage, electrons of clusters become free with respect to their atomic cores and partially leave the parent clusters. As a result, a nonuniform hot plasma is formed where a part of the electrons is captured by a cluster self-consistent field. In the next stage of cluster evolution, individual clusters expand and fill the region between clusters, so that a uniform hot plasma is formed. Later on this almost uniform plasma also expands, and this process determines the lifetime of the total plasma. Figure 16 represents typical times of separate stages of evolution of cluster beams excited by a superintense ultrashort laser pulse.

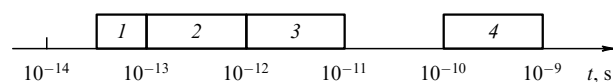


Figure 16. The time scale for processes accompanying excitation of a cluster beam by a superintense ultrashort laser beam: 1 — typical time of laser pulse; 2 — typical lifetime of clusters with respect to their expansion; 3 — time of formation of a uniform plasma after expansion of the plasma of clusters; 4 — time of decay of uniform plasma.

The process of interaction of a cluster beam with an intense laser pulse is used as an effective and compact source of X-rays [220–234]. As a result of absorption of laser radiation, a plasma is formed, consisting of electrons and multicharged ions [216–218]. In the course of evolution of irradiated clusters, multicharged ions of this plasma are excited, and other excitations are created in the plasma. These excitations lead subsequently to emission of hard photons. Note that the possibility to emit short-wave radiation is a property of any hot plasma that contains excited multicharged ions, and the peculiarity of this plasma relates to fast processes in it, so that the duration of the first stage of plasma development is shorter than the time of emission of radiation. This leads to specifics of radiative processes, and excitations are created in the first stages of plasma evolution before expansion of the clusters, whereas radiation is emitted in the subsequent stages of plasma evolution after expansion of the clusters. Nevertheless, this plasma provides a high efficiency of transformation of the laser pulse energy into the energy of X-ray photons — that is, $\sim 1\%$.

Similar processes are developed in a cluster beam if it is used as a compact source of neutrons [235–239]. Then a beam of deuterium clusters is irradiated by an ultrashort laser pulse that leads to ionization of the clusters. This induces a high electric potential for the cluster consisting of deuterium ions, and fast ions are formed as a result of the decay of this

cluster under the action of the self-consistent cluster field. The kinetic energy of deuterium ions reaches several keV, and collisions of fast deuterium ions in the next stage of plasma evolution, when the plasma becomes uniform, can lead to a fusion nuclear reaction. This scheme does not allow one to construct a thermonuclear reactor since the Lawson parameter for this system is less than the threshold one by four–five orders of magnitude. Nevertheless, in this way, on the basis of beams of deuterium or deuterium-contained clusters, one can construct a compact source of neutrons. Thus, combination of cluster beams with intense ultrashort laser beams gives new compact sources of X-rays and neutrons.

6.3 Collision of cluster beams

We now call attention to one more example of cluster applications, which relates to cluster excitation and is similar to the previous case of cluster irradiation by an intense femtosecond laser pulse. This example is connected with the collision of two beams of fast clusters, when the kinetic energy of the colliding clusters is transformed into the excitation energy of the clusters. Though under contemporary possibilities of cluster acceleration this method does not lead to high cluster excitations compared to the laser method, it is a prospective method for exciting the cluster matter. The processes of excitation in cluster collisions resemble the processes of cluster excitation by a laser pulse. As a result of the collision between two clusters, a united cluster is formed in the course of the collision process, and the kinetic energy of cluster atoms is converted into the excitation of electrons. Then a part of electrons leaves the united cluster, and after a lapse of a typical time of motion of nuclei, the plasma formed expands into the surrounding space as a result of ion interaction with a self-consistent cluster field. This leads to formation of a uniform hot plasma which occupies all the volume of cluster beams. This plasma decays later by expansion into the surrounding space.

A general scheme of the collision of two cluster beams is depicted in Fig. 17. Parameters of each cluster beam are taken according to evaluations of Section 4.5, so that the density of clusters in a beam, N_{cl} , the number density of bound atoms in the space, N_b , and the cluster size, n , are taken from Table 11, while the beam shape depends on the nozzle. Taking a nozzle in the form of a narrow slit, we obtain a cluster beam of a rectangular cross section. Clusters of this beam are charged by a crossing electron beam, atoms of a buffer gas are pumped out, and a beam of charged clusters is operated by electric optics. Cluster beams with a rectangular cross section are convenient for collisions. Considering frontal collisions of cluster beams with a small angle between them, we obtain the following criterion for the beam length L :

$$N_{cl}\sigma L \geq 1, \tag{6.1}$$

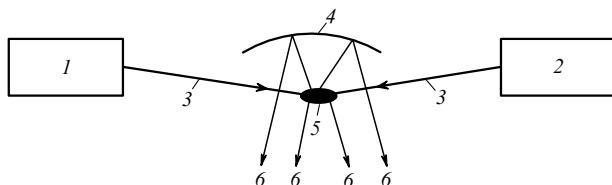


Figure 17. Character of collision of two pulse cluster beams: 1, 2 — generators of pulse cluster beams, 3 — cluster beams, 4 — reflector, 5 — region of intersection of cluster beams, 6 — X-ray beams.

which provides for the collision of most of the clusters in the beam. Here, $\sigma = 4\pi r_W^2 n^{2/3}$ is the cross section of collisions of two identical clusters, and r_W is the Wigner–Seitz radius of clusters. Since $N_{cl} = N_m/n$, where N_m is the number density of bound metallic atoms in clusters of the beam, we have criterion (6.1) in the form

$$4\pi r_W^2 N_m L \geq n^{1/3}. \tag{6.2}$$

Criterion (6.2) is optimal for cluster collisions. In the case of the clusters under consideration (Mo, W and Ir clusters for which $r_W \approx 1.6 \text{ \AA}$ according to Table 1), and taking according to Table 11 the number density of bound metallic atoms as $N_m \sim 3 \times 10^{19} \text{ cm}^{-3}$, we reduce this criterion to the following one:

$$\frac{L}{n^{1/3}} \geq 10^{-5} \text{ cm}. \tag{6.3}$$

In particular, taking a typical cluster size $n \sim 10^6$, we obtain from formula (6.3) that $L > 10 \text{ \mu m}$, which shows the reality of realizing the collision of two cluster beams, if each cluster of one beam can collide with clusters of the other beam.

The character of cluster collisions is determined by the interaction of the clusters with matter where they are moving [240, 241]. Then it depends on the collision velocity of clusters and a degree of cluster excitation as a result of this collision. We consider such a degree of cluster excitation when chemical bonds between atoms are broken, and atomic particles of one cluster penetrate freely into another one. Then the subsequent cluster excitation results from the energy transfer from heavy atomic particles, which carry the kinetic energy of the colliding clusters, to excitation of the electron subsystem. In collisions of large clusters, as well as in collisions of a cluster with a solid, collective degrees of freedom, like shock waves and plasma oscillations, are excited along with excitation of the electron subsystem. There are various models for the analysis of these processes in the plasma which is produced in such collisions (see, for example, Refs [242–247]). We restrict ourselves below to the simple schemes which describe the transformation of the nuclear kinetic energy into the energy of electron excitation.

We assume that each cluster in the course of collision is divided into individual ions, so that each ion interacts with the surrounding matter and is moving in it independently. We consider two limiting cases of ion deceleration under this assumption, considering the electron subsystem to be weakly and strongly excited. In the first case, a test ion is decelerated as a result of motion in the system of degenerate electrons, and this gives the lower limit for the deceleration rate, if we model the cluster matter by a degenerate electron gas at zero temperature. Because in this case the degenerate electron gas is located inside the Fermi sphere in a momentum space, we have for the deceleration rate [248, 249]:

$$-\frac{dE}{dx} = \frac{2Z\hbar v}{3\pi a_0^2} \left(\ln \frac{4}{\alpha} - 3 + 3\alpha \ln \frac{4}{\alpha} - \frac{11}{2} \alpha \right) = C(\alpha) \frac{Z\hbar v}{a_0^2},$$

$$\alpha = \frac{e^2}{\hbar\pi v_F}. \tag{6.4}$$

Here, a small parameter of this expansion is $\alpha \approx e^2/(\hbar\pi v_F)$, e is the electron charge, a_0 is the Bohr radius, Z is the effective charge of a nucleus which is moving with a velocity v inside the cluster, v_F is the Fermi velocity for a dense degenerate

electron gas, and the criterion

$$v \ll v_F \quad (6.5)$$

holds true. In this case, the velocity distribution of electrons corresponds to their location inside a sphere of radius v_F in the velocity space. From this it follows that an incident nucleus interacts only with electrons located near the Fermi surface, because the scattered electron changes its velocity by a value of order $v \ll v_F$, and the scattered electron cannot be found inside the Fermi sphere. Hence, the expression (6.4) corresponds to the lower limit of the deceleration rate, because when cluster electrons are excited, the prohibition for transitions of internal electrons due to the Pauli exclusion principle is lost, and the deceleration rate increases.

We now determine the parameters of formula (6.4) for real clusters. Considering cluster electrons as a degenerate electron gas, we obtain the Fermi velocity for these electrons:

$$v_F = \frac{\hbar}{m_e} (3\pi^2 N_e)^{1/3},$$

where N_e is the electron number density. Assuming that each atom in a metallic cluster gives Z electrons, we get for a small parameter of formula (6.4) the following relationship

$$\alpha = \frac{0.11 r_W}{a_0 Z^{1/3}},$$

where a_0 is the Bohr radius, and r_W is the Wigner–Seitz radius, and if we take its values from Table 1 for Mo, Ir, and W clusters, we obtain

$$\alpha = \frac{0.34}{Z^{1/3}}. \quad (6.6)$$

In this problem, Z , the effective charge of an atomic ion moving in the cluster matter, depends on the ion velocity. For the velocities under consideration $Z = 5–10$, and the function $C(\alpha)$ varies from 0.15 up to 0.19 in this range of Z . Correspondingly, the mean free path of atomic ions of one cluster, which transfers its kinetic energy to electrons of another cluster, is equal in this case to

$$\lambda \approx (5–6) \frac{m_i v a_0^2}{Z \hbar}, \quad (6.7)$$

where m_i is the atomic ion mass.

We now consider another limiting case of the behavior of the electron subsystem in the course of its excitation as a result of ion motion inside the electron subsystem, assuming any final states of scattered electrons to be free. Then the deceleration rate for an ion with respect to the excitation of electrons is given by [250]

$$-\frac{dE}{dt} = N_e v \frac{4\pi Z e^4}{m_e v^2} \ln A. \quad (6.8)$$

Here, v is the ion velocity inside the electron subsystem, and it is assumed that the scattering of individual electrons proceeds independently; $A = p_{\max}/p_{\min}$, where $p_{\max} = m_e v$ is the maximum momentum transferred to a scattered electron, and p_{\min} is its minimum value that is determined by the structure of the electron subsystem. We use for estimation the

Coulomb logarithm $\ln A \approx 5–10$. According to the definition of the Wigner–Seitz radius r_W , we obtain for the electron number density

$$N_e = \frac{3Z}{4\pi r_W^3}.$$

Formula (6.8) gives the mean free path of ions in the electron medium:

$$\lambda = \frac{E m_e v^2 r_W^3}{3Z^2 e^4 \ln A}. \quad (6.9)$$

In these two limiting cases of ion deceleration in an electron matter, the mean free paths evaluated on the basis of formulas (6.7) and (6.9) differ by several orders of magnitude. Therefore, these models are able to give the limiting estimates for parameters of cluster collisions.

Figure 17 gives a scheme of collision of two cluster beams. In the final stage of cluster generation, clusters are charged by an electron beam and are then accelerated in an electric field. We take the maximum cluster charge to be, according to formula (3.51) and data from Table 7, approximately $n^{1/2}e$, and the voltage of cluster acceleration to be $V = 1$ MV. For clusters of size $n \sim 10^6$, in this case each cluster is accelerated up to an energy ~ 1 MeV per unit charge or ~ 1 keV per nucleus. This corresponds to a relative velocity $v \approx 10^7$ cm s⁻¹ of motion with respect to other clusters. Under these conditions we get for the mean free path of ions on the basis of formula (6.7): $\lambda \sim 10^3 a_0$, and on the basis of formula (6.9): $\lambda \ll a_0$. Hence, the optimal cluster size depends on the initial stage of the deceleration process that leads to transformation of the kinetic energy into the energy of excitation of the electron subsystem. When all the kinetic energy of nuclei is transformed into the excitation energy of the electron subsystem, the latter will be heated up to the temperature ~ 100 eV.

Thus, as a result of the collision of two clusters, a plasma is produced with a high electron temperature. The properties of this plasma are similar to the case of a plasma obtained by the excitation of a cluster beam with an ultrashort and superpower laser pulse. The lifetime of the nonuniform plasma resulting from the collision of two clusters is $\sim r_W n^{1/3}/v \sim 10^{-13}$ s. During this time excited multicharged ions are formed and they emit X-ray radiation in the next stage of plasma evolution, when this plasma expands into the surrounding space. As a result, the collision of cluster beams leads to the emission of X-rays, and the efficiency of transformation of the kinetic energy of colliding atoms into the energy of X-rays is expected to be similar to that in the laser case, i.e., $\sim 1\%$.

Evolution of a cluster plasma formed in the collision of cluster beams has common features with a plasma generated by the excitation of a cluster beam by an ultrashort and superpower laser pulse. Assuming that the collision of two clusters leads to the transformation of their kinetic energy into the energy of excitation of the electron subsystem of clusters, we obtain the following typical times for the example under consideration. The lifetime of a system of two colliding clusters, $\sim 10^{-13}$ s, is also a time of cluster expansion when the cluster is excited by a laser pulse. A typical time of transformation of this nonuniform plasma into a uniform one as a result of the expansion of cluster ions in a surrounding space is $\sim 10^{-12}–10^{-11}$ s in both cases, and a

typical time of collision of two cluster beams, which characterizes the lifetime of the total system, is $\sim 10^{-10}$ s. In addition, the electric potential of beams of charged clusters is equal to 10–100 kV in the case of the collision of cluster beams, and is ~ 10 kV in the case of irradiation of a cluster beam by a laser pulse. Thus, both considered cases of cluster excitation are characterized by the identical nature of the processes and correspond to the same applications. The possibility of using above concepts for applications depend on the experimental technique used and can lead to new possibilities in the future.

Thus, the basic application of cluster beams relates to the transport of a material to a target in the form of cluster beams. Thin films and new materials, which are uniform films with embedded solid clusters of almost identical sizes, are manufactured on the basis of the method of cluster beams. The other cluster application relates to the excitation of cluster beams and the generation of a nonuniform hot plasma in this way. This excitation is realized on the basis of a superpower ultrashort laser pulse, as well as a result of the collision of cluster beams. The plasma formed may be used as a source of X-ray emission or as a source of neutrons if the clusters of a beam contain deuterium.

7. Conclusions

Cluster beams present one form of contemporary micro-technology and nanotechnology, where they are used for the fabrication of thin films and the manufacturing of new materials. This path for such a fine and science-consuming technology requires understanding cluster properties and processes involving clusters, which is the basis for creating new concepts of cluster technology and optimization of appropriate technological processes. Because clusters conserve their individuality in cluster beams, these beams are of interest for the study of cluster properties and cluster processes. In turn, generation of cluster beams includes many processes, the study of which allows one to optimize cluster generation. Therefore, the fundamental and applied aspects of clusters are entangled, so that the development of the physics of clusters and cluster technology involves an interrelationship. Appearance of new application aspects promotes a deeper understanding of related processes and is conducive to this. This review demonstrates this fact, so that the applied problem of the generation of cluster beams is supported by the study of processes involving clusters. This leads both to a deeper understanding of this problem and to its connection with fundamentals.

This paper is supported in part by RFBR grant # 03-02-16059.

References

- Johnson B F G (Ed.) *Transition Metal Clusters* (Chichester: J. Wiley, 1980)
- Cotton F A et al. *Clusters* (Structure and Bonding, Vol. 62) (Berlin: Springer-Verlag, 1985)
- Moskovits M (Ed.) *Metal Clusters* (New York: Wiley, 1986)
- Sugano S *Microcluster Physics* (Berlin: Springer-Verlag, 1991)
- Smirnov B M *Kompleksnye Iony* (Complex Ions) (Moscow: Nauka, 1983) [Translated into English: *Cluster Ions and Van der Waals Molecules* (Philadelphia: Gordon and Breach Sci. Publ., 1992)]
- González-Moraga G *Cluster Chemistry: Introduction to the Chemistry of Transition Metal and Main Group of Element Molecular Clusters* (Berlin: Springer-Verlag, 1993)
- Haberland H (Ed.) *Clusters of Atoms and Molecules II: Salvation and Chemistry of Free Clusters, and Embedded, Supported, and Compressed Clusters* (Springer Ser. in Chem. Phys., Vol. 56) (New York: Springer-Verlag, 1994)
- Kreibig U, Vollmer M *Optical Properties of Metal Clusters* (Berlin: Springer-Verlag, 1995)
- Haberland H (Ed.) *Clusters of Atoms and Molecules I: Theory, Experiment, and Clusters of Atoms* (Springer Ser. in Chem. Phys., Vol. 52) (Berlin: Springer-Verlag, 1994)
- Smirnov B M *Clusters and Small Particles in Gases and Plasmas* (New York: Springer, 2000)
- Becker E W, Bier K, Henkes W Z. *Phys.* **146** 333 (1956)
- Henkes W Z. *Naturforsch. A* **16** 842 (1961)
- Henkes W Z. *Naturforsch. A* **17** 786 (1962)
- Hagena O F, Obert W J. *Chem. Phys.* **56** 1793 (1972)
- Hagena O F, in *Molecular Beams and Low Density Gasdynamics* (Gasdynamics, Vol. 4, Ed. P P Wegener) (New York: M. Dekker, 1974) p. 93
- Hagena O F *Surf. Sci.* **106** 101 (1981)
- Gspann J Z. *Phys. D: At. Mol. Clust.* **3** 143 (1986)
- Aleksandrov M L, Kusner Yu S *Gazodinamicheskie Molekulyarnye Ionnye i Klasterne Puchki* (Gasdynamic Molecular Ion and Cluster Beams) (Leningrad: Nauka, 1989)
- Takagi T, Yamada I, Sasaki A *J. Vac. Sci. Technol.* **12** 1128 (1975)
- Yamada I, Usui H, Takagi T *J. Phys. Chem.* **91** 2463 (1987)
- Takagi T *J. Vac. Sci. Technol. A* **2** 382 (1984)
- Yamada I, Inokawa H, Takagi T *J. Appl. Phys.* **56** 2746 (1984)
- Takagi T et al. *Thin Solid Films* **126** 149 (1985)
- Takaoka G H, Yamada I, Takagi T *J. Vac. Sci. Technol. A* **3** 2665 (1985)
- Usui H, Yamada I, Takagi T *J. Vac. Sci. Technol. A* **4** 52 (1986)
- Yamada I et al. *J. Vac. Sci. Technol. A* **4** 722 (1986)
- Takagi T *Vacuum* **36** 27 (1986)
- Takagi T *Ionized-Cluster Beam Deposition and Epitaxy* (Park Ridge, NJ: Noyes Publ., 1988)
- Perez A et al. *J. Phys. D: Appl. Phys.* **30** 709 (1997)
- Perllarin M et al. *Chem. Phys. Lett.* **277** 96 (1997)
- Mélinon P et al. *J. Chem. Phys.* **107** 10278 (1997)
- Palpant B et al. *Phys. Rev. B* **57** 1963 (1998)
- Ray C et al. *Phys. Rev. Lett.* **80** 5365 (1998)
- Gleiter H *Nanostruct. Mater.* **6** 3 (1995)
- Echt O, Sattler K, Recknagel E *Phys. Rev. Lett.* **47** 1121 (1981)
- Knight W D et al. *Phys. Rev. Lett.* **52** 2141 (1984)
- Harris I A, Kidwell R S, Northby J A *Phys. Rev. Lett.* **53** 2390 (1984)
- Martin T P et al. *Chem. Phys. Lett.* **172** 209 (1990)
- Valkealahti S, Manninen M *Z. Phys. D: At. Mol. Clust.* **26** 255 (1993)
- Lide D R (Ed.) *Handbook of Chemistry and Physics* 79th ed. (London: CRC Press, 1998–1999)
- Smirnov B M *Usp. Fiz. Nauk* **170** 495 (2000) [*Phys. Usp.* **43** 453 (2000)]
- Ino S *J. Phys. Soc. Jpn.* **27** 941 (1969)
- Smirnov B M *Plasma Chem. Plasma Process.* **13** 673 (1993)
- Smirnov B M *Usp. Fiz. Nauk* **164** 665 (1994) [*Phys. Usp.* **37** 621 (1994)]
- ter Haar D, Wergeland H *Elements of Thermodynamics* (Reading, Mass.: Addison-Wesley Publ. Co., 1966)
- Landau L D, Lifshitz E M *Statisticheskaya Fizika* (Statistical Physics) Pt. 1 (Moscow: Nauka, 1976) [Translated into English (Oxford: Pergamon Press, 1980)]
- Smirnov B M *Statistical Physics and Kinetic Theory of Atomic Systems* (Moscow: IVT RAN Publ., 2001)
- Zel'dovich Ya B *Zh. Eksp. Teor. Fiz.* **12** 525 (1942)
- Frenkel' Ya I *Kineticheskaya Teoriya Zhidkosti* (Kinetic Theory of Liquids) (Moscow–Leningrad: Izd. AN SSSR, 1945) [Translated into English (Oxford: The Clarendon Press, 1946)]
- Abraham F F *Homogeneous Nucleation Theory* (New York: Academic Press, 1974)
- Landau L D, Lifshitz E M *Statisticheskaya Fizika* (Statistical Physics) Pt. 2 (Moscow: Nauka, 1978) [Translated into English (Oxford: Pergamon Press, 1980)]
- Gutzow I, Schmelzer J *The Vitreous State* (Berlin: Springer-Verlag, 1995)

53. Voloshchuk V M *Kineticheskaya Teoriya Koagulyatsii* (Kinetic Theory of Coagulation) (Leningrad: Gidrometeoizdat, 1984)
- [doi](#) 54. Blum J et al. *Phys. Rev. Lett.* **85** 2426 (2000)
55. Ostwald W Z. *Phys. Chem.* **34** 495 (1900)
56. Aleksandrov L N *Kinetika Obrazovaniya i Struktury Tverdykh Sloev* (Kinetics of Formation and Structures of Solid Layers) (Novosibirsk: Nauka, 1972)
57. Geguzin Ya E, Kaganovskii Yu S *Usp. Fiz. Nauk* **125** 489 (1978) [*Sov. Phys. Usp.* **21** 611 (1978)]
58. Lewis B, Anderson J C *Nucleation and Growth of Thin Films* (New York: Academic Press, 1978)
59. Slezov V V, Sagalovich V V *Usp. Fiz. Nauk* **151** 67 (1987) [*Sov. Phys. Usp.* **30** 23 (1987)]
60. Trofimov V I, Osadchenko V A *Rost i Morfologiya Tonkikh Plenok* (Growth and Morphology of Thin Films) (Moscow: Energoatomizdat, 1993)
61. Kukushkin S A, Slezov V V *Dispersnye Sistemy na Poverkhnosti Tverdykh Tel* (Disperse Systems on Solid Surfaces) (St. Petersburg: Nauka, 1996)
- [doi](#) 62. Kukushkin S A, Osipov A V *Usp. Fiz. Nauk* **168** 1083 (1998) [*Phys. Usp.* **41** 983 (1998)]
63. Lifshitz I M, Slezov V V *Zh. Eksp. Teor. Fiz.* **35** 479 (1958) [*Sov. Phys. JETP* **8** 331 (1959)]
64. Lifshitz I M, Slezov V V *Fiz. Tverd. Tela* **1** 1401 (1959)
- [doi](#) 65. Lifshitz I M, Slyozov V V *J. Phys. Chem. Solids* **19** 35 (1961)
66. Kondrat'ev V N *Konstanty Skorostei Gazofaznykh Reaktsii* (Rate Constants of Gas Phase Reactions) (Moscow: Nauka, 1970) [Translated into English (Washington: Office of Standard Reference Data, National Bureau of Standards, U.S. Dept. of Commerce, 1972)]
67. Rao B K, Smirnov B M *Phys. Scripta* **56** 439 (1997)
- [doi](#) 68. Smirnov B M *Usp. Fiz. Nauk* **167** 1169 (1997) [*Phys. Usp.* **40** 1117 (1997)]
- [doi](#) 69. Chu J H, Lin I *Phys. Rev. Lett.* **72** 4009 (1994)
- [doi](#) 70. Thomas H et al. *Phys. Rev. Lett.* **73** 652 (1994)
71. Hayashi Y, Tachibana K *Jpn. J. Appl. Phys. Pt. 2* **33** L804 (1994)
- [doi](#) 72. Melzer A, Trottenberg T, Piel A *Phys. Lett. A* **191** 301 (1994)
- [doi](#) 73. Nefedov A P, Petrov O F, Fortov V E *Usp. Fiz. Nauk* **167** 1215 (1997) [*Phys. Usp.* **40** 1163 (1997)]
74. Bouchoule A “Technological impacts of dusty plasmas”, in *Dusty Plasmas: Physics, Chemistry, and Technological Impacts in Plasma Processing* (Ed. A Bouchoule) (Chichester: Wiley, 1999)
75. Kaplan S A, Pikel'ner S B *Interstellar Medium* (Cambridge, Mass.: Harvard Univ. Press, 1982)
- [doi](#) 76. Tsytoich V N *Usp. Fiz. Nauk* **167** 57 (1997) [*Phys. Usp.* **40** 53 (1997)]
- [doi](#) 77. Morfill G E et al. *Phys. Plasmas* **6** 1769 (1999)
78. Weber B, Scholl R *J. Illum. Eng. Soc.* (Summer) 93 (1992)
79. Scholl R, Weber B, in *Physics and Chemistry of Finite Systems: from Clusters to Crystals* Vol. 2 (Eds P Jena, S N Khana, B K Rao) (Dordrecht: Kluwer Acad. Publ., 1992) p. 1275
- [doi](#) 80. Weber B, Scholl R *J. Appl. Phys.* **74** 607 (1993)
81. Scholl R, Natour G, in *Phenomena in Ionized Gases* (AIP Conf. Proc., Vol. 363, Eds K H Becker, W E Carr, E E Kunhardt) (Woodbury, NY: American Institute of Physics, 1996) p. 373
82. Smirnov B M *Phys. Scripta* **58** 363 (1998)
- [doi](#) 83. Smirnov B M *J. Phys. D: Appl. Phys.* **33** 115 (2000)
- [doi](#) 84. Smirnov B M *J. Appl. Phys.* **87** 3279 (2000)
- [doi](#) 85. Smirnov B M *Phys. Scripta* **62** 148 (2000)
86. Smirnov B M, in *Proc. 12th Symp. on Application of Plasma Processes: SAPP, Liptovský Ján, Feb. 9–13, 1999. Symp. Proc.* (Eds J D Skalný, J Ráhel) (Bratislava: Comenius Univ., 1999) p. 45
87. Chapman S, Cowling T G *The Mathematical Theory of Non-Uniform Gases* (Cambridge: Univ. Press, 1952)
88. Ferziger J H, Kaper H G *Mathematical Theory of Transport Processes in Gases* (Amsterdam: North-Holland Publ. Co., 1972)
- [doi](#) 89. Smirnov B M *Phys. Scripta* **64** 152 (2001)
90. Smirnov B M *Physics of Ionized Gases* (New York: Wiley, 2001)
91. Cobine J D *Gaseous Conductors* (New York: Dover Publ., 1958)
92. Hoyaux M F *Arc Physics* (New York: Springer-Verlag, 1968)
93. Neumann W *The Mechanism of the Thermoemitting Arc Cathode* (Berlin: Academic-Verlag, 1987)
- [doi](#) 94. Haberland H et al. *J. Vac. Sci. Technol. A* **12** 2925 (1994)
95. Landau L D, Lifshitz E M *Elektrodinamika Sploshnykh Sred* (Electrodynamics of Continuous Media) (Moscow: Nauka, 1982) [Translated into English (Oxford: Pergamon Press, 1984)]
96. Emeleus K, Breslin A *Int. J. Electron.* **54** 195 (1983)
97. Eletskaia A V, Smirnov B M *Usp. Fiz. Nauk* **159** 45 (1989) [*Sov. Phys. Usp.* **32** 763 (1989)]
- [doi](#) 98. Ding A, Hesslich J *Chem. Phys. Lett.* **94** 54 (1983)
- [doi](#) 99. Märk T D, Scheier P J *Chem. Phys.* **87** 1456 (1987)
- [doi](#) 100. Echt O et al. *Phys. Rev. A* **38** 3236 (1988)
- [doi](#) 101. Scheier P, Stamatovic A, Märk T D *J. Chem. Phys.* **89** 295 (1988)
- [doi](#) 102. Lezius M et al. *J. Chem. Phys.* **91** 3240 (1989)
103. Barlak T M et al. *J. Phys. Chem.* **85** 3840 (1981)
104. Barlak T M et al. *J. Am. Chem. Soc.* **104** 1212 (1982)
- [doi](#) 105. Ens W, Beavis R, Standing K G *Phys. Rev. Lett.* **50** 27 (1983)
- [doi](#) 106. Martin T P *Phys. Rep.* **95** 167 (1983)
107. Martin T P *Ber. Bunsenges. Phys. Chem.* **88** 300 (1984)
108. Fayet P, Woste J Z. *Phys. D: At. Mol. Clust.* **3** 177 (1986)
109. Begemann W et al. *Z. Phys. D: At. Mol. Clust.* **3** 183 (1986)
110. Ganteför G et al. *Z. Phys. D: At. Mol. Clust.* **9** 253 (1988)
111. Begemann W et al. *Z. Phys. D: At. Mol. Clust.* **12** 229 (1989)
112. Ganteför G et al. *J. Chem. Soc. Faraday Trans.* **86** 2483 (1990)
113. Lutz H O, Meiwes-Broer K H *Nucl. Instrum. Meth. B* **53** 395 (1991)
114. Takagi T *Pure Appl. Chem.* **60** 781 (1988)
115. Sosnowski M, Yamada I *Nucl. Instrum. Meth. B* **46** 397 (1990)
- [doi](#) 116. Huq S E, McMahon R A, Ahmed H *Semicond. Sci. Technol.* **5** 771 (1990)
- [doi](#) 117. Takaoka G H, Ishikawa J, Takagi T *J. Vac. Sci. Technol. A* **8** 840 (1990)
118. Sosnowski M, Usui H, Yamada I *J. Vac. Sci. Technol. A* **8** 1470 (1990)
119. Smalley R E *Laser Chem.* **2** 167 (1983)
- [doi](#) 120. Hopkins J B et al. *J. Chem. Phys.* **78** 1627 (1983)
- [doi](#) 121. Liu Y et al. *J. Chem. Phys.* **85** 7434 (1986)
- [doi](#) 122. Yang S H et al. *Chem. Phys. Lett.* **139** 233 (1987)
- [doi](#) 123. Cheshnovsky O et al. *Rev. Sci. Instrum.* **58** 2131 (1987)
- [doi](#) 124. Milani P, de Heer W A *Rev. Sci. Instrum.* **61** 1835 (1990)
- [doi](#) 125. Blanc J et al. *J. Chem. Phys.* **102** 680 (1995)
- [doi](#) 126. Nowak C et al. *J. Electron Spectrosc. Relat. Phenom.* **101–103** 199 (1999)
127. Anisimov S I et al. *Deistvie Izlucheniya Bol'shoi Moshchnosti na Metally* (Action of High-Power Radiation on Metals) (Eds A M Bonch-Bruевич, M A El'yashevich) (Moscow: Nauka, 1970)
128. Vedenov A A, Gladush G G *Fizicheskie Protsessy pri Lazernoĭ Obrabotke Materialov* (Physical Processes in Laser Treatment of Materials) (Moscow: Energoatomizdat, 1985)
129. Vorob'ev V S *Usp. Fiz. Nauk* **163** (12) 51 (1993) [*Phys. Usp.* **36** 1129 (1993)]
130. Bunkin F V, Kirichenko N A, Luk'yanchuk B S *Usp. Fiz. Nauk* **138** 45 (1982) [*Sov. Phys. Usp.* **25** 662 (1982)]
131. Bunkin F V, Kirichenko N A, Luk'yanchuk B S *Izv. Akad. Nauk SSSR Ser. Fiz.* **47** 2000 (1983); **48** 1485 (1984); **49** 1054 (1985)
132. Karlov N V, Kirichenko N A, Luk'yanchuk B S *Lazernaya Termokhimiya* (Laser Thermochemistry) (Moscow: Nauka, 1992)
133. Danshchikov E V et al. *Kvantovaya Elektron.* **12** 1863 (1985) [*Sov. J. Quantum Electron.* **15** 1231 (1985)]
134. Vorob'ev V S, Maksimenko S V *Teplofiz. Vys. Temp.* **25** 430 (1987)
135. Bronin S Ya, Polishchuk V P *Teplofiz. Vys. Temp.* **22** 7550 (1984)
136. Brykin M V, Vorob'ev V S, Shelyukhaev B P *Teplofiz. Vys. Temp.* **25** 468 (1987)
137. Lushnikov A A, Pakhomov A V, Chernyaeva G A *Dokl. Akad. Nauk SSSR* **292** 86 (1987) [*Sov. Phys. Dokl.* **32** 45 (1987)]
- [doi](#) 138. Lushnikov A A, Maksimenko V V, Pakhomov A V *J. Aerosol Sci.* **20** 865 (1989)
- [doi](#) 139. Lushnikov A A, Negin A E, Pakhomov A V *Chem. Phys. Lett.* **175** 138 (1990)
140. Lushnikov A A et al. *Usp. Fiz. Nauk* **161** (2) 113 (1991) [*Sov. Phys. Usp.* **34** 160 (1991)]
141. Smirnov B M *Teplofiz. Vys. Temp.* **29** 185 (1991)
142. Smirnov B M *Plasma Chem. Plasma Process.* **12** 177 (1992)
143. Launder B E, Spalding D B *Lectures in Mathematical Models of Turbulence* (London: Academic Press, 1972)

144. Hagena O F, Knop G, Linker G, in *Physics and Chemistry of Finite Systems: from Clusters to Crystals* Vol. 2 (Eds P Jena, S N Khanna, B K Rao) (Dordrecht: Kluwer Acad. Publ., 1992) p. 1233
145. Leontovich M A *Vvedenie v Termodinamiku. Statisticheskaya Fizika* (Introduction to Thermodynamics. Statistical Physics) (Moscow: Nauka, 1983) [Translated into German: *Einführung in die Thermodynamik* (Hochschulbücher für Physik, Bd. 6) (Berlin: Deutscher Verlag der Wissenschaften, 1953)]
146. Hagena O F *Z. Phys. D: At. Mol. Clust.* **4** 291 (1987)
147. Hagena O F *Z. Phys. D: At. Mol. Clust.* **17** 157 (1990)
148. Hagena O F *Z. Phys. D: At. Mol. Clust.* **20** 425 (1991)
149. Hagena O F, Knop G, Ries R *KFK Nachr.* **23** 136 (1991)
- [doi](#) 150. Hagena O F *Rev. Sci. Instrum.* **63** 2374 (1992)
151. Hagena O F, Knop G, in *Rarefied Gas Dynamics: Space Science and Engineering: Proc. of the 18th Symp., July 26–31, 1992, Vancouver, Canada* (Prog. in Astronautics and Aeronautics, Vol. 159, Eds B D Shizgal, D P Weaver) (Washington, DC: AIAA, 1994)
- [doi](#) 152. Smirnov B M *Pis'ma Zh. Eksp. Teor. Fiz.* **68** 741 (1998) [*JETP Lett.* **68** 779 (1998)]
- [doi](#) 153. Smirnov B M *Pis'ma Zh. Eksp. Teor. Fiz.* **71** 588 (2000) [*JETP Lett.* **71** 403 (2000)]
154. Gspann J *Z. Phys. D: At. Mol. Clust.* **3** 143 (1986)
155. Vargaftik N B *Spravochnik po Teplofizicheskim Svoistvam Gazov i Zhidkostei* (Tables of Thermophysical Properties of Liquids and Gases) 2nd ed. (Moscow: Nauka, 1972) [Translated into English (New York: Halsted Press, 1975)]
156. Vargaftik N B et al. *Spravochnik po Teploprovodnosti Zhidkostei i Gazov* (Handbook of Thermal Conductivity of Liquids and Gases) (Moscow: Energoatomizdat, 1990) [Translated into English (Boca Raton: CRC Press, 1994)]
- [doi](#) 157. Preuss D R, Pace S A, Gole J L *J. Chem. Phys.* **71** 3553 (1979)
- [doi](#) 158. Smirnov B M *Usp. Fiz. Nauk* **171** 1291 (2001) [*Phys. Usp.* **44** 1229 (2001)]
- [doi](#) 159. Haberland H et al. *J. Vac. Sci. Technol. A* **10** 3266 (1992)
- [doi](#) 160. Haberland H et al. *Mater. Sci. Eng. B* **19** 31 (1993)
161. Haberland H et al. *Surf. Rev. Lett.* **3** 887 (1996)
162. Mesyats G A, Proskurovsky D I *Impul'snyĭ Elektricheskii Razryad v Vakuume* (Pulsed Electrical Discharge in Vacuum) (Novosibirsk: Nauka, 1984) [Translated into English (Berlin: Springer-Verlag, 1989)]
163. Mesyats G A *Ektony* (Ectons) (Ekaterinburg: UIF Nauka, 1993)
- [doi](#) 164. Mesyats G A *Usp. Fiz. Nauk* **165** 601 (1995) [*Phys. Usp.* **38** 567 (1995)]
165. Mesyats G A *Ektony v Vakuumnom Razryade: Proboi, Iskra, Duga* (Cathode Phenomena in a Vacuum Discharge: the Breakdown, the Spark, and the Arc) (Moscow: Nauka, 2000) [Translated into English (Moscow: Nauka Publ., 2000)]
- [doi](#) 166. Mesyats G A, Barenogol'ts S A *Usp. Fiz. Nauk* **172** 1113 (2002) [*Phys. Usp.* **45** 1001 (2002)]
167. Mesyats G A *Pis'ma Zh. Eksp. Teor. Fiz.* **60** 514 (1994) [*JETP Lett.* **60** 527 (1994)]
- [doi](#) 168. Mesyats G A *IEEE Trans. Plasma Sci.* **PS-23** 879 (1995)
- [doi](#) 169. Sanger C C, Secker P E *J. Phys. D: Appl. Phys.* **4** 1940 (1971)
170. Daalder J E *IEEE Trans. Power Ap. Syst.* **PAS-93** 1747 (1974)
171. Mesyats G A et al. *Pis'ma Zh. Tekh. Fiz.* **11** 398 (1985) [*Sov. Tech. Phys. Lett.* **11** 164 (1985)]
- [doi](#) 172. Vogel N, Jüttner B J *Phys. D: Appl. Phys.* **24** 922 (1991)
- [doi](#) 173. Smirnov B M *Usp. Fiz. Nauk* **170** 495 (2000) [*Phys. Usp.* **43** 453 (2000)]
- [doi](#) 174. Jüttner B J *Phys. D: Appl. Phys.* **28** 516 (1995)
175. Jüttner B J *Phys. IV* (Paris) **7** C4-31 (1997)
- [doi](#) 176. Jüttner B J *Phys. D: Appl. Phys.* **34** R103 (2001)
177. Pavlov P A *Dinamika Vskipaniya Sil'no Peregretykh Zhidkostei* (Dynamics of Boiling of Strongly Overheated Liquids) (Sverdlovsk: Izd. UrO AN SSSR, 1988)
- [doi](#) 178. Vorob'ev V S, Malyschenko S P *Phys. Rev. E* **56** 3959 (1997)
- [doi](#) 179. Vorob'ev V S et al. *Pis'ma Zh. Eksp. Teor. Fiz.* **75** 445 (2002) [*JETP Lett.* **75** 373 (2002)]
- [doi](#) 180. Vorob'ev V S, Malyschenko S P, Tkachenko S I *Pis'ma Zh. Eksp. Teor. Fiz.* **76** 503 (2002) [*JETP Lett.* **76** 428 (2002)]
181. Kartsev G K et al. *Dokl. Akad. Nauk SSSR* **192** 309 (1970)
- [doi](#) 182. Utsumi T, English J H *J. Appl. Phys.* **46** 126 (1975)
- [doi](#) 183. Daalder J E *J. Phys. D: Appl. Phys.* **8** 1647 (1975)
184. Spitzer L *Physics of Fully Ionized Gases* 2nd ed. (New York: Interscience Publ., 1962)
185. Smirnov B M *Atomnye Stolkoveniya i Elementarnye Protsessy v Plazme* (Atomic Collisions and Elementary Processes in Plasma) (Moscow: Atomizdat, 1968)
186. Nezhlin M V *Dinamika Puchkov v Plazme* (Dynamics of Beams in a Plasma) (Moscow: Energoizdat, 1982) [Translated into English: *Physics of Intense Beams in Plasmas* (Bristol: Institute of Physics Publ., 1993)]
187. Pierce J R *J. Appl. Phys.* **15** 721 (1944)
188. Popov Yu S *Pis'ma Zh. Eksp. Teor. Fiz.* **4** 352 (1966) [*JETP Lett.* **4** 238 (1966)]
189. Plyutto A A, Ryzhkov V N, Kapin A T *Zh. Eksp. Teor. Fiz.* **47** 494 (1964) [*Sov. Phys. JETP* **20** 328 (1965)]
190. Kassirov G M, Mesyats G A *Zh. Tekh. Fiz.* **34** 1476 (1964) [*Sov. Phys. Tech. Phys.* **9** 1141 (1965)]
191. Bugaev S P et al. *Zh. Tekh. Fiz.* **37** 2206 (1967) [*Sov. Phys. Tech. Phys.* **12** 1358 (1968)]
192. Boxman R L, Sanders D M, Martin P J (Eds) *Handbook of Vacuum Arc Science and Technology: Fundamentals and Applications* (Park Ridge, NJ: Noyes Publ., 1995)
- [doi](#) 193. de Heer W A, Milani P, Chtelain A *Phys. Rev. Lett.* **65** 488 (1990)
- [doi](#) 194. Khanna S N, Linderoth S *Phys. Rev. Lett.* **67** 742 (1991)
195. Jena P et al. *Mater. Res. Soc. Symp. Proc.* **206** 3 (1991)
- [doi](#) 196. Khanna S N, Jena P *Phys. Rev. Lett.* **69** 1664 (1992)
197. Wiel R Z *Phys. D: At. Mol. Clust.* **27** 89 (1993)
198. Gspann J *Nucl. Instrum. Meth. B* **37–38** 775 (1989)
199. Gspann J *Nucl. Instrum. Meth. B* **80/81** 1336 (1993)
200. Henkes P R W, Klingelhofer R *J. Phys. (Paris)* **50** 159 (1989)
- [doi](#) 201. Henkes P R W, Klingelhofer R *Vacuum* **39** 541 (1989)
- [doi](#) 202. Gspann J *Microelectron. Eng.* **27** 517 (1995)
- [doi](#) 203. Gruber A, Gspann J *J. Vac. Sci. Technol. B* **15** 2362 (1997)
- [doi](#) 204. Gruber A, Gspann J, Hoffmann H *Appl. Phys. A* **68** 197 (1999)
205. Gspann J, in *Physics and Chemistry of Finite Systems: from Clusters to Crystals* Vol. 2 (NATO ASI Series, Ser. C, Vol. 374, Eds P Jena, S N Khanna, B K Rao) (Dordrecht: Kluwer Acad. Publ., 1992) p. 1115
206. Gspann J, in *Large Clusters of Atoms and Molecules* (NATO ASI Series, Ser. E, Vol. 313, Ed. T P Martin) (Dordrecht: Kluwer Acad. Publ., 1996) p. 443
207. Beuhler R, Friedman L *Chem. Rev.* **86** 521 (1986)
208. Matthew M W et al. *J. Phys. Chem.* **90** 3152 (1986)
209. Becker E W *Laser Part. Beams* **7** 743 (1989)
- [doi](#) 210. Beuhler R J, Friedlander G, Friedman L *Phys. Rev. Lett.* **63** 1292 (1989)
211. Leonas V B *Usp. Fiz. Nauk* **160** (11) 135 (1990) [*Sov. Phys. Usp.* **33** 956 (1990)]
- [doi](#) 212. Beuhler R J et al. *Phys. Rev. Lett.* **67** 473 (1991)
213. Gspann J *Trans. Mat. Res. Soc. Jpn.* **17** 107 (1994)
214. Haberland H et al., in *Beam Processing of Advanced Materials: Proc. of the Second Intern. Conf., Cleveland, Ohio, USA, 1995* (Eds J Singh, J Mazumder, S M Copley) (Materials Park, OH: ASM Intern., 1996) p. 1
- [doi](#) 215. Orloff J *Rev. Sci. Instrum.* **64** 1105 (1993)
- [doi](#) 216. Krainov V P, Smirnov M B *Phys. Rep.* **370** 237 (2002)
- [doi](#) 217. Krainov V P, Smirnov M B *Usp. Fiz. Nauk* **170** 969 (2000) [*Phys. Usp.* **43** 901 (2000)]
- [doi](#) 218. Ditmire T et al. *Phys. Rev. Lett.* **75** 3122 (1995)
- [doi](#) 219. Ditmire T et al. *Appl. Phys. Lett.* **71** 166 (1997)
- [doi](#) 220. Dobos S et al. *Pis'ma Zh. Eksp. Teor. Fiz.* **68** 454 (1998) [*JETP Lett.* **68** 485 (1998)]
221. Ditmire T et al. *J. Phys. B: At. Mol. Opt. Phys.* **31** 2825 (1998)
- [doi](#) 222. Larsson J, Sjögren A *Rev. Sci. Instrum.* **70** 2253 (1999)
- [doi](#) 223. Honda H et al. *Phys. Rev. A* **61** 023201 (2000)
- [doi](#) 224. Auguste T et al. *Pis'ma Zh. Eksp. Teor. Fiz.* **72** 54 (2000) [*JETP Lett.* **72** 38 (2000)]
- [doi](#) 225. Mocek T et al. *Appl. Phys. Lett.* **76** 1819 (2000)
- [doi](#) 226. Miura E et al. *Appl. Phys. B* **70** 783 (2000)
- [doi](#) 227. Schnürer M et al. *Eur. Phys. J. D* **14** 331 (2001)
- [doi](#) 228. Mocek T et al. *Phys. Rev. E* **62** 4461 (2000)
- [doi](#) 229. Stenz C et al. *Kvantovaya Elektron.* **30** 721 (2000) [*Quantum Electron.* **30** 721 (2000)]
- [doi](#) 230. Ter-Avetisyan S et al. *Phys. Rev. E* **64** 036404 (2001)

- [doi>](#) 231. Abdallah J (Jr) et al. *Phys. Rev. A* **63** 32706 (2001)
- [doi>](#) 232. Mori M et al. *J. Appl. Phys.* **90** 3595 (2001)
233. Rozet J-P et al. *Phys. Scripta* **T92** 113 (2001)
234. Junkel-Vives G C et al. *Phys. Rev. A* **64** 021201(R) (2001)
- [doi>](#) 235. Ditmire T et al. *Nature* **398** 489 (1999)
- [doi>](#) 236. Ditmire T et al. *Phys. Plasmas* **7** 1993 (2000)
- [doi>](#) 237. Zweiback J et al. *Phys. Rev. Lett.* **84** 2634 (2000)
- [doi>](#) 238. Zweiback J et al. *Phys. Rev. Lett.* **85** 3640 (2000)
- [doi>](#) 239. Hilscher D et al. *Phys. Rev. E* **64** 16414 (2001)
- [doi>](#) 240. Schmidt R, Seifert G, Lutz H O *Phys. Lett. A* **158** 231 (1991)
- [doi>](#) 241. Seifert G, Schmidt R, Lutz H O *Phys. Lett. A* **158** 237 (1991)
- [doi>](#) 242. Basbas G, Ritchie R H *Phys. Rev. A* **25** 1943 (1982)
243. Eliezer S, Martinez-Val J M, Deutsch C *Laser Part. Beams* **13** 43 (1995)
- [doi>](#) 244. Bret A, Deutsch C *Fusion Eng. Des.* **32** – **33** 517 (1996)
245. Deutsch C et al. *Fusion Technol.* **31** (1) 1 (1997)
- [doi>](#) 246. Zwicknagel G, Deutsch C *Phys. Rev. E* **56** 970 (1997)
247. Bret A, Deutsch C *Nucl. Instrum. Meth. A* **415** 703 (1998)
- [doi>](#) 248. Fermi E, Teller E *Phys. Rev.* **72** 399 (1947)
249. Smirnov B M *Zh. Eksp. Teor. Fiz.* **44** 192 (1963) [*Sov. Phys. JETP* **17** 133 (1963)]
250. Landau L D, Lifshitz E M *Kvantovaya Mekhanika: Nerelyativistskaya Teoriya* (Quantum Mechanics: Non-Relativistic Theory) (Moscow: Nauka, 1974) [Translated into English (Oxford: Pergamon Press, 1977)]